REQ. NO. 9-9082

CONTRACT REPORT NO. 15L80-00027

UNIVERSITY OF WATERLOO
WATERLOO RESEARCH INTITUTE

Project No. 910-03

FIELD AND LABORATORY INVESTIGATIONS OF ACIDIC PORE WATER IN PYRITIC URANIUM TAILINGS AT ELLIOT LAKE, ONTARIO

Final Report
1980-1982

Principal Investigators:
J.A.Cherry and R.W.Gillham
Research Assistants:
N.Dubrovsky, R.V.Nicholson and D.J.A.Smyth
Department of Earth Sciences
University of Waterloo
Waterloo, Ontario, N2L3G1

Sponsored by:

Energy, Mines and Resources Canada
555 Booth St
Ottawa, Ontario

June, 1982

223 pp

ABSTRACT

Field investigations of the hydrogeochemistry of inactive tailings areas in the Elliot Lake uranium mining district and laboratory studies of pyrite oxidation cotrols were conducted during the 1980-1981 and 1981-1982 fiscal years. The three major divisions of this study dealt with: 1) the hydrogeochemical processes above the water table, 2) acidification and contaminant migration below the water table and 3) physiochemical factors that affect pyrite oxidation rates.

The first objective of this study was to delineate the active zone of pyrite oxidation and to identify other geochemical processes that play an important role in the evolution of the pore water in the zone above the water table. The pore-water, soil-gas and solid-phase geochemistry, and the physical characteristics of tailings were monitored at three sites at the Nordic Main tailings impoundment.

The tailings are a heterogeneous mixture of sand- and silt-sized material, generally deposited in thin layers. In the zone above the water table the silt-rich lenses are typically more than 70% saturated and the sand lenses are approximately 25% saturated. Pyrite content within the tailings generally ranges from 3% to 7% except in the vicinity of the tailings discharge pipe where concentrations exceed 15%.

The most significant pyrite oxidation has occurred within the upper metre of the tailings which is depleted in pyrite relative to points deeper in the tailings. Profiles of oxygen concentration in the soil gas delineate the active

zone of pyrite oxidation. In fine, wet sediments, oxygen concentrations decrease markedly in a narrow zone from about 0.5 to 0.7 m below the surface, but in drier sands, where oxygen diffusion is more rapid, the decrease occurs in a zone from 0.5 to 1.5 m below the surface of the tailings.

Pyrite oxidation occurring at shallow depths and the translocation of reaction products downward towards the water table with infiltration water are the major controls on the pore-water characteristics. Both the August and May profiles of iron and sulphate concentrations in the pore water exhibit major concentration peaks just below the surface and immediately above the water table; however, the upper peak in the May profiles has been displaced downward by 0.5 to 1.0 m by the infiltration water associated with the spring recharge event.

The pH is lowest in the upper metre, ranging from about 1.4 to 3.0, and generally increases with depth. Carbonate minerals are present at depths of more than 1.0 m in the tailings in concentrations of less than 0.001% $CaCO_3$ by weight and their dissolution probably contributes significantly to the neutralization of low pH waters.

The second objective of the study was to develop a detailed hydrogeochemical explanation for the extent and degree of acidification observed in the Nordic Main and Nordic West Arm tailings. In particular, the investigation was focused on evaluating the influence of physical hydrology on tailings chemical evolution, the mechanisms of pyrite oxidation that have produced acidity during the tailings history, and chemical processes that control the rate of migration of iron, aluminum and low pH conditions.

Data gathered from piezometers installed in the tailings and underlying aquifer indicate that a two layer groundwater system has developed in which recharging precipitation, with high concentrations of SO_4, Fe and heavy metal, and a low pH, has moved downward into the tailings gradually displacing the original high pH, low Fe residual process water. Depth of contaminant penetration is controlled by the physical properties and hydrologic setting of the tailings, with the greatest penetration occurring in areas of coarser grained tailings and high downward hydraulic gradients. The limit of the depth of displacement is marked by decreasing concentrations of Fe and SO_4, coincident with increasing concentrations of Cl.

High concentrations of Fe^{3+} at shallow depths in the unsaturated zone indicates that ferric iron is an important oxidizer of pyrite under low pH conditions in Elliot Lake tailings. These results also suggest that iron oxidizing bacteria play an important role in the oxidation process.

The pe of the groundwaters is controlled by the ferric-ferrous iron redox couple, and trends in the data indicate iron solubility control by siderite at high pH, ferric hydroxide at moderate to slightly acid pH values, and possibly jarosite at low pH. Transport of low pH conditions is retarded relative to the rate of groundwater flow in the tailings. This is due to the dissolution of small amounts of carbonate minerals added during tailings neutralization, primary aluminosilicates such as sericite, and secondary aluminum hydroxides and basic aluminum sulfates. The pH neutralization also results in retardation of the rate of transport of heavy metals and the radionuclides uranium and lead-210, probably due to sorption and coprecipitation reactions. Aluminum solubility controls are complex, and precipitation of amorphous aluminum hydroxide, allophane, and basic aluminum sulfates occurs over different pH.

The third objective of this study was to determine the relative importance of critical factors that control pyrite oxidation rates. Six variables that were cited in the literature as influencing pyrite oxidation rates were investigated in the laboratory under controlled conditions. Oxygen content, microbial mediation, surface area, carbonate buffering, pyrite content and temperature were the variables used in a two level factorial design experiment. The sulphate that was leached from the tailings at the end of the 56 day oxidation period was used as an indication of the extent of oxidation.

The results of this experiment indicated that temperature and surface area are highly significant variables that affect pyrite oxidation rates. A difference in oxygen contents between 20 and 0.5% did not significantly alter the production of sulphate over the period of oxidation. The presence of carbonate buffering and pyrite content did not significantly affect the sulphate yield. Microbial mediation did not affect the results probably because the experimental conditions did not allow sufficient time for culture growth.

CONTENTS

ABSTRACT ii

page

HYDROGEOLOGICAL AND GEOCHEMICAL STUDIES ABOVE THE WATER TABLE 1

Introduction 1
Background 1
Purpose and Scope 4
The Study Area 6
Methods 8
Coring and Pore-Water Extraction 8
Soil-Gas Sampling 10
Soil-Moisture and Bulk-Density Measurements 12
Analytical Techniques 13
Pore-Water Chemistry 13
Solids 14
Soil Gas 15
Results 15
Physical Characteristics of the Tailings 15
Pore-Water Chemistry 17
Solid-Phase Chemistry 21
Soil-Gas Composition 22
Discussion 22
Summary and Conclusions 39
List of Tables in Chapter 1 43
List of Figures in Chapter 1 44
Tables in Chapter 1 46
Figures in Chapter 1 53

SATURATED ZONE GEOCHEMISTRY AND HYDROLOGY 73

Introduction 73
Objectives and Scope 75
Methods 76
Physical Hydrology 79
Aqueous Geochemistry 83
Hydrochemical Conditions 83
Acid Production 88
Major Ion Geochemistry 91
Acid Neutralizing Processes 99
Summary of Conclusions 104
List of Tables in Chapter 2 108
List of Figures in Chapter 2 109

Tables in Chapter 2 112
Figures in Chapter 2 121

LABORATORY INVESTIGATION OF FACTORS AFFECTING PYRITE OXIDATION 137

Introduction 137
Literature Review 138
Research Rationale 147
Experimental Methods 148
Experimental Design 149
Sample Preparation 150
Sample Processing 154
Statistical Treatment 155
Results and Discussion 156
Summary of Conclusions 161
List of Tables in Chapter 3 164
List of Figures in Chapter 3 165
Tables in Chapter 3 166
Figures in Chapter 3 178

REFERENCES 180

Appendix page

A. DATA ON PHYSICAL HYDROLOGY 187

B. ANALYSES OF SATURATED-ZONE PORE-WATER CHEMISTRY . . . 192

C. DEVELOPMENT OF A TECHNIQUE FOR THE DETERMINATION OF SOLID CARBONATE MINERAL CONTENT AND RESULTS . 203

D. TEMPERATURE DATA FOR THE FOUR INCUBATORS DURING THE OXIDATION PERIOD 212

E. OXYGEN AND CARBON DIOXIDE CONTENTS OF THE INCUBATOR ATMOSPHERES 216

HYDROGEOLOGICAL AND GEOCHEMICAL STUDIES ABOVE THE WATER TABLE

INTRODUCTION

Background

The base-metal mining industry in Ontario produces large volumes of waste material which, following the milling and extraction processes, are deposited in extensive tailings impoundments. Generally the ore bodies are associated with metal sulphides. Iron sulphides such as pyrite, marcasite and pyrrhotite are not desired products and are released to the tailings as part of the mill wastes (Hawley, 1972). In recent years the identification of acid mine draingage conditions associated with these tailings piles has caused considerable environmental concern.

The development of highly acidic conditions in the tailings impoundments results from the oxidation of pyrite and other iron sulphides. The oxidation of pyrite and the subsequent leaching of the tailings material by the acidic waters creates a pore water containing significant concentrations of iron, sulphate and heavy metals. The migration of the water from the tailings by either surface runoff or subsurface groundwater flow can lead to a serious deterioration in quality of adjacent natural water systems.

During the operating life of a mine the water quality of the surface water and groundwater seepage from tailings impoundments can be controlled by on-site neutralization and treatment facilities. The potential for the production of acidic waters from pyrite oxidation should, however, persist for

decades in abandoned tailings areas. Thus, the mining industry is faced with the difficult task of devising long term abandonment schemes that minimize pyrite oxidation and prevent the release of contaminated waters to the environment. These schemes need to be cost-effective and should require very little future maintenance or monitoring.

As a result of uranium mining operations, major tailings impoundments currently exist in the Elliot Lake area. Pyrite is associated with the uranium ore of the region and occurs in the tailings at concentrations between 3 and 7% by weight. As the major iron sulphide mineral, pyrite is a dominant factor in the generation of acid mine water conditions in the uranium tailings.

The oxidation of pyrite and the subsequent production of acidic conditions occurs in a complex series of reactions (Nordstrom, 1979; Nordstrom et al., 1979). The first step in the pyrite oxidation process is the release of ferrous ions and elemental sulphur from pyrite;

$$FeS_2(s) \Longrightarrow Fe^{2+} + S_2^0 + 2e^- \qquad (1.1)$$

The second step involves the oxidation of elemental sulphur in water producing sulphate and hydrogen ions. This step can be summarized as

$$S_2^0 + 8H_2O \Longrightarrow 2SO_4^{2-} + 16H^+ + 12e^- \qquad (1.2)$$

Below a pH of 3 ferric ion replaces oxygen as the only oxidizing agent of pyrite; however, in abiotic systems the oxidation of ferrous to ferric ion is a very slow process. When combined with the half-reaction for the reduction of oxygen to water the oxidation of ferrous ion can be represented as

$$2Fe^{2+} + 1/2\ O_2(aq) + 2H^+ \Longrightarrow 2Fe^{3+} + H_2O \qquad (1.3)$$

Because ferric ion is the only oxidizing agent of pyrite under these conditions, its rate of production is the rate-determining step in the pyrite-oxidation process (Singer and Stumm, 1970). In the development of acid mine waters ferrous to ferric ion oxidation is performed by the iron-oxidizing bacterium, Thiobacillus ferrooxidans, with only sufficient oxygen for bacterial respiration required (Nordstrom et al., 1979). The oxidation of pyrite by ferric ion with the subsequent production of ferrous and sulphate ions and acidic condition can be represented as

$$FeS_2(s) + 14Fe^{3+} + 8H_2O \Longrightarrow 15Fe^{2+} + 2SO_4^{2-} + 16H^+ \qquad (1.4)$$

The oxidation of pyrite in the presence of T. ferrooxidans and small amounts of oxygen is thus, a self-perpetuating process that results in the creation of severe acid mine drainage conditions. The problem is compounded in the Elliot Lake area because radionuclides deposited with the tailings are more soluble in low pH waters. The likelihood of the migration of radionuclides to adjacent groundwater and surface water systems is increased as a consequence of the generation of the acid drainage.

Moffett and Tellier (1978) were the first to study the chemical characteristics of groundwater in tailings in the Elliot Lake area. Two main types of water were identified. A highly acidic water with elevated concentrations of Fe, Zn, ^{210}Pb, ^{232}Th, ^{230}Th, ^{228}Th, ^{226}Ra and U was found in the coarse-grained tailings close to the area where the tailings were discharged. In the finer tailings material a low-pH water with low concentration of iron, zinc and radionuclides, with the exception of ^{226}Ra, was identified. Seepage waters from the base of the impoundment dam contained concentrations intermediate between those present in the high and low-pH waters but above desirable water quality limits (O.M.E., 1978).

Blair et al. (1980) and Blair (1981) documented a hydrogeological study of the inactive Nordic Main tailings adjacent to the impoundment described by Moffett and Tellier (1978). A zone of highly acidic water with a pH of approximately 3 was identified immediately below the water table. This water had elevated concentrations of iron, sulphate, heavy metals and ^{226}Ra.. Below this zone, but within the tailings, neutral waters were found with much lower total dissolved solids (TDS). They proposed that downward hydraulic gradients caused the low pH waters to displace the neutral pore waters at depth. In the vicinity of the tailings dam the water table is deepest and the saturated zone of the tailings is thin. Some discontinuities in a peat layer immediately beneath the tailings in this section of the tailings area have permitted the movement of tailings water into the underlying sand and gravel aquifer. An iron, sulphate and ^{226}Ra contaminant plume has subsequently developed beyond the lateral boundaries of the tailings impoundment (Blair et al., 1980; Blair, 1981; Morin et al., 1982). It was also indicated that the low pH waters probably develop as a result of pyrite oxidation within the zone above the water table.

Purpose and Scope

The purpose of this study is to identify the geochemical characteristics of the pore water, soil gas and solid-phase material within the zone above the water table in the inactive Nordic Main tailings. It was anticipated, that based on the geochemical trends, the zones of active pyrite oxidation could be delineated, and that other geochemical processes that have a significant effect on the pore-water chemistry could be identified.

The Nordic Main tailings impoundment, which has been inactive since the termination of mining operations at the Nordic Mine in 1968, was selected as the study area. It was chosen because the hydrogeological and geochemical conditions below the water table were previously documented in more detail than in any other tailings area in the Elliot Lake region (Blair et al., 1980; Blair, 1981). In these studies the authors suggested that chemical processes which occurred within the zone above the water table played a major role in the chemical evolution of the tailings, but no data was available to verify this hypothesis.

This study included the measurement of several parameters at three sites in the zone above the water table. The sites were chosen to provide different depth-to-the-water table and grain-size characteristics representative of the various conditions prevalent in the tailings.

The geochemical characteristics of the pore water were monitored on two occasions; in August, 1980 and in early May, 1981, to determine general trends and to indicate the significance of seasonal variations. The water was obtained from continuous cores of the tailings material by squeezing and immiscible displacement techniques. The specific conductance and pH of the water were measured in addition to the major cations, anions and heavy metals.

The geochemical analysis of the solid-phase material included determinations of total sulphur, soluble sulphate, and carbonate content. Radionuclide concentrations were measured for selected samples. The solid samples were taken from continuous cores during the August sampling period.

The soil-gas samples were collected in early October, 1980. Changes in the relative abundances of N_2, O_2 and CO_2 with depth were monitored at each site.

Grain-size analyses were performed on portions of the samples used for solid-phase geochemical determinations to indicate the general grain-size characteristics at each site and the variability of the tailings material with depth.

Volumetric water contents were determined gravimetrically from a separate suite of cores taken in the fall. Bulk-density measurements of the tailings material were also made from the same set of cores.

The Study Area

The Nordic Mine and associated tailings impoundments are located 4 km east of Elliot Lake, Ontario (Fig. 1). The physiography is characterized by rugged bedrock exposures, with a thin and discontinuous cover of glacial drift typical of the Canadian Shield. The region has a modified continental climate due to the influence of the Great Lakes, which lie to the south and west (Chapman and Thomas, 1968). The area receives about 84 cm (33 in) of rain annually distributed relatively enenly throughout the year. Snow cover is generally present from late November to April. The temperature ranges from a January monthly average of $-11^{0}C$ ($12^{0}F$) to a July monthly average of $18^{0}C$ ($65^{0}F$).

The tailings impoundments lie in an east-west trending valley that is flanked by ridges of Huronian sedimentary rocks (Robertson, 1968) and are underlain almost continuously by a black peat layer 0.5 to 1.0 m thick. Below this, Pleistocene deposits with a thickness of as much as 30 m are present. These consist of an upper glaciofluvial sand and gravel unit and a lower sandy bouldery till (Blair et al., 1980).

The uranium ore exists in a pyritiferous quartz-pebble conglomerate. Associated sulphides, in addition to pyrite, include pyrrhotite, chalcopyrite, and minor arsenopyrite, galena and cobalite (Robertson, 1968). The ore was crushed, treated by a sulphuric acid-leach process and the uranium extracted by passing the resulting liquor through ion-exchange columns. The method removed as much as 95% of the uranium (Robertson, 1968). The effluent and leached crushed rock were neutralized with lime and limestone and the resultant slurry was subsequently discharged to the tailings impoundment at a pH of 8 (Blair, 1981).

The Nordic Main tailings were deposited from 1957 to 1968 during the operation of the mine. Following closure the tailings were subject to controlled drainage; however the north-eastern segment of the tailings impoundment remained submerged by ponded water. A vegetative program was initiated in 1972. The ponded water was drained off, the barren surface of the tailings was treated with lime and crushed limestone to maintain neutral pH conditions and fertilizers were applied to provide nutrients necessary for plants growth. A grass cover, consisting of several species (Murray and Moffett, 1977), was successfully established in the ensuing years.

The three sampling sites chosen for investigation in this study were T1, T3 and T5 (Fig. 2). At T5, in predominantly coarser tailings adjacent to the tailings discharge pipe, the depth to the water table varies from 4 to 4.5 m. T1 and T3 are located in finer-grained tailings. The depth to the water table at T1, which is adjacent to a small stream, ranges from 1 to 3 m and at T3, which is approximately midway between the stream and the dam, the depth to the water table ranges from 6 to 7 m.

METHODS

Coring and Pore-Water Extraction

Pore-water and solid phase samples were obtained from cores collected from the ground surface to the water table at each site. The cores were taken in 1 m long aluminum tubes with an external diameter of 7.62 cm (3 in) and a wall thickness of 0.127 cm (0.05 in). The cores were taken in sections to ensure complete recovery and to facilitate handling. The tubes were driven using a hand-operated Cobra percussion drill and removed from the ground using a block and tackle apparatus supported by a metal tripod.

The section of tubing was attached to a drive head. A threaded male connector on the drive head was joined to a machined adaptor for the percussion drill when shallow cores were taken or A-type drill rods which were required when cores from depths of more than 1 m were desired. After the core was removed from the ground the hole was covered to minimize air movement and compositional changes of gas in the hole. The core was cut into 0.2 m segments and the squeezing technique, described below, was used to obtain water from each segment. When the drill rods were used for deeper cores, the section of aluminum tubing and drive head were lowered down the hole to the point of deepest penetration of the previous core. The adaptor for the percussion drill was fitted to the protruding drill rod and the core was taken. The holes generally remained open in the unsaturated zone and therefore 100% core recovery was possible; however, in the saturated and near-saturated zone just above the water table the hole frequently caved in and complete recovery was not possible.

To extract water samples from the cores, a squeezing device similar to that described by Patterson et al. (1978) was used. The apparatus (Fig. 3)

consisted of a plunger, a sealing disc with o-ring which fit tightly into the upper end of the aluminum tubing, a filter in the base of the tubing consisting of a porous plate bounded by two sheets of no. 40 filter paper, and a hollowed-out base with a port through which the water sample could be collected.

To operate the device, a sufficient volume of tailings was removed from the upper end of the 0.2 m core to allow for the positioning of the sealing disc within the tubing. The filter papers and porous plate were emplaced following the removal of sufficient tailings material from the lower end of the core. The tube was then fitted on the protrusion of the base. The plunger was positioned on top of the sealing disc and the entire unit was placed between a fixed plate and moveable plate which rested on a hydraulic jack (Fig. 3). Pressure increases were applied by slowly raising the hydraulic jack; thereby expelling water at the base of the device. A rubber septum was inserted into the port in the base following the passage of the initial few drops of water. Each water sample was collected in a 50 ml syringe fitted with a 25 mm filter holder and syringe needle (Fig. 3). To collect a sample, the septum was pierced by the syringe needle and the water drawn through a 0.45 micron Sartorius membranfilter directly into the syringe.

In fine materials with a high water content, the squeezing procedure proved to be quite satisfactory; however, in the coarser, less compressible fractions of the tailings the procedure did not yield sufficient quantities of water. In these materials immiscible displacement of the water with Paraplex, an expoxy plasticizer, was used. The mechanical squeezing method was modified slightly for this purpose. Approximately 0.06 m of tailings material was removed from the upper part of the core and was replaced

with Paraplex leaving enough space for the emplacements of the sealing disc. The rest of the procedure was similar except that the pressure was applied in smaller increments with longer time periods between successive increases. Rapidly applied pressure increases forced the Paraplex through larger pores or cracks in the core, causing the Paraplex to appear in the sample port before sufficient water had been collected. The process of immiscible displacement required between 0.75 and 1.5 hours before sufficient water for analytical purposes was obtained. The volumes of water collected ranged from 3 ml to in excess of 35 ml.

The tailings material removed from individual cores in preparation for either the squeezing or immiscible displacement technique was retained for solid-phase geochemical analyses and grain-size analyses.

Soil-Gas Sampling

Gas samplers, similar to those described by Reardon et al., (1979), were installed in the zone above the water table in the tailings. The samplers consisted of inverted Eppendorf pipette tips packed tightly with glass wool and attached to 2 mm Tygon tubing. These were placed at the desired depth in the holes used for the coring operations. The holes were backfilled with silica sand and sealed at the surface with a layer of bentonite. The ends of the Tygon tubing at the ground surface were also attached to inverted Eppendorf pipette tips which were capped by rubber septa. These allowed gas samples to be collected in 10 ml glass syringes. Gas sampling points were positioned every 0.5 m throughout the profile, except within the upper metre.

An initial sequence of test sampling indicated that significant soil-gas compositional changes occurred within a metre of the ground surface. To facilitate more detailed monitoring in this zone gas samplers made from stainless-steel tubes with an exterior diameter of 3.175 mm (0.125 in) and a wall thickness of 0.794 mm (0.0312 in) were used. Each tube was punctured with several small holes close to its tip which was pinched into a sharp point. This end was pushed into the tailings to the desired depth of sampling. The part of the stainless-steel tube protruding above the ground surface was joined to a short segment of Tygon tubing with an inverted Eppendorf pipette tip capped by a rubber septum on its free end. Thus, gas sampling could be performed in the same manner from both types of gas sampling devices.

In preparation for sampling, the plungers of the glass syringes were wetted with distilled water to provide an adequate seal. During sampling, extraction of gas from the samplers was conducted with the pipette tip and syringe sampler submerged in a distilled water bath. Prior to the actual sample collection, a 30 ml volume of gas was flushed from each sampler. Following sample collection the needle of each syringe was sealed by inserting it into a rubber stopper. The syringes were then stored vertically in a bucket of distilled water such that the water covered the entire barrel and part of the protruding plunger. This procedure was followed to reduce the possibility of gaseous interchange at the needle-syringe connection.

Soil-Moisture and Bulk-Density Measurements

Soil-moisture profiles were determined gravimetrically at each site in late September, 1980. The soil-moisture measurements were made from 7.62 cm (3 in) cores that were collected in the same manner as that described for pore-water extraction purposes. The 1 m core sections were cut into 0.25 m lengths. A smaller sample was taken in a 2.54 cm (1 in) long thin-walled stainless-steel cylinder with a diameter of 2.54 cm from the freshly exposed face at the base of each length. The ends of the small sample were cut flush with those of the small cylinder using a knife and the sample was then transferred into a 15 ml Nalgene container. The weight of the moist sample was measured prior to being dried in an oven at 105^0C for more than twenty-four hours. Following drying, the dry weight of the sample was measured. The values of the wet and dry bulk weights, the initial volume of the small samples and an assumed specific gravity of 1.0, permitted the determination of volumetric and gravimetric water contents and bulk density. The degree of saturation was calculated at each sample point. The porosity, n, was determined using the equation

$$n = 1 - \text{bulk density/particle density} \quad (1.5)$$

The particle density was assumed to be 2.75 g/cm^3 in light of the predominence of silicate minerals in the tailing material and the lesser quanities of pyrite and gypsum. The degree of saturation is the ratio of the volumetric water content to the porosity.

Analytical Techniques

Pore-Water Chemistry.

The filtered water samples collected by the squeezing and immiscible displacement techniques were separated into four portions. Approximately 2 ml of water were required for a pH measurement. The pH of each sample was measured in a stoppered 5 ml syringe with plunger removed, using a small Markson 1885 electrode and a Cole-Parmer Digi-Sense pH meter with a reported accuracy of $\pm$ 0.02 pH units. The pH measurements were performed in the field immediately following the squeezing operation and the collection of water samples.

A 3 to 5 ml portion of each sample was stored in a 5 ml syringe for electrical conductance measurements. These were performed in the laboratory at a later date using a Beckman 50-18 A conductivity bridge.

A 10 ml unacidified volume of water for anion analyses and a 5 ml volume, acidified with 37% HCl to a pH of less than 2, for cation analyses were refrigerated and distributed to the appropriate laboratories. Anion analyses were performed in the Geochemistry Laboratory at the University of Waterloo. Sulphate, chloride and bromide were analysed by column chromatography using the Dionex Ion Analyser and the silica analyses were performed using an automatic photometric method on a Technicon Auto-Analyzer. The cation analyses included Ca, Na, K, Mg, Pb, Zn, Ni, Co, Mn, Fe(total), Cu and Al and were performed at the Process and Development Laboratory of Rio Algom Limited, Elliot Lake. Atomic adsorption was used for all determinations except Fe(total) which was measured using a redox titration with potassium dichromate.

When circumstances arose such that insufficient quantities of water could be obtained, water analyses were performed on smaller volume or, in extreme cases, analyses for some constituents were not done.

Solids.

Solid-phase geochemical analyses were performed for total sulphur, soluble sulphate, carbonate and radionuclides. The content of total sulphur was determined using the photometric starch-iodine technique. The analyses were performed with a Leco Ignition Furnace and a Leco DB-64 is (Model 765-100) Digital Titrator at the University of Waterloo.

For sulphate analyses, a 0.5 g sample was washed in 20 ml of distilled water for a 24 hour period. The resultant water samples were analysed for sulphate using column chromatography in the Geochemistry Laboratory at the University of Waterloo.

For the carbonate analyses, 5 g of material was placed in a 30 ml syringe with approximately 10 ml of distilled water and centrifuged immediately following core collection. This step was performed to flush the high concentrations of ferrous ion from the pore water associated with the sample. The sample was retained for analysis and the water discarded. The carbonate-mineral content of the sample was determined by acidifying the material in a helium atmosphere. The amount of CO_2 gas liberated from the dissolution of carbonate minerals was measured on a Hewlett-Packard gas chromatograph with a TCD detector. The method is described by Barker (in preparation).

The analyses for radionuclides in the solid materials were performed by Monenco Analytical Laboratories, Calgary, Alberta. ^{228}Th, ^{230}Th, ^{232}Th and ^{226}Ra were analysed using alpha spectroscopy, while beta spectroscopy was

used to determine ^{210}Pb concentrations. U(total) was measured by colorimetry and ion exchange and colorimetry were used to analyse for Th(total).

In addition to solid-phase geochemistry, grain-size distributions were determined on representative portions of each sample at the CANMET Elliot Lake Laboratory. Sieving was used to separate the coarser fractions. The material passing the 45 um screen was further described by eriometry, a technique that estimates the size distribution of fine particles based upon the diffraction pattern which results when a beam of light is transmitted through a sample of dust particles (Kirk, 1981).

Soil Gas.

The samples of soil gas were analysed using a Hewlett-Packard gas chromatograph with a TCD detector within 48 hours of collection. The O_2 and N_2 fractions were measured using a molecular sieve and a poropak was used for CO_2 determinations. The analyses were conducted in the Geochemistry Laboratory at the University of Waterloo.

RESULTS

Physical Characteristics of the Tailings

The tailings are a heterogeneous mixture of sand and silt. They are generally a light grey colour, with sandy lenses being lighter in colour than the silt-rich lenses. A distinctive weathering profile has developed, however. The material within a half metre of the ground surface is generally yellow to brown-yellow, often with a mottled appearance. Horizontal and sub-vertical dessication cracks within this zone tend to be a darker rust brown. This zone grades into a lighter yellow, white and pale grey zone at a depth

of 0.5 m. At depths between 0.8 and 1.0 m the effects of post-depositional weathering are less apparent and the grey-coloured material typical of the tailings mass predominates. A summary of the soil profiles including a documentation of the soil colour and texture at the three study sites is presented in Table 1.

The graphic mean, a parameter defined by Folk (1974), which requires the use of the d_{84}, d_{50}, and d_{16} points on the grain-size distribution curve, was used as a statistical measure of the general grain-size characteristics at selected sampling points. The graphs of mean grain size versus depth for sites, T1, T3 and T5 (Fig. 4a, b) indicate the variability of the tailings material areally across the impoundment and vertically through the soil profiles. Silt and very fine sand are predominant at T1 and T3. At T1 the mean grain size ranges from 0.05 to 0.1 mm. At T3 the mean grain size is typically less than 0.05 mm but may range as high as 0.1 mm in coarser lenses at depths of more than 4.0 m below ground surface. The tailings material at T5 is generally a fine sand, with the mean grain size ranging from 0.15 to 0.2 mm.

The moisture-content and bulk-density profiles (Fig. 4a, b) also show considerable variability. The volumetric moisture contents, as measured in late September, range from 10% in the coarser lenses to 60% in the finer sediments. At T1 and T3, in predominantly fine sediments, the bulk density of the tailings material ranges from 0.9 to 1.3. In coarser material at T5 the bulk density is generally higher, ranging form 1.2 to 1.5.

The profiles of degree of saturation versus depth (Fig. 4a, b) indicate that much of the tailings in the zone above the water table is close to saturation. In the finer sediments at T1 and T3 the degree of saturation

commonly exceeds 75% and may be greater than 90%; whereas in sandy lenses the degree of saturation is less than 30%. In the fine sands at T5, degree of saturation values are typically between 20 and 40%.

Pore-Water Chemistry

The pH and electrical conductance profiles determined for the August and May sampling periods are shown in Fig. 5a and b. The August pH profile exhibits low pH in the upper 1.5 m and a characteristic increase with depth. The pH at T1 increases from 3.0 at 1.0 m to 3.65 m at 2.4 m, about 0.5 m above the water table. At T3, in silt and very fine sand, the pH decreases from 3.7 at 0.2 m to 1.9 at 1.0 m. Below this depth the pH gradually increases to above 5.0 at 3.0 m. At T5, in coarser material, the pH increases from 1.4 at a depth of 1.0 m to 3.6 at a depth of 3.8 m.

The May pH profiles are somewhat different. At T1 the water table in May is only 1.05 m below ground surface. The pH increases from 2.8 at 0.2 m to 3.15 at a depth of 1.0 m. At T3 the May pH profile is similar to that of August. The pH decreases from 3.0 at 0.4 m to 2.07 at 1.2 m. A gradual increase in pH with depth to above 5.0 at a depth of 4.0 m occurs. At T5 the pH profile in May differs markedly from that described for August. The pH decreases from 2.22 at 0.6 m to less than 1.5 at a depth of 3.6 m, about 0.5 m above the water table.

The August profiles of electrical conductance (Fig. 5a) are irregular. At T1 the electrical conductance increases from approximately 3000 uS at 0.8 m to 7000 uS at 2.4 m. At T3 a peak of over 20000 uS exists at a depth of 1.0 m, but at 2.0 m it drops to 2700 uS. The rest of the profile is characterized by a gradual increase with depth to about 700 uS within 0.5 m

of the water table. The electrical conductance at T5 increases from about 7000 uS at a depth of 1.8 m to a peak of 19000 uS at 3.0 m. At 3.8 m, just above the water table, the electrical conductance is 12000 uS.

The May profiles of electrical conductance (Fig. 5b) show similar trends to those of August. The profile at T1 indicates an increase from 3400 uS at 0.2 m to 3800 uS at a depth of 1.0 m. At T3 an electrical conductance peak of 5600 uS at a depth of 1.2 m is present, although this is significantly lower than the 20000 uS apparent in August. Over the rest of the profile the electrical conductance ranges from 2500 to 4000 uS. The May profile at T5 is similar in form to the August profile; however, the electrical conductance values are much higher. They increase from 3500 uS at 0.6 m to more than 30000 uS at depths below 2.4 m.

The major-ion and heavy metal profiles for August (Fig. 6a-f) and May (Figs. 7a-e) show some significant seasonal variations. The August Fe(total) and SO_4 profiles exhibit two major concentration peaks; one within the upper 1.5 m and a second immediately above the water table. This pattern is distinctive at T3 and T5. At T3 the upper peak occurs at a depth of 1.2 m, while at T5 it appears at 1.0 m. Both sites have a second significant peak within 1.0 m of the water table. At T5 higher concentrations of both SO_4 and Fe(total) are present with SO_4 levels in excess of 32000 mg/L and Fe(total) concentrations of more than 10000 mg/L. The August profiles at T1 do not show two peaks but rather a general increase in concentration with depth. SO_4 concentrations increase from 2000 mg/L at 0.8 m to approximately 7000 mg/L at 2.6 m and Fe(total) concentrations increase from less than 400 mg/L to more than 3000 mg/L over the same interval.

The May profiles of Fe(total) and SO_4 concentrations at T3 and T5 also show two peaks. At T3 the upper peak occurs between 1.6 and 2.4 m below the ground surface with SO_4 and Fe (total) concentrations as high as 3500 mg/L and 1400 mg/L respectively. The peak at T5 exists at a depth of 2.0 to 2.8 m and is characterized by SO_4 levels in excess of 20000 mg/L and Fe(total) concentrations of more than 10,000 mg/L. At both sites concentration peaks are also present just above the water table. The May profiles at T1, although shallower than those of August due to the raised water table, indicate an increase in concentration of both SO_4 and Fe(total) with depth.

Similar profiles to those of Fe(total) and SO_4 exist for the metals: Mn, Ni and Co. The concentrations of these metals, however, are generally limited to less than 10 mg/L. Cu and Zn also occur at significant concentrations but show no regular trends.

The profiles of Na, K, and Mg generally show gradual increases in concentration with depth for both sampling periods. Na values are typically less than 10 mg/L and K concentrations are somewhat higher, ranging from less than 10 to 200 mg/L. Mg has maximum values as high as 130 mg/L but generally concentrations range between 10 and 60 mg/L.

The Al profiles show trends similar to those exhibited by Fe(total) and SO_4. Al concentrations are generally high ranging from 0 to 250 mg/L at T1 and T3. At T5 exceptionally high Al concentrations of 1500 mg/L in August and 500 mg/L in May are present. Only where the pH values rise above 3.5 at depths of more than 3.0 m at T3 do Al levels drop to less than 1 mg/L. In this segment the profiles differ from those of Fe(total) and SO_4. Si concentrations are also high and variable, ranging from 10 to 100mg/L.

The profiles do not show the same characteristics as those exhibited by Al, Fe(total) or SO_4.

Cl concentrations are variable, typically ranging from 5 to 40 mg/L except at T5, where the May profile indicates Cl concentrations of in excess of 150 mg/L.

Selected water analyses were evaluated using WATEQ2 to identify tendencies for the precipitation and dissolution of various mineral phases. WATEQ2 is a computer program for the calculation of aqueous speciation and the degree of saturation with respect to a wide variety of mineral phases. Developed by Ball, Nordstrom and Jenne (1980), WATEQ2 originated as a result of extensive additions and revisions to the thermodynamic data and computing capabilities of WATEQF, an earlier program developed by Truesdell and Jones (1974). WATEQ2 requires that the cation and anion charge balance for each sample, expressed in equivalents per million (EPM), be within 30%. When this error in charge balance was exceeded, as was the case for several of the high Fe and SO_4 waters, the SO_4 concentrations were adjusted to suitable levels to satisfy this criterion. The WATEQ2 results, expressed as the logarithms of the saturation indeces (Log S.I) are summarized in Table 2. The results indicate that the Log S.I. values are: much greater than 1 for gibbsite ($Al(OH)_3$); at or very near 0 for gypsum ($CaSO_4 \cdot 2H_2O$) and silica gel (SiO_2); much less than 0 for amorphous aluminum hydroxide ($Al(OH)_3$). Thus the waters are supersaturated with respect to gibbsite, at or near saturation with respect to gypsum and silica gel and undersaturated with respect to amorphous aluminum hydroxide.

Solid-Phase Chemistry

The results of the solid-phase analyses for soluble-sulphate, pyrite and carbonate are included in Figs. 8a, b. The weight percent pyrite was calculated by assuming that pyrite was the only sulphide mineral present and subtracting the soluble-sulphate values from the total-sulphur determinations.

The profiles indicate that sulphate exists in the soluble sulphate form throughout the tailings in amounts ranging from 0.2 to 3% S by weight as SO_4. No distinct trends are discernible. The distribution of pyrite throughout the profile does, however, show some definite trends. The upper half metre at each site is depleted in pyrite in comparison to points deeper in the profile. At T1, 0.28% pyrite by weight is found within the upper 0.3 m, while deeper in the profile at 3.3 m 3.65% pyrite is present. At T3 the pyrite content increases from 0.19% at 0.15 m to 6.68% at a depth of 5.6 m. The pyrite content at T5 ranges from 5.28% at a depth of 0.3 m to 14.33% at 3.7 m. The data also indicate that the pyrite content varies from site to site. In the coarse sediments at T5, adjacent to the tailings discharge pipe, as much as 15% pyrite is present; whereas, in the silt and very fine sand at T1 and T3, more than 500 m from the tailings discharge pipe, the pyrite content is less than 7%, but generally ranges from 3 to 5%.

The carbonate mineral-content in the zone above the water table is quite small. In the upper 0.5 m there are non-detectable levels of carbonate (less than 0.001% by weight as $CaCO_3$). At a depth of 0.8 m at T1, 0.0024% by weight of carbonate is found, and at T3 the carbonate content increases from 0.0015% at a depth of 1.4 m to 0.011% at 4.6 m. At T5, in the coarser tailings and where lower pH conditions prevail, no detectable carbonate is present.

The results of the selected radionuclide analyses are presented in Table 3. Generally the highest concentrations of radionuclides are associated with fine-grained sediments; however, significant concentrations are also present in the coarser tailings at T5. ^{228}Th ranges from 7 to 168 pCi/g, ^{230}Th from 15 to 740 pCi/g and ^{232}Th from 10 to 350 pCi/g in the samples tested. ^{226}Ra ranges from 79 pCi/g at a depth of 2.1 m at T5 to 294 pCi/g in silty material at T3. ^{210}Pb ranges from 82 pCi/g to 492 pCi/g for the same samples. U is present in concentrations of less than 100 ug/g and elemental Th ranges from 20 to nearly 300 ug/g.

Soil-Gas Composition

The results of the soil-gas analyses are presented in Figs. 8a, b. The profiles at each site show relatively high levels of O_2 within a metre of the ground surface. Below depths of 0.8 m at T1 and T3, and 1.3 m in the sandy material at T5, relatively constant levels of approximately 1.5% O_2 by volume are present. CO_2 levels are considerably higher than atmospheric levels at each site. The profiles tend to show an increase in CO_2 with depth. Generally levels are less than 1% CO_2 except at T3 where a maximum level of 1.1% is present at 6.5 m. N_2 levels also tend to increase with depth from less than 80% to as much as 98% by volume.

DISCUSSION

During operation of the mine, the tailings were deposited with process water containing high concentrations of calcium and sulphate with appreciable amounts of ammonium and nitrate (Blair, 1981). In the years following the Nordic Mine closure in 1968 the hydrogeologic and geochemical conditions of

the impoundment have changed dramatically. Initially a large portion of the tailings area, especially in the north eastern section, was covered with ponded water. After the ponded water was drained off in 1972, the surface of the tailings was neutralized with crushed limestone and fertilizer was applied in preparation for the growth of a grass cover. The first attempts at revegetation met with limited success but by 1978, with additional limestone and fertilizer treatments, a thick grass cover was established across the tailings impoundment.

It is reasonable to expect the geochemical conditions, as they currently exist in the tailings to reflect, in some complex manner, the combined influence of:

1) the presence of the initial process water.
2) continued infiltration of precipitation and snow-melt water.
3) surface treatments used in the revegetation program.
4) the geochemical processes and the evolution of these processes within the tailings.

In this section, an attempt will be made to provide a rational explanation of the data in light of the above factors.

Blair (1981), considering both the hydraulic gradients and the geochemical characteristics of the pore water below the water table, concluded that the original process water had been displaced to depths of greater than 7.5 m in the Nordic Main tailings. Above this depth the pore water originated as recharge water. The downward rate of groundwater flow, and hence the boundary between the original process water and the recharge water, is estimated to range from 0.5 to 1.5 m/yr (Blair, 1981). It is therefore

reasonable to conclude that, with the exception of a very shallow zone affected by the revegetation program, the chemical trends are principally the result of geochemical processes, that are spatially and temporally variable, and translocation processes, that are associated with infiltration events.

The data clearly indicate pyrite oxidation in the upper metre to be a significant process in the tailings, and further suggests that the major zone of oxidation may occur as a relatively narrow front.

The depth profiles of pyrite content indicate that the upper metre is depleted in pyrite relative to points deeper in the tailings (Figs. 8a, b). This characteristic is the result of the consumption of pyrite in the oxidation process. At T1 and T3, in fine-grained tailings, the pyrite content in the upper 0.5 m is less than 0.5% pyrite by weight; whereas, at depth of more than 1.0 m, the pyrite cotent exceeds 3%. In the sandy, coarse-grained tailings at T5 the pyrite content is approximately 5% in the upper 0.5 m, but at depths below 2.0 m, it is greater than 10%. Thus, the actual quantity of pyrite consumed in the oxidation process at this site is larger than at T1 and T3.

The concentrations of pyrite at depth in the tailings, which are an indication of the initial pyrite concentrations at the time of deposition, vary with the overall grain-size characteristics of the tailings material from site to site. The coarsest, sand-sized sediments are found at T5 in close proximity to the mouth of the tailings discharge pipe. This is also the site of the highest concentrations of pyrite, which at depths of more than 2.0 m exceed 10%. The fine-grained sediments consisting of silt and very fine sand that predominate at T1 and T3 more than 500 m from the mouth of the discharge pipe contain lower concentrations of pyrite. Below the leached

layer the pyrite content at these two sites generally ranges from 3 to 5%, although pyrite levels as high as 7% are found in some coarser sand lenses. Because pyrite is a heavy mineral with a specific gravity of 5.01, much of it, especially the coarse grained pyrite would have preferentially settled out with the coarse-grained tailings. The finer material containing lesser quantities of pyrite of a fine-grained nature would have settled further from the point of discharge.

Without continuous oxygen consumption at shallow depths diffusion would cause high levels of oxygen to exist throughout the zone above the water table. This, however, is not the case. In combination, the pyrite and soil-gas profiles (Fig. 8a, b) suggest that a pyrite-oxidation front exists in the upper 1.5 m of the tailings. This situation requires that pyrite oxidation be restricted to a particular zone. Above this zone relatively low concentrations of pyrite are expected because the oxidation process earlier in the history of the tailings resulted in significant pyrite removal. The soil gas of this upper zone should also have relatively high concentrations of oxygen since the rate of pyrite oxidation would be slow and oxygen consumption would be low. Intermediate concentrations of pyrite and an abrupt decrease in the level of oxygen would be expected across the zone where the rate of pyrite oxidation is highest. At depths below the front pyrite concentrations should be quite high and soil-oxygen levels low since only minimal pyrite oxidation should have occurred.

A pyrite-oxidation front is clearly delineated in the fine-grained sediments at T3 at a depth of 0.7 m . The oxygen levels in the soil gas decrease rapidly from more than 13% at 0.6 m to approximately 1.5% at 0.8 m. No analysis for pyrite was performed at exactly this depth; however,

analyses at 0.55 and 0.95 m indicate concentrations of 0.62 and 2.92% pyrite respectively. The zone above 0.5 m is virtually depleted in pyrite. In the silt and very fine sand at T1 an oxidation front occurs at a depth of approximately 0.5 m, although at this site the front is not as distinct as at T3. The oxygen levels decrease significantly, but at a less steep gradient, from 7.11% at a depth of 0.4 m to 1.38% at a depth of 0.8 m. Pyrite has clearly been leached from the upper 0.25 m but at a depth of 0.75 m the pyrite content is 3.46%.

In the sandy sediments at T5 oxidation appears to be occurring in a broader zone from approximately 0.3 to 1.5 m below the ground surface. Oxygen levels decrease from 9.74% to less than 2.21% through this zone and incomplete pyrite removal from the profile is apparent.

The different characteristics of the pyrite-oxidation front across the tailings reflect variations in the pattern of oxygen diffusion from site to site. The diffusion coefficient for a gas in partially-saturated porous media is dependent upon the water content and porosity of the media (Millington, 1959; Currie, 1970; Lai et al., 1976) and the rate of consumption of the gas by biological and chemical processes (Papendick and Runkles, 1965).

Currie (1970) presented a general equation for the determination of the diffusion coefficient of a gas in a wet sand; however, Lai et al., (1976) indicate that, because of heterogeneities and complicated pore geometry in soils it is necessary to empirically determine the diffusion coefficient of a gas in a partially-saturated soil for specific conditions. Both studies neglect the consumption of gas in inorganic or biologically mediated geochemical processes. The equation of Currie (1970) is

$$D/D_0 = (Ea/E) * (E)^{3/2} \qquad (1.6)$$

where D is the diffusion coefficient of gas in soil, Do is the diffusion coefficient of gas in the atmosphere, Ea is the gas filled porosity and E is the total porosity. This equation was used with the data from the upper metre to give an indication of the variability of the diffusion coefficient of oxygen in the tailings from site to site. The results are listed in Table 4. At T3, where the sharpest oxidation front exists, the tailings within the upper metre are more than 75% saturated and the oxygen-diffusion coefficient was calculated to be less than 0.01% of that in air. At T1 the tailings of the upper 0.4 m are more than 80% saturated, but below this depth a drier zone with a 25% degree of saturation exists. The oxygen-diffusion coefficient in the tailings at this site was determined to be approximately 1.7% that in air. At T5 the upper metre is relatively dry compared to the other two sites and has a degree of saturation of less than 30%. The diffusion coefficient for oxygen in the tailings at this site was calculated to be approximately 12% of that in air. Thus, at T5, where the void space is predominantly filled with air, oxygen diffusion is more rapid and occurs to a greater depth; however, at T3 and T1 the void space is predominantly filled with water and oxygen diffusion into the ground is somewhat restricted.

The grain-size characteristics of the tailings material, and hence the pyrite, influences the development of the pyrite-oxidation front at each of the three sites. Caruccio (1975) indicated that fine-grained pyrite is more reactive than coarser grained pyrite. In the silty sediments at T3 the pyrite has been almost totally consumed by oxidation above the pyrite-oxidation front. In addition, oxygen does not diffuse below the depth of the front because it is being almost completely used up in the oxidation of the more

reactive pyrite. At T1, where slightly coarser sediments and pyrite exists, the pyrite is somewhat less reactive than at T3. Nearly all the pyrite is being consumed by oxidation; however, due to the lower reactivity of the pyrite and the higher diffusion coefficient of oxygen, some oxygen diffuses marginally beyond the primary zone of oxidation. The resultant pyrite-oxidation front is not as clearly defined as at T3. In the sandy material at T5 the pyrite-oxidation front encompasses a broad zone. The coarse-grained pyrite is not being totally consumed in the oxidation process because it is not as reactive as the finer pyrite at T3 and T1. Additionally, the rate of oxygen diffusion into the tailings is considerably higher at this site. These factors combine to create a wider oxidation front and result in the oxidation of larger quantities of pyrite.

The peak concentrations of the products of pyrite oxidation; iron, sulphate and hydrogen ion, (Figs. 5a, b; 6a-f; 7a-e) in the pore waters of the zone above the water table are found at or just below the depths of active pyrite oxidation as delineated by pyrite-content and soil-gas data. Thus, it is apparent that pyrite oxidation within the upper metre exerts a major influence in determining the characteristics of the pore waters at these depths.

Below the zone of active pyrite oxidation, the soil-gas apparently has oxygen levels of approximately 1.5%. The rate of pyrite oxidation at such concentrations of oxygen has not been discussed in detail in the available literature, although some pyrite oxidation should occur at such levels of oxygen, especially in the presence of T.ferroxidaans (J. Scharer, pers. comm.). The analytical value of 1.5% may represent an actual concentration of 0% O_2 because of consistent methodological errors in sample collection

and analysis. This could be the case because it appears that the oxidation of pyrite is inhibited at depths below the oxidation front.

Pyrite oxidation occurring at shallow depths, combined with the translocation of reaction products by infiltration water, appear to be the major controls on the observed characteristics of pore-water chemistry in the tailings. Some general geochemical characteristics are pervasive throughout the tailings. The August profiles of pore-water chemistry show major concentration peaks of iron and sulphate (Figs. 6a, b, c) within 2.0 m of the surface of the tailings and within 1.0m of the water table. No smaller peaks are apparent between these two peaks. The May profiles (Figs. 7a, b, d) also show a significant peak above the water table but the upper peak is found somewhat deeper than in August. Due to the large fluctuations in the water table at T1 seasonal comparisons of the profiles are obscured; however, at T3 the upper peak has been displaced downward by approximately 0.5 m and at T5 this displacement is approximately 1.2 m.

Using an assumed infiltration volume of 0.305 m (12 in) and approximate water contents of 55% at T3 and 20% at T5 the anticipated peak displacements at each site are approximately 0.55 m (21.8 in) and 1.5 m (60 in) respectively. The infiltration volume is based upon a mean annual precipitation of approximately 0.813 m (32 in) less a mean annual actual evapotranspiration of approximately 0.51 m (20 in) (Chapman and Thomas, 1968). This calculation does not account for surface runoff, which should be quite small on the relatively flat surface of the tailings. An infiltration volume of this size provides displacements similar to those observed in the geochemical profiles between the August and May sampling periods.

Because there are no smaller concentration peaks in the segments of the August profiles between the upper peak and the one immediately above the water table, it is reasonable to assume that the translocation of the products of pyrite oxidation to points deeper in the profile did not occur during the rainfall events in the summer months prior to August. The downward displacement of the upper peak in the May profile indicates that the chemical constituents were transported by recharge events between the two sampling periods. Some infiltration would likely accompany the fall rains, which occur in a season of low evapotranspiration, but most of the infiltration would occur following the winter snowmelt. The downward displacement of the upper peak is accompanied by spreading of the peak as a result of dispersion.

The concentration peaks in pore water near the surface and above the water table represent the successive annual generations of the reaction products of pyrite oxidation. The high-TDS water immediately above the water table in the August profiles is assumed to represent the products of the previous year's production within the upper metre of the tailings, which was subsequently transported to the water table by the spring recharge. The downward displacement of the upper peak in the May profiles in relation to those of the previous August represents an intermediate stage in this process.

The process of pyrite oxidation would likely be most significant in the late spring, summer and fall seasons when the temperature of the shallow soil zone is high enough to permit rapid rates of pyrite oxidation. The optimal temperature range for the oxidation of sulphide minerals is between 25^0C and 45^0C; however, active bacterial iron oxidation has been noted in soils at 10^0C (Lundgren and Silver, 1980). In the winter months, depending

upon the thickness of snow cover, the upper metre of soil would normally be penetrated by frost. Lundgren and Silver (1980) indicate that 0^0C is generally accepted as the lower limit of the activity of iron-oxidizing bacteria. Thus, it is unlikely that significant pyrite oxidation would occur within the upper metre of the tailings during the winter months. Below the depth to which the soil freezes pyrite oxidation would also be minimal because the influx of oxygen to the system would be small. Throughout the winter the high-TDS water produced during the previous summer and fall would remain near the surface of the tailings. The chemical constituents would not move deeper into the system until they were transported downward with the pulse associated with the spring recharge. Following this a new season's production of high-TDS water within the upper metre would begin as conditions favourable for pyrite oxidation develop.

Pyrite oxidation at shallow depths and translocation will, of course, not account for all of the observed trends. The geochemical processes that alter the pore water chemistry as infiltration transports reaction products downward towards the water table will now be considered.

With the exception of the May pH profile at T5, all the pH profiles (Figs. 5a, b) exhibit low-pH conditions within the upper metre and increasing pH with depth. The consumption of hydrogen ions is a major process below the shallow zone in which pyrite oxidation is very active. This consumption may occur as a result of the dissolution of the following solid phases: calcite, dolomite, iron hydroxides, aluminum hydroxide, and aluminosilicate minerals such as feldspar.

The presence of even small amounts of calcite would contribute significantly to the neutralization capacity of the tailings. The consumption

of hydrogen ions in the reaction of low-pH water with calcite can be represented by the equation

$$CaCO_3 + 2H^+ \langle==\rangle Ca^{2+} + H_2CO_3^0(aq) \qquad (1.7)$$

Calcite and other carbonate minerals were present in the lime and limestone used in the neutralization of the tailings slurry prior to its discharge. It is reasonable to assume that some carbonate material should still be present. The results of the analyses for carbonate in the solid phase indicate that carbonate concentrations in the upper half metre throughout the tailings are below the detection limit of 0.001% $CaCO_3$ by weight. At T1, 0.8 m below the surface of the tailings, 0.0024% carbonate exists. At T3, the analyses gave results ranging from 0.0015% at a depth of 1.4 m to 0.011% at 4.6 m. At T5, where low pH conditions predominate throughout the profile, no detectable carbonate is present.

The potential consumption of hydrogen ions by very small quantities of carbonate is illustrated below. If the porosity of the tailings is assumed to be 50% and the specific gravity of the sediments is 2.75, then a cell of 1 m^3 within the tailings would contain 500 L of water and 1.375×10^6 g of tailings material. A carbonate content of 0.002% would mean that the solid material of the cell contains 2.75×10^3 g (2.75×10 moles) of $CaCO_3$; and one of 0.01% would yield 1.375×10^4 g (1.274×10^2 moles). From equation 1.7 it is apparent that two moles of H^+ ions are consumed with each mole of $CaCO_3$. If the pH of the pore water in the tailings is considered to be 2, then 5 moles of H^+ ions are present in the cell. Therefore, with a carbonate content of 0.002%, one cubic metre of tailings has the potential to neutralize 11 cell volumes of pore water but, with a carbonate content of 0.01%, 55 cell volume of pore water could be neutralized.

The high concentrations of iron in the pore water throughout the tailings make the collection of solid-phase samples for the purpose of the carbonate analyses difficult. Following sample collection and exposure to air ferrous ion in the pore water is oxidized and precipitated as ferric hydroxide ($Fe(OH)_3$). This process releases hydrogen ions to solution which consume carboante according to equation 1.7. To alleviate this problem the samples were flushed with distilled water in a centrifuge immediately following collection in an attempt to remove the iron-rich pore water. Any ferrous ion that remained in the sample following the flushing procedure would serve to consume carbonate. The results obtained from the analytical procedure are, therefore, considered to be conservative estimates.

The results of the carbonate analyses are expressed as weight % $CaCO_3$. This, however, does not mean that other carbonate minerals such as siderite ($FeCO_3$) are not present in the tailings. They, too, could cause hydrogen ion consumption upon dissolution; however, if the carbonate mineral phase present is siderite rather than calcite, there would be less tendency for dissolution because ferrous ion concentrations are so high. The results also do not indicate the form of the carbonate minerals. They may have surface coatings of such minerals as gypsum which would inhibit dissolution.

Support for the hypothesis that carbonate-mineral dissolution plays an important role in the consumption of hydrogen ions in the pore water in the tailings is provided by the high partial pressures of carbon dioxide in the soil gas. The generation of carbon dioxide is released following the dissolution of carbonate minerals (equation 1.7) by degassing from the neutral species, $H_2CO_3^0(aq)$ which can be represented as

$$H_2CO_3^0(aq) \text{ <==> } H_2O + CO_2(g) \qquad (1.8)$$

The soil-gas profiles are characterized by increasing levels of carbon dioxide with depth ranging from a low of 0.2% ($10^{-2.7}$ atm.) in the upper 0.5 m at T5 to a high of 1.17% ($10^{-1.95}$ atm) immediately above the water table at T3. These profiles in the tailings resemble those recorded by Reardon et al. (1979) in a natural sandy soil where the development of such profiles was attributed to the upward diffusion of carbon dioxide from the shallowest portions of the saturated zone. In the Nordic Main tailings the elevated pCO_2 values in the zone above the water table are a result of the dissolution of carbonate in this zone or dissolution of carbonate immediately below the water table and the subsequent diffusion of carbon dioxide upwards towards the surface of the tailings. The production of carbon dioxide in the root zone by microbial activity appears to be of minor importance in the tailings since carbon dioxide levels are lowest within the upper metre of tailings.

In low-pH waters the dissolution of amorphous aluminum hydroxide ($Al(OH)_3$) and ferric hydroxide ($Fe(OH)_3$) can increase pH by consuming hydrogen ions. The reactions of the dissolution processes and the respective equilibrium constants are

$$Al(OH)_3 \text{ <==> } Al^{3+} + 3OH^-, \quad k=10^{-32} \tag{1.9}$$

$$Fe(OH)_3 \text{ <==> } Fe^{3+} + 3OH^-, \quad k=10^{-37} \tag{1.10}$$

Both of these amorphous compounds are expected to exist in the tailings becuase, in the milling process, high concentrations of iron and aluminum were present during acid leaching. Because of neutralization of the mill wastes to a pH of 8 with lime and limestone, these compounds would have precipitated following the discharge of the slurry to the tailings

impoundment. WATEQ2 results indicate that the pore waters throughout the zone above the water table are presently undersaturated with respect to amorphous aluminum and ferric hydroxide. Thus, the dissolution of these compounds may contribute to the rise in pH with depth.

The dissolution of aluminosilicates can also consume hydrogen ions, thereby increasing pH. The dissolution of a feldspar such as albite can be represented as

$$H^+ + NaAlSi_3O_8 + H_2O \text{ <==> } Al(OH)_3 + Na^+ + 3H_4SiO_4 \qquad (1.11)$$

The rate at which such reactions occur within the tailings is not known. High concentrations of Al and Si in the low-pH pore waters indicate that the dissolution of aluminosilicate minerals may be contributing to the rise in pH with depth in the pore waters of the zone above the water table.

The profiles for Mn, Co, Cu, Ni and Zn (Figs. 6a, c, f; 7a, c, e) generally mirror those of iron and sulphate, although the concentration peak within the upper 1.5 m is much less prominent. This seems reasonable because many of the metals occur as impurities in pyrite and would be released to the pore water as the pyrite is oxidized. Accessory sulphide minerals such as pyrrhotite, chalcopyrite, arsenopyrite, galena and cobaltite, which occur in the ore (Robertson, 1968), are also subject to oxidation in the tailings and therefore are expected to contribute heavy metals to the system. The metals would be distributed through the system by major infiltration events with the same trends as iron and sulphate.

The dissolution of aluminosilicate minerals in low-pH waters release aluminum and silicon into solution. An additional source of aluminum is the dissolution of amorphous aluminum hydroxides. Both aluminum and silicon

are present in high concentrations. According to the WATEQ2 results (Table 2) the pore water is saturated with respect to silica gel (SiO_2), supersaturated with respect to gibbsite ($Al(OH)_3$) and undersaturated with respect to amorphous aluminum hydroxide. At T3, where the pH increases from 2.0 at a depth of 1.0 m to above 4.0 at 3.0 m, the aluminum and silicon profiles show concentration peaks at approximately 1.5 m below the surface and much lower concentrations at depths below 3.0 m in both the August and May profiles. Because no peak exists above the water table, and because the trends are the inverse of the trend in pH, it appears likely that an aluminosilicate mineral phase is acting as a solubility constraint on aluminum and silicon at the higher pH levels. Lindsay (1979) suggests that kaolinite and Mg-montmorillonite can depress the activity of Al^{3+} below the gibbsite-solubility limit when levels of silicic acid are controlled by amorphous silica gel. WATEQ2 calculations indicate that the pore waters are not saturated with respect to either kaolinite or Mg-montmorillonite so they do not appear to be acting as a solubility constraint in this case.

At T5, both the August and May profiles show a silicon concentration peak at a depth of approximately 2.0 m, where aluminum concentrations are low, and an aluminum concentration peak at depths from 2.0 m to 3.0 m, where silicon concentrations are somewhat depressed. The pH conditions at T5 are low throughout the profile; ranging from 1.4 to just over 3 in August and are consistently lower than 2.0 in May. Supersaturation with respect to gibbsite and saturation with respect to silica gel exist at all depths but other solubility controls are not indicated by WATEQ2 results.

The dissolution of aluminosilicate minerals in low-pH water also releases sodium, potassium and magnesium to the pore water. Fertilizers applied to

the surface of the tailings in conjunction with the revegetation program may release additional quantities of these ions into solution. The profiles of these elements show minor concentration peaks near the surface and a general increase in concentration with depth.

The concentration of calcium is relatively constant in the pore water throughout the zone above the water table, ranging from 400 to 600 mg/L. The calcium is present as a result of the dissolution of carbonate material, mainly limestone and lime, used in the post-milling neutralization process and, at the time of its release to the tailings impoundment, the discharge water was probably saturated with respect to gypsum. At present, as indicated by WATEQ2 results, the pore-water is saturated or near-saturated with respect to gypsum which acts as a solubility constraint on the amount of calcium present in solution. The concentration of sulphate ion throughout the zone above the water table varies from about 200 mg/L to more than 20000 mg/L but, because sulphate complexes with other aqueous species such as ferrous and calcium ion, the activity of sulphate is not nearly as variable. Only small contributions of calcium are made to the water in the tailings by the dissolution of carbonate, so the pore water remains at or close to saturation with respect to gypsum with relatively constant concentrations of calcium.

The chloride concentrations typically range from 5 to 40 mg/L, although elevated values of 150 mg/L are found in the May profile at T5. Chloride, which was present in concentrations of approximately 10 mg/L in the effluent originally discharged to the tailings impoundment (Moffett, 1976), is probably released from fertilizers. At T5 chrloride may also be derived from sewage sludge that has been applied to the surface of the tailings.

The role of differing grain-size and soil-moisture characteristics between sites was discussed in conjunction with the process of pyrite oxidation. The profiles of pore-water geochemistry, though, do not appear to be influenced by the heterogeneity that exists between layers at each particular site. The profiles of mean grain size and degree of saturation versus depth indicate that the physical characteristics of different layers are quite variable. This variability is not reflected by changes in the trends of the profiles of pore-water geochemistry at the corresponding depths. The general trend of two major concentration peaks, one within the upper two metres and another above the water table, with a low-concentration, intermediate zone in the pore-water profiles is not disrupted by the layered nature of the tailings.

The occurrence of radionuclides in the solid phase will be considered briefly. The highest concentrations of radionuclides are generally associated with fine-grained sediments at T3. The lowest concentrations are found in sandy material at T5. An estimate of the original radionuclide concentrations in the tailings at their time of deposition is provided by Moffett and Tellier (1978). They estimate that the concentration of uranium was approximately 36 ug/g and that of thorium was about 170 ug/g. The samples analyzed in this study generally have uranium and thorium concentrations that exceed the estimated initial concentrations. Radium-226 concentrations, however, are consistently lower than the 344 pCi/g predicted for the original tailings by Moffett and Tellier (1978). The measured concentrations of lead-210 are also consistently lower than the levels predicted, except for two samples from fine-grained sediments at T3.

The estimate of radionuclide concentrations in the tailings at the time of their deposition (Moffett and Tellier, 1978) is based upon radionuclide levels

encountered in the milling circuit. They did not attempt to account for the preferential association of radionuclides with fine-grained sediments; thus, the observed radionuclide concentrations at T3 may be reasonable. One general trend that is apparent from the estimated original composition and the concentrations measured in this study is that radium-226 levels are much lower than predicted. Because the half-life of radium-226 is more than 1600 years, the lower concentrations cannot be explained by radioactive decay but, rather, must be attributed to leaching of radium-226 by the low-pH waters that have developed in the tailings.

SUMMARY AND CONCLUSIONS

The sediments of the Nordic Main tailings impoundment vary from fine sand to silt and are typically deposited in thin layers. The depth to water table is about 1 m along the northern boundary and greater than 7.0 m at the tailings dam along the southern boundary of the impoundment. The water content of the tailings in the zone above the water table ranges from approximately 10% in the coarsest sand to more than 60% in the silt-rich lenses.

Pyrite oxidation in the zone above the water table is responsible for the generation of a low-pH water with high concentrations of iron and sulphate characteristic of the shallow groundwater zone in the Nordic Main tailings. Measurements of the pyrite content with depth in the tailings indicate that pyrite is depleted within the upper metre relative to that at points deeper in the profile. In silt and very fine sand at T3 and T1, almost complete pyrite consumption within the upper metre has occurred, but pyrite is still present at greater depths in concentrations that range from 3 to 7% by weight. In

sandy material at T5, where pyrite is more abundant, concentrations of approximately 5% exist within the upper metre, but those at depth are as high as 15%. Significant decreases in oxygen levels in the soil from in excess of 10% by volume to constant levels of approximately 1.5% delineate the zones of most active pyrite oxidation. In the finest and generally wettest sediments at T3, oxygen diffusion is restricted and the zone of active pyrite oxidation occurs as a sharp front at a depth of 0.7 m. At T1, in coarser silt and very fine sand, conditions are slightly drier and the pyrite-oxidation front occurs in a zone from 0.4 to 0.7 m. In the drier and sandy material at T5, oxygen diffusion is rapid and the pyrite-oxidation front encompasses a broad zone from about 0.5 to 1.5 m.

Pyrite oxidation at shallow depths in the tailings and the subsequent transport of the reaction products downward towards the water table with infiltration water play the major role in the development of the observed chemical characteristics of the pore water. The August profiles of iron and sulphate indicate the presence of two concentration peaks, one within 2.0 m of the surface of the tailings and another within a metre of the water table. The May profiles also show two peaks, but the upper peak is between 0.5 and 1.0 m deeper in the profile compared with that of August. This downward displacement can be attributed to translocation of the chemical constituents with the infiltration water associated with the spring snowmelt.

The pH of the pore water is generally lowest at a depth of about 1.0 m and increases with depth. An exception to this occurs in May at T5 where, in the coarse sandy material with pyrite concentrations in excess of 5%, the pH is lower than 2 at all points above the water table. The increases in pH reflect consumption of hydrogen ions with depth and can be attributed to the

dissolution of calcite and dolomite, amorphous aluminum and ferric hydroxides; or aluminosilicates such as feldspar. Analyses show that minor amounts of carbonate, ranging from less than 0.001% $CaCO_3$ by weight to 0.011%, are present in the zone above the water table. Elevated values of CO_2 in the soil gas as high as 1% by volume are evidence that CO_2 gas is being exsolved in the carbonate dissolution process.

The profiles of the metals (Mn, Co, Ni, Cu and Zn) in the pore waters of the zone above the water table show the same general trends as those exhibited by iron and sulphate, although the concentrations are much lower. These metals occur as impurities in pyrite or in other sulphide minerals associated with the ore and are released to the pore water following oxidation.

High concentrations of aluminum and silicon are present in the pore water as a result of the dissolution of aluminosilicate minerals and amorphous aluminum hydroxides. The trends in the profiles are similar to those of iron and sulphate, except above pH levels of 3.5 to 4, silicon and aluminum concentrations decrease significantly. The pore waters are saturated with respect to gibbsite and silica gel throughout the zone above the water table.

Na, K and Mg are also released to the pore water in the process of aluminosilicate dissolution. The concentration of these elements generally increase slightly with depth. The dissolution of fertilizers, applied to the surface of the tailings in conjunction with the vegetative program adds Na, K, Mg and Cl to the pore water. Ca concentrations consistently range from 400 to 600 mg/L throughout the tailings. It is present in the water in the tailings because of the use of lime and limestone as neutralization agents in

the mill waters. The pore water is saturated with respect to gypsum throughout the tailings which acts as a solubility constraint on the amount of Ca in solution.

Because of a lack of detailed information about concentrations of radionuclides in the solid phase in the tailings at their time of deposition, the degree of leaching of uranium and thorium from the tailings is unclear. It is apparent, however, that significant radium-226 leaching has occurred in the Nordic Main tailings since mining operations ceased in 1968.

List of Tables in Chapter 1

1.1 General soil profiles at T1, T3 and T5

1.2 Log S.I. values for selected mineral phase in pore-water samples collected in August, 1980 and May, 1981 as calculated by WATEQ2.

1.3 Radionuclide concentrations in solid-phase samples.

1.4 Calculations of gas-diffusion coefficients in the sediments at T, T3 and T5 relative to the diffusion coefficient of a gas in air (after Currie, 1970).

List of Figures in Chapter 1

Figure

1.1 The nordic Main and other tailings impoundments in the Elliot Lake uranium mining district.

1.2 Location map of the Nordic tailings showing the monitored sites.

1.3 Diagrammatic representation of the squeezing apparatus and stand.

1.4a Volumetric moisture content, degree of saturation, mean grain size and bulk density profiles at T1 and T5.

1.4b Volumetric moisture content, degree of saturation mean grain size and bulk density profiles at T3.

1.5a August profiles of pH and electrical conductance at T1, T3 and T5. pH levels below the water table are included.

1.5b May profiles of pH and electrical conductance at T1, T3 and T5.

1.6a Pore-water geochemistry at T1 in August, 1980.

1.6b Pore-water geochemistry at T3 in August, 1980 (SO_4, Fe(total), Na, K, Mg, Ca).

1.6c Pore-water geochemistry at T3 in August, 1980 (Al, Si, Mn, Co, Cu, Ni, Zn).

1.6d Pore-water geochemistry at T3 in August, 1980 (Cl, Br).

1.6e Pore-water geochemistry at T5 in August, 1980

(SO_4, Fe(total), Mg, K, Na, Ca, Al, Si).

1.6f Pore-water geochemistry at T5 in August, 1980 (Mn, Co, Cu, Ni, Zn, Cl).

1.7a Pore-water geochemistry at T1 in May, 1981.

1.7b Pore-water geochemistry at T3 in May, 1981 (SO_4, Fe(total), Na, K, Mg, Ca, Al, Si, Cl).

1.7c Pore-water geochemistry at T3 in May, 1981 (Mn, Co, Cu, Ni, Zn).

1.7d Pore-water geochemistry at T5 in May, 1981 (SO_4, Fe(total), Na, K, Mg, Ca, Al, Si).

1.7e Pore-water geochemistry at T5 in May, 1981 (Mn, Co, Cu, Ni, Zn, Cl).

1.8a Soil-gas composition and solid-phase geochemistry profiles at T1 and T5.

1.8b Soil-gas composition and solid-phase geochemistry profiles at T3.

Tables in Chapter 1

TABLE 11: GENERAL SOIL PROFILES AT T1, T3 and T5. COLOURS ARE CODED ACCORDING TO MUNSELL SOIL CHARTS

Depth(m)	Description
T1 0.1	- pale yellow (5Y8/3), clay-like
	- yellow (2.5Y7/6) and red (2.5Y3/6) mottles.
0.35	- pale yellow (5Y8/3), clay-like
	- yellow-red (5Y5/8) and yellow (10YR7/6) vertical fractures
0.60	- light grey (5Y7/1), silty sand
0.85	- grey (5Y6/1), fine sand
1.10	- grey (5Y5/1), clay-like
1.35	- dark grey (5Y4/1), clay-like
1.60	- dark grey (5Y4/1), clay-like
1.85	- very dark grey (5Y3/1), clay-like
2.10	- dark grey (5Y4/1), silty sand
2.35	- dark grey (5Y4/1), silty sand

Depth(m)	Description
T3 0.1	- pale yellow (5Y8/3), clay-like
	- brown (10YR6/8) and yellow (2.5Y8/8) mottles.
0.35	- yellow (5Y8/3), clay-like
	- yellow-red (5YR4/8) vertical fracture
0.60	- pale yellow (5Y8/3), clay-like
	- yellow (10YR8/8) and brown (7.5 YR5/8) mottles
0.85	- dullwhite (5Y8/2), clay-like
1.10	- grey (5Y6/1), silty clay
1.35	- olive brown (2.5Y5/6), clay-like
1.60	- grey (5Y4/2), clay-like
1.85	- grey (5Y4/3), clay-like
2.10	- grey (5Y6/2), fine sand
2.35	- grey (5Y5/2), silt
2.60	- grey (5Y6/2), fine sand
2.85	- grey (5Y5/2), fine sand
3.10	- grey (5Y5/1), sandy silt
3.35	- grey (5Y6/1), fine sand
3.60	- grey (5Y5/1), clay-like
4.60	- grey (5Y5/1), clay-like
4.85	- grey (5Y5/1), sand
5.10	- grey (5Y6/1), fine sand
5.35	- grey (5Y6/1), fine sand
5.60	- grey (5Y4/1), clay-like

Depth(m)	Description
T5 0.1	- pale yellow (5Y8/4), fine sand
0.35	- light grey (5Y7/2), fine sand
0.60	- light grey (5Y7/2), fine sand
	- grey (5Y4/1) fracture traces
0.85	- grey (5Y6/1), fine sand
1.10	- light grey (5Y7/2), fine sand
	- grey (5Y4/1) fracture traces
1.35	- grey (5Y6/1) fine sand
1.60	- grey (5Y5/1) fine sand
2.35	- grey (5Y5/1) fine sand
2.60	- grey (5Y5/1) silty sand
3.35	- dark grey (5Y4/1), silty sand
3.60	- dark grey (5Y4/1) silty sand.

TABLE12: LOG S.I. VALUES FOR SELECTED MINERAL PHASES IN PORE-WATER SAMPLES COLLECTED IN AUGUST, 1980 AS CALCULATED BY WATEQ2

SAMPLE	DEPTH(m)	LOG S.I. GYPSUM ($CaSO_4 \cdot 2H_2O$)	Al(OH)3 amph	SILICA GEL (SiO_2 amph)	GIBBSITE (Al(OH)3)
T 1-4	0.8	0.058	-5.723	0.540	38.357
1-7	1.4	0.058	-3.726	0.484	40.355
1-10	2.0	0.050	-4.115	0.424	39.965
1-12	2.4	0.080	-3.97	0.497	40.111
T 3-5	1.0	-0.041	-9.251	0.659	34.829
3-6	1.2	0.106	-7.264	0.742	36.816
3-10	2.0	0.040	-4.209	0.409	39.872
3-13	2.4	0.047	-4.441	0.349	39.639
3-16	2.6	0.093	-4.014	0.023	40.067
3-18	3.2	0.088	-4.257	0.100	39.823
3-20	3.8	0.096	-3.749	-0.181	40.331
3-22	4.2	0.139	-2.768	-0.086	41.313
3-25	4.8	0.126	-3.192	-0.038	40.889
3-28	5.4	0.183	-2.790	-0.069	41.291
T 5-5	1.0	0.123	-10.053	0.729	34.028
5-9	1.8	-0.009	-8.079	0.390	36.002
5-13	2.6	0.149	-6.307	0.776	37.773
5-15	3.0	0.287	-4.800	0.778	39.281
5-17	3.4	0.198	-3.889	0.807	40.191
5-19	3.8	0.196	-3.624	0.593	40.456

TABLE 12 (CONT): LOG S.I VALUES FOR SELECTED MINERAL PHASES IN PORE-WATER SAMPLES COLLECTED IN MAY, 1981 AS CALCULATED BY WATEQ2

SAMPLE	DEPTH(m)	LOG S.I. GYPSUM ($CaSO_4 \cdot 2H_2O$)	Al(OH)3 amph	SILICA GEL (SiO_2 amph)	GIBBSITE (Al(OH)3)
TS1-3	0.2	-0.029	-8.118	0.563	35.963
1-5	0.6	-0.040	-7.128	0.728	36.953
1-7	1.0	-0.022	-4.451	0.604	39.630
TS3-2	0.4	0.013	-7.383	0.371	36.697
3-5	1.0	-0.023	-9.091	0.431	34.989
3-8	1.6	-0.051	-4.038	0.704	40.042
3-10	2.0	-0.012	-4.282	0.596	39.799
3-13	2.6	-0.022	-3.784	0.129	40.297
3-16	3.2	-0.026	-4.326	0.119	39.754
3-18	3.6	-0.013	-5.587	0.032	38.493
3-20	4.0	-0.016	-2.585	-0.121	41.496
3-22	4.4	0.032	0.12	-0.174	44.200
3-27	5.4	0.044	0.589	-0.060	44.670
TS5-3	0.6	-0.050	-9.595	0.515	34.486
5-5	1.0	-0.162	-9.236	0.700	34.844
5-7	1.4	-0.183	-9.347	0.723	34.733
5-9	1.8	-0.047	-9.786	0.716	34.310
5-10	2.0	-0.051	-9.546	0.635	34.350
5-13	2.6	-0.028	-10.521	0.623	33.559
5-15	3.0	-0.050	-9.924	0.700	34.157

TABLE 13: RADIONUCLIDE ANALYSES OF SOLID-PHASE SAMPLES

			pCi/g					ug/g	
SAMPLE LOCATION	DEPTH(m)	MEAN GRAIN SIZE(mm)	^{228}Th	^{230}Th	^{232}Th	^{226}Ca	^{210}Pb	u	Th
T1	1.90	0.0558	36	197	79	194	193	51	62
T3	1.35	0.0354	42	388	143	183	220	45	297
	2.95	0.0608	51	336	136	293	398	104	242
	3.15	0.0384	35	372	133	131	265	68	136
	3.65	0.0442	168	740	350	294	492	54	283
T5	2.10	0.172	7	15	10	79	82	10.5	20
	2.95	0.171	17	206	85	135	128	63	225
	3.50	0.136	20	139	90	146	167	85	118

TABLE 14. CALCULATIONS OF GAS DIFFUSION COEFFICIENTS IN THE SEDIMENTS AT T1, T3 and T5 RELATIVE TO THE DIFFUSION COEFFICIENT OF A GAS AIR (AFTER CURRIE, 1970).

SITE	TOTAL POROSITY	GAS-FILLED POROSITY	D/D_o
T1	0.589	0.258	0.0166
T3	0.604	0.077	0.000124
T5	0.512	0.387	0.119

Figures in Chapter 1

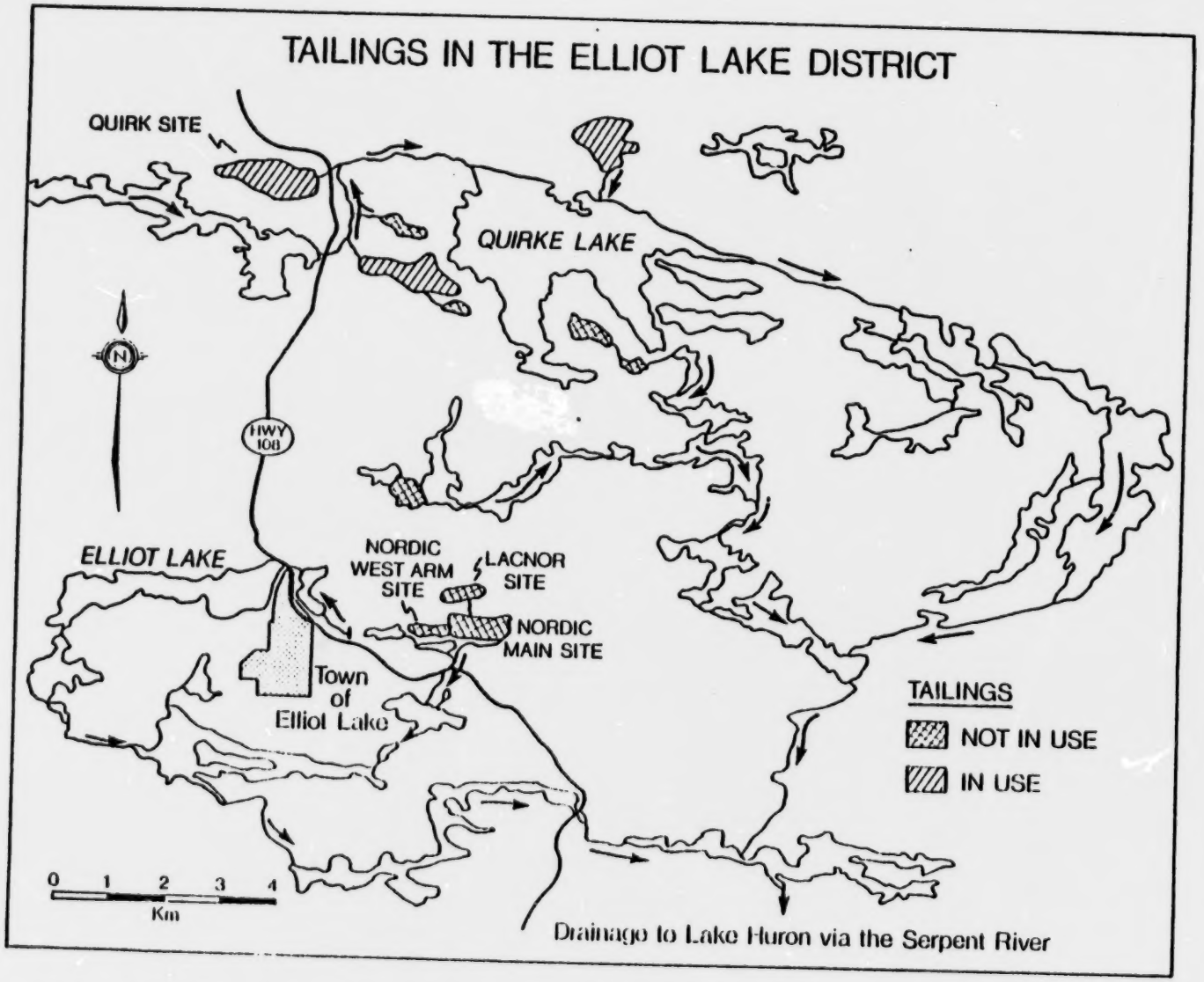

Figure 11. The Nordic Main and other tailings impoundments in the Elliot Lake uranium mining district.

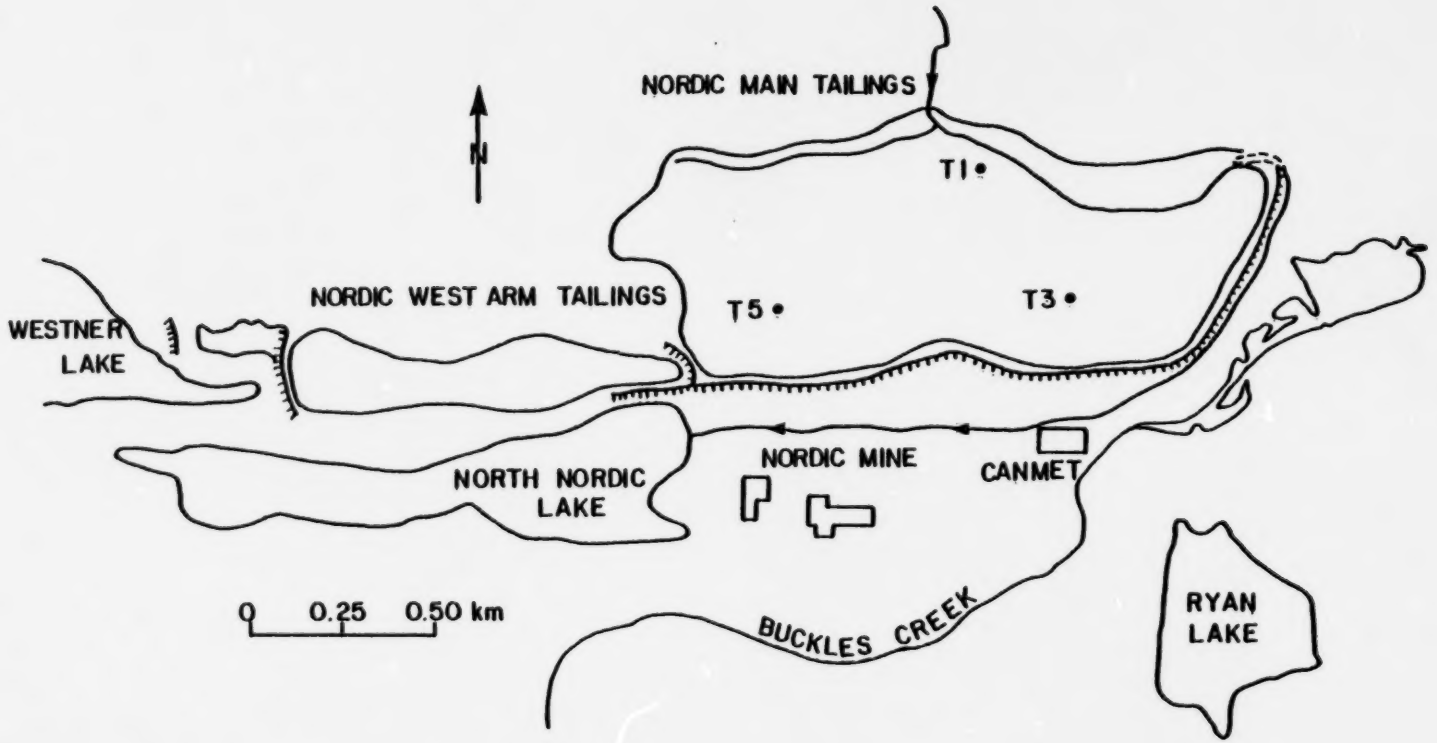

Figure 1.2 Location map of the Nordic tailings showing the monitored sites.

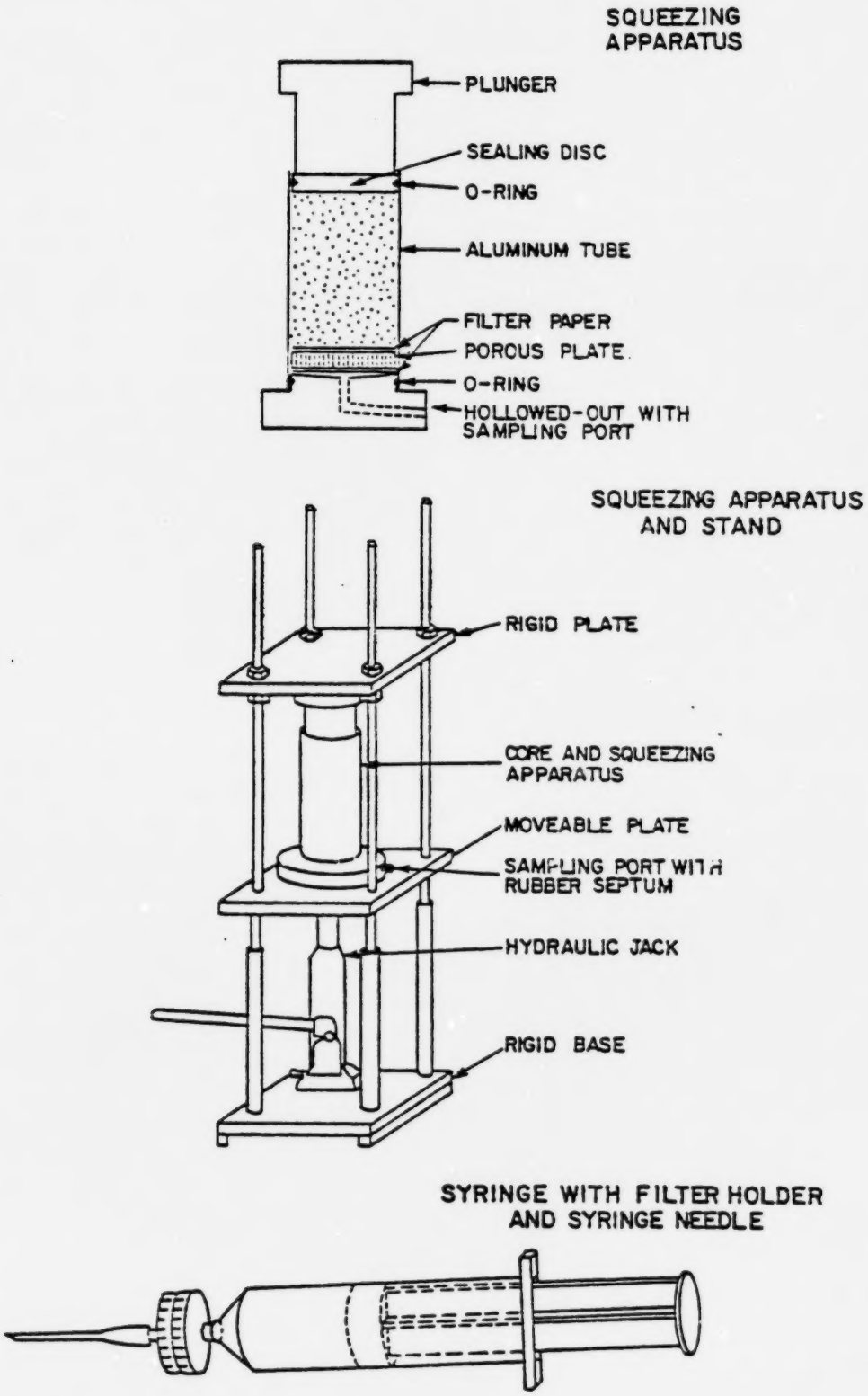

Figure 13. Diagrammatic representation of the squeezing apparatus and stand.

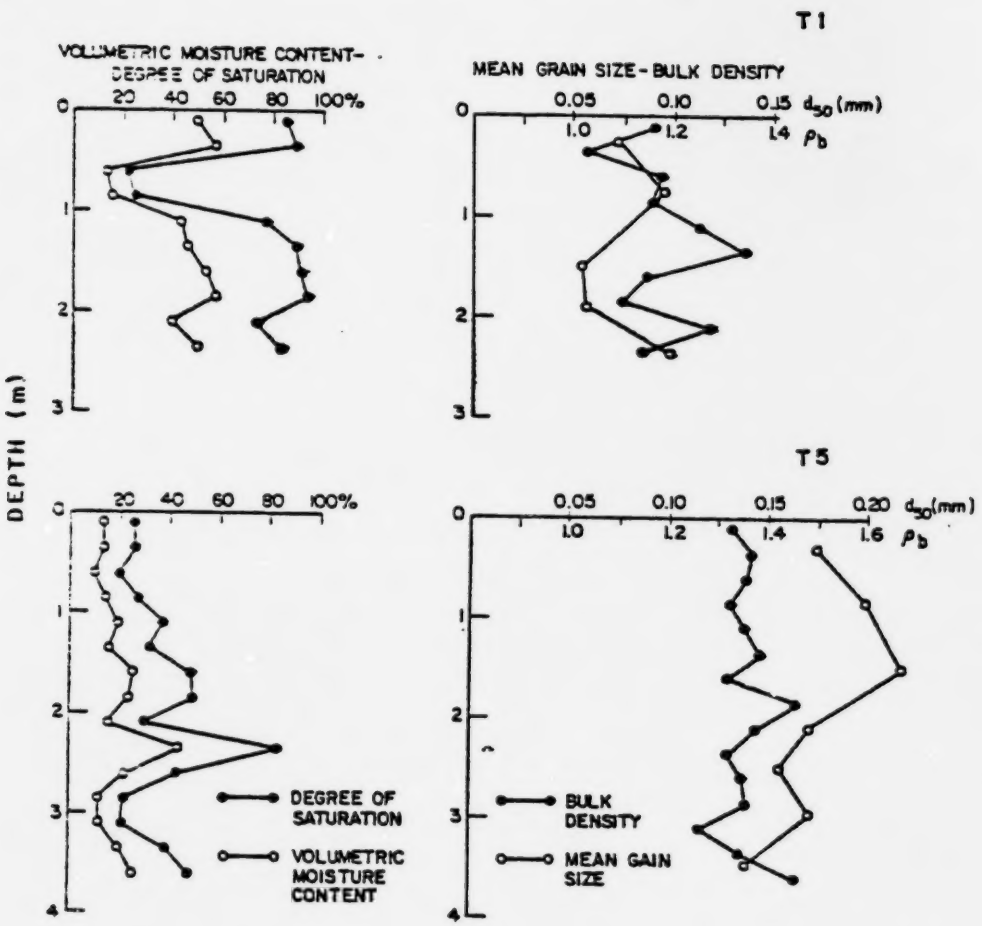

Figure14a. Volumetric moisture content, degree of saturation, mean grain size and bulk density profiles at T1 and T5.

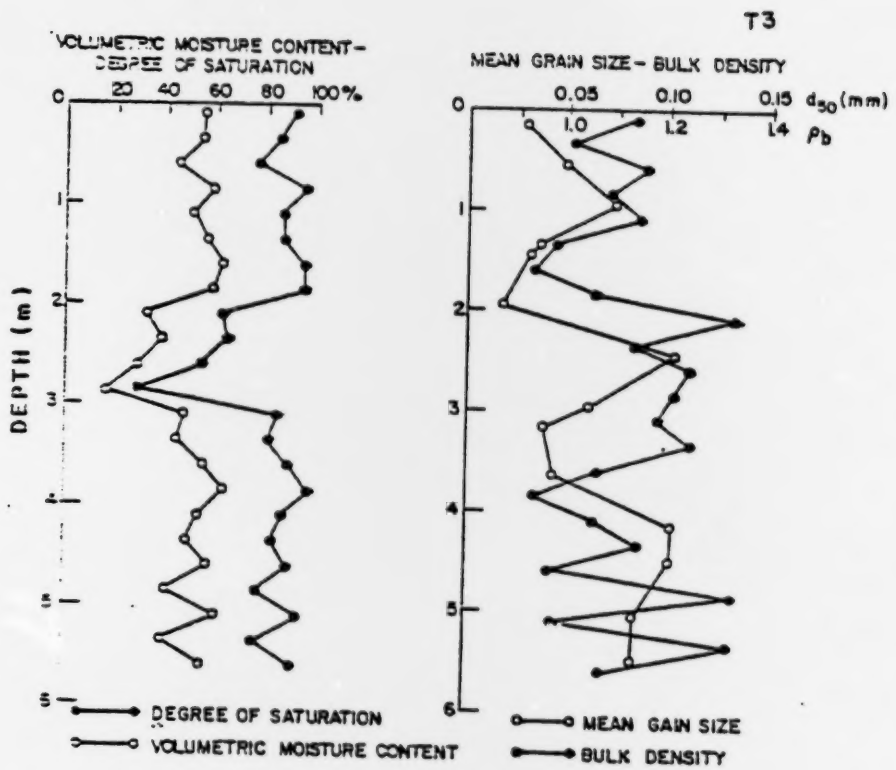

Figure 4b. Volumetric moisture content, degree of saturation, mean grain size and bulk density profiles at T3.

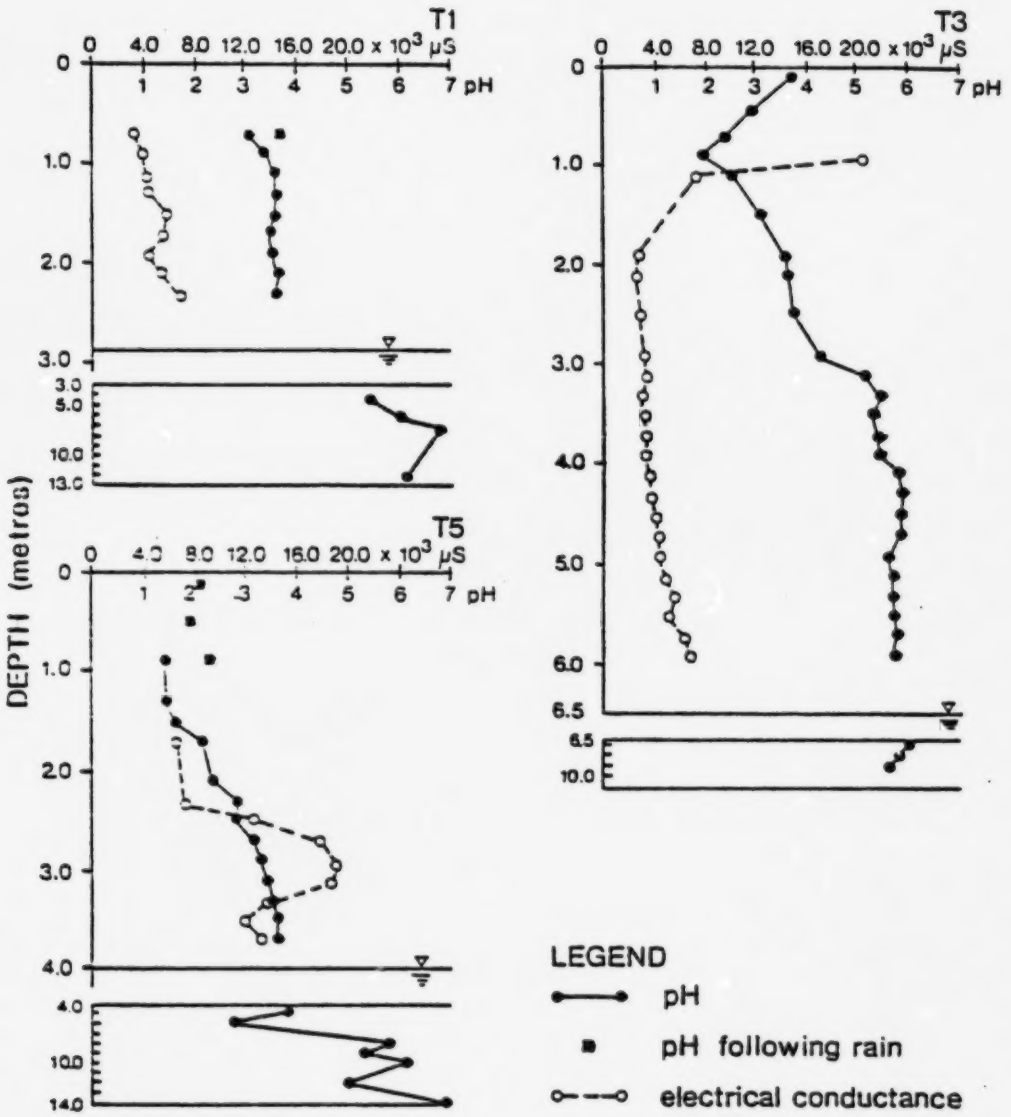

Figure15a. August profiles of pH and electrical conductance at T1, T3 and T5. pH levels below the water table are included.

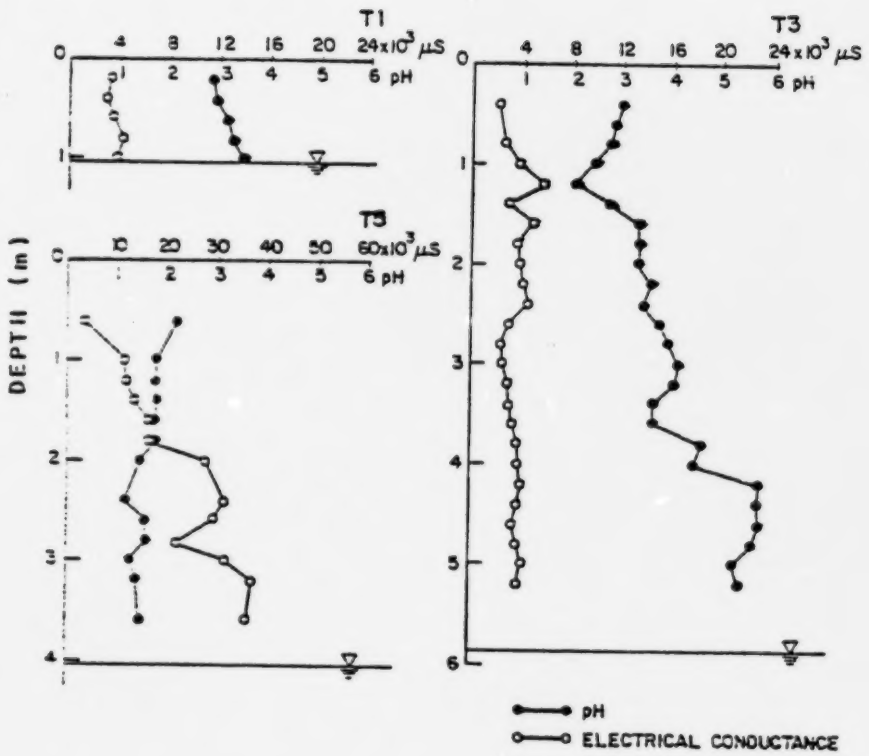

Figure 5b. May profiles of pH and electrical conductance at T1, T3 and T5.

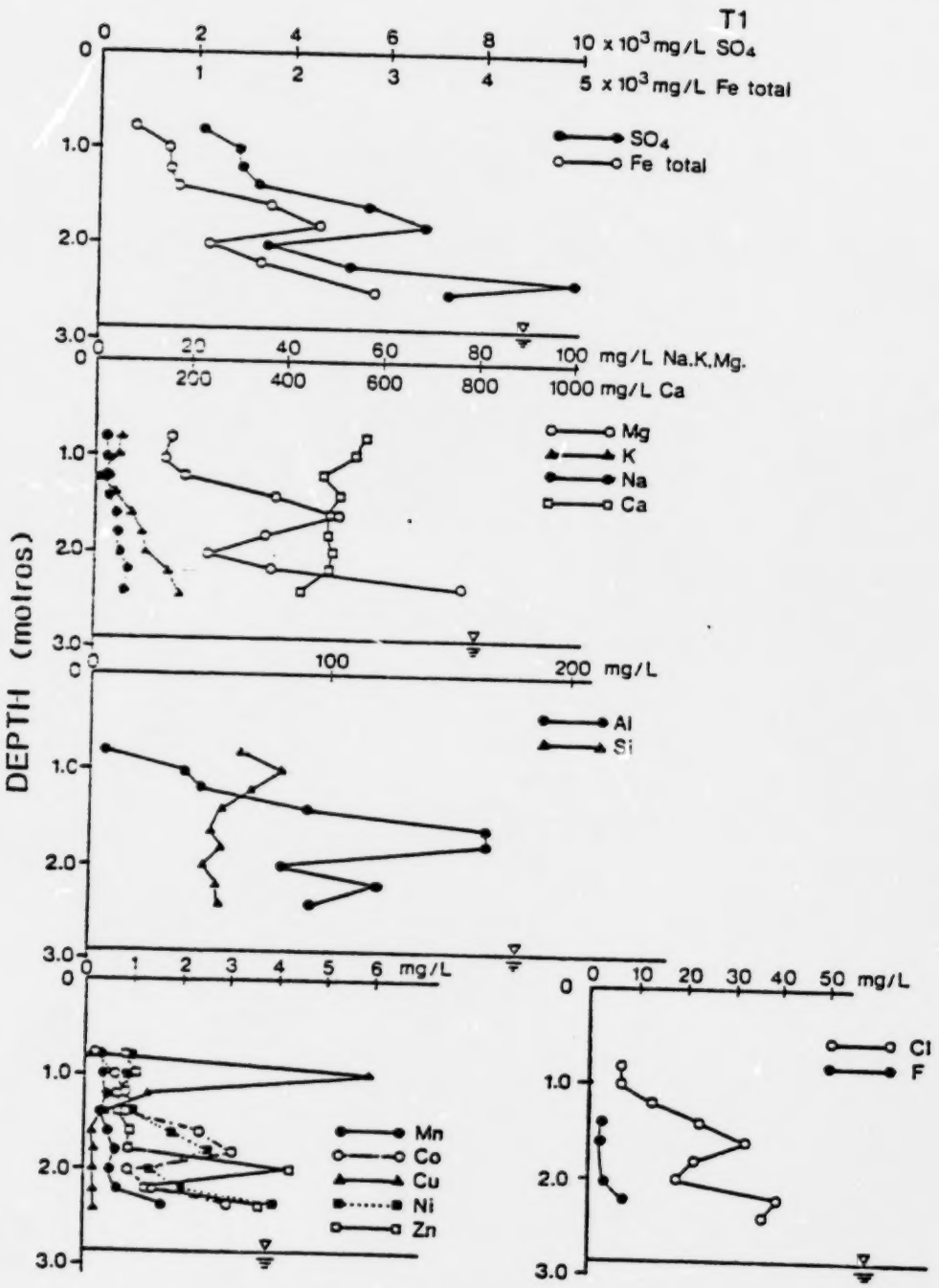

Figure 16a. Pore-water geochemistry at T1 in August, 1980.

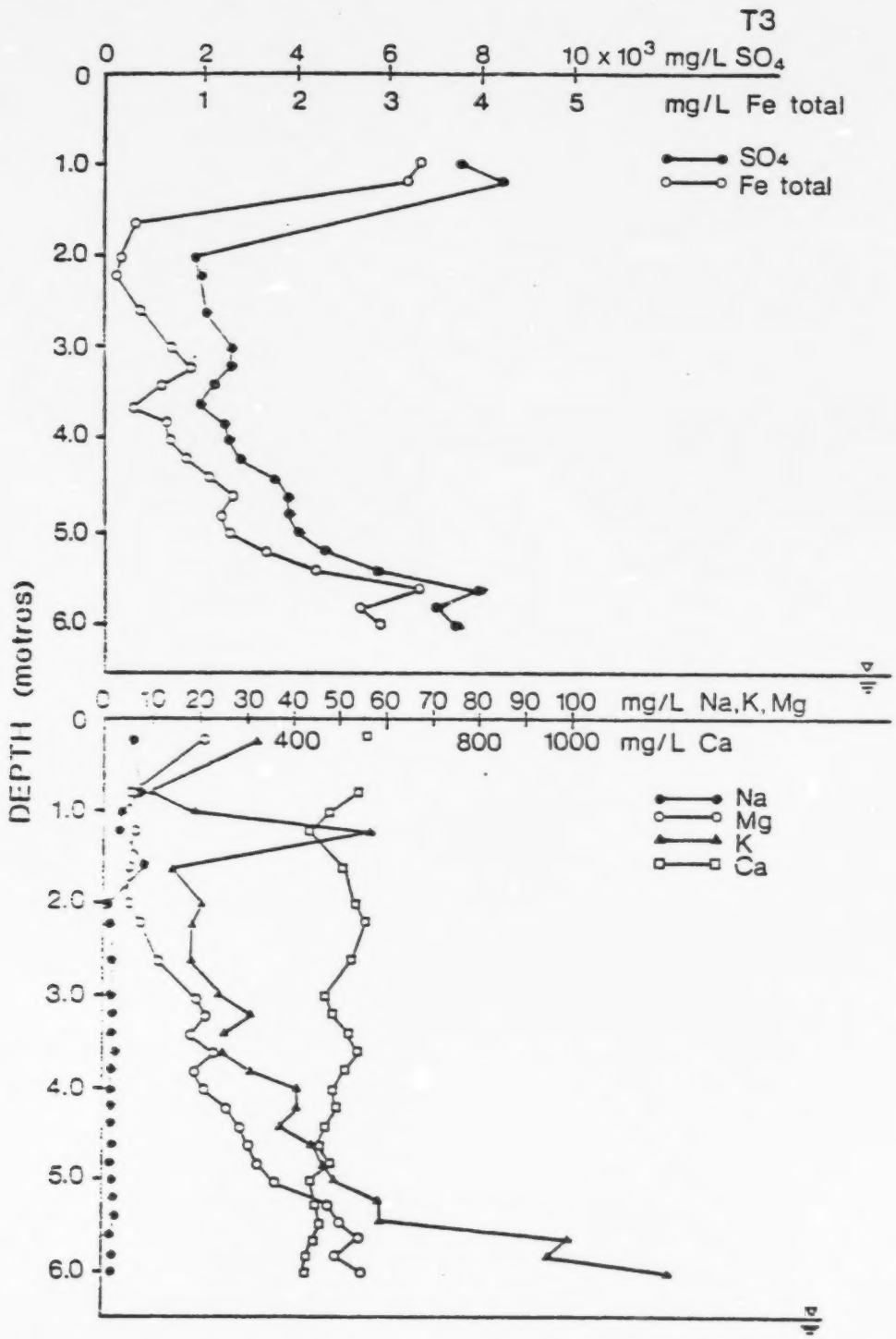

Figure 16b. Pore-water geochemistry at T3 in August, 1980 (SO_4, Fe(total), Na, K, Mg, Ca).

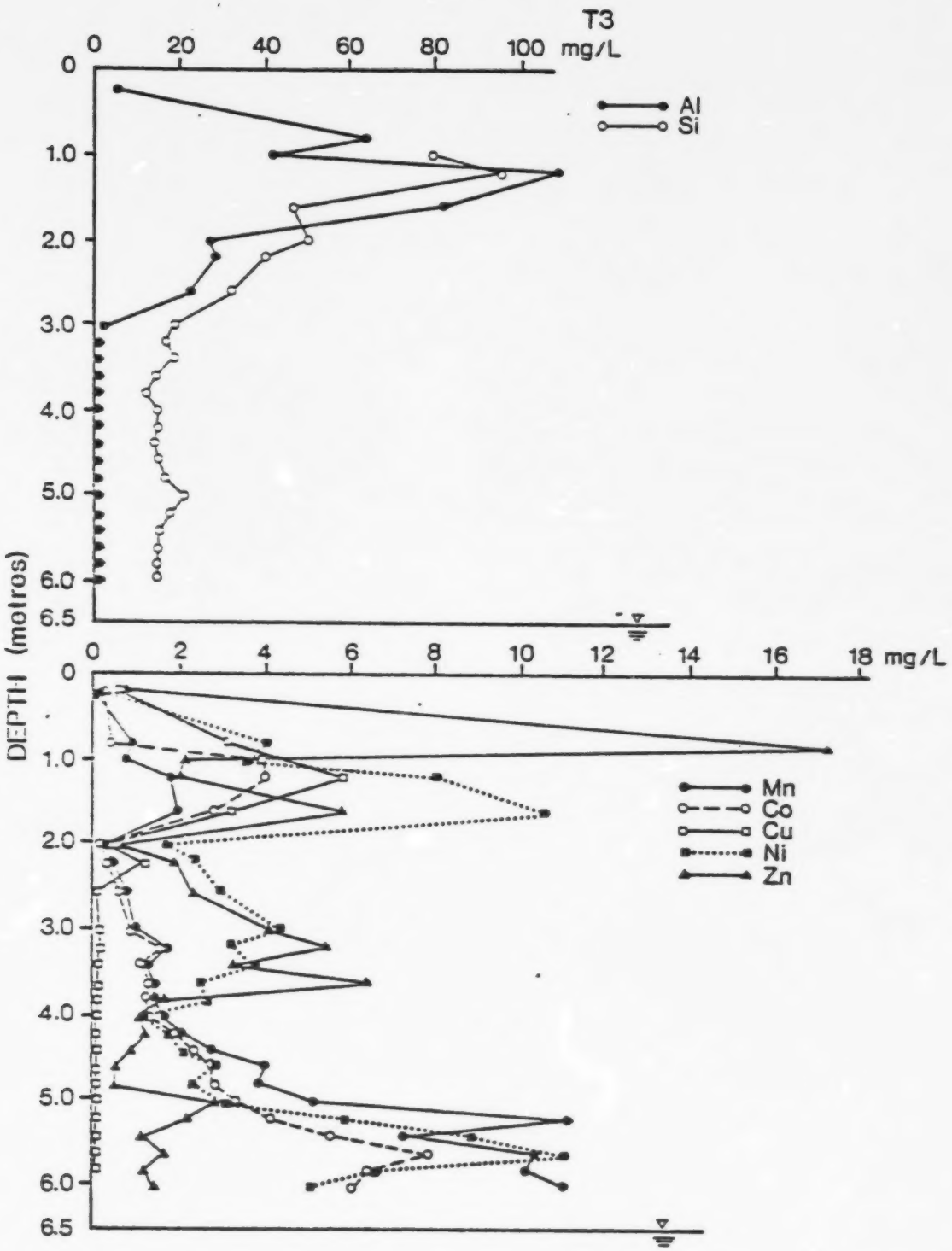

Figure 16c. Pore-water geochemistry at T3 in August, 1980 (Al, Si, Mn, Co, Cu, Ni, Zn).

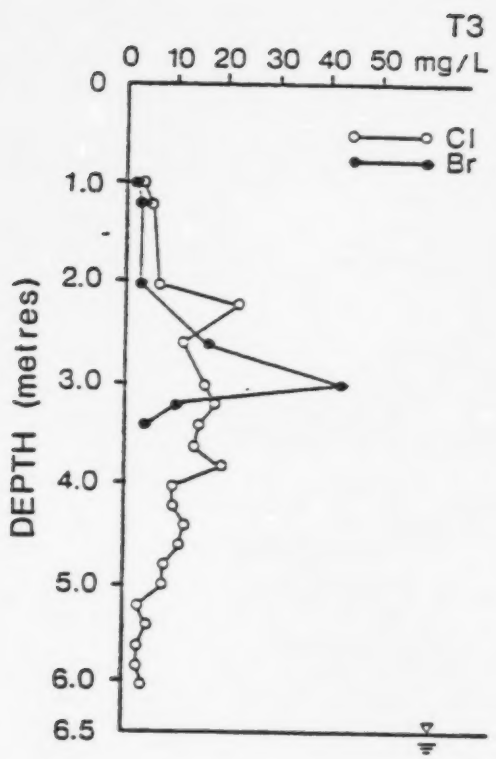

Figure 16d. Pore-water geochemistry at T3 in August, 1980 (Cl, Br).

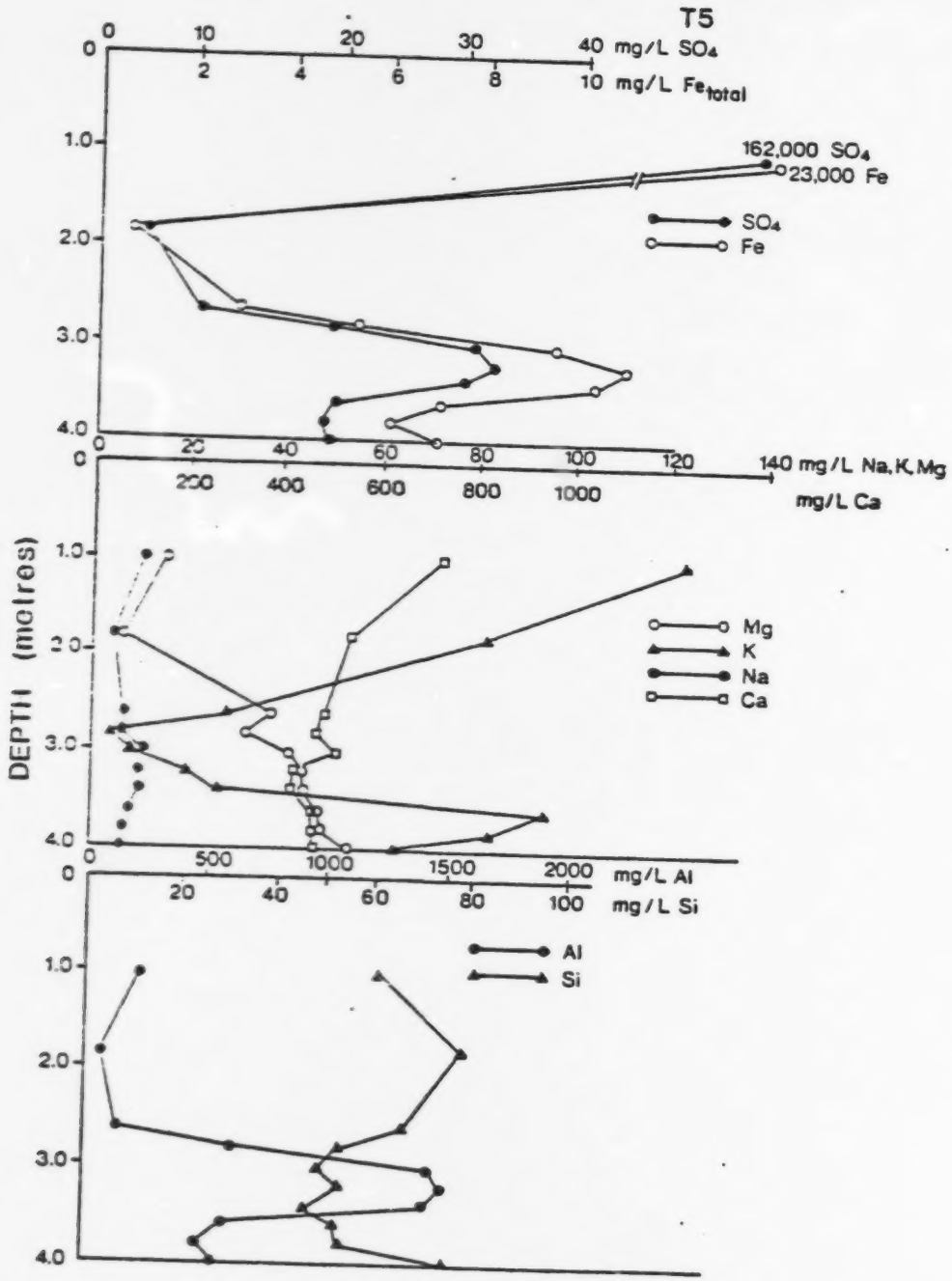

Figure 16e. Pore-water geochemistry at T5 in August, 1980 (SO_4, Fe(total), Mg, K, Na, Ca, Al, Si).

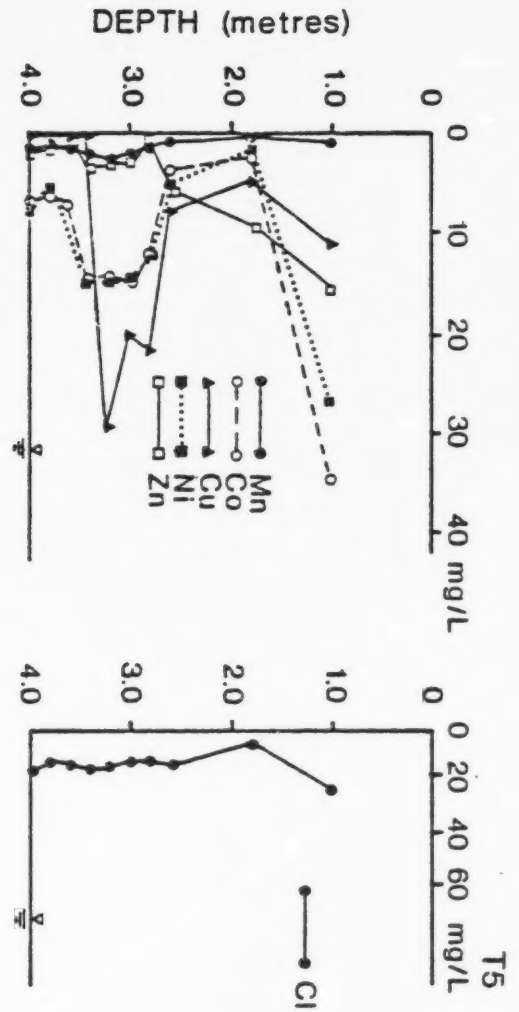

Figure 15f. Pore-water geochemistry at T5 in August, 1980 (Mn, Co, Cu, Ni, Zn, Cl).

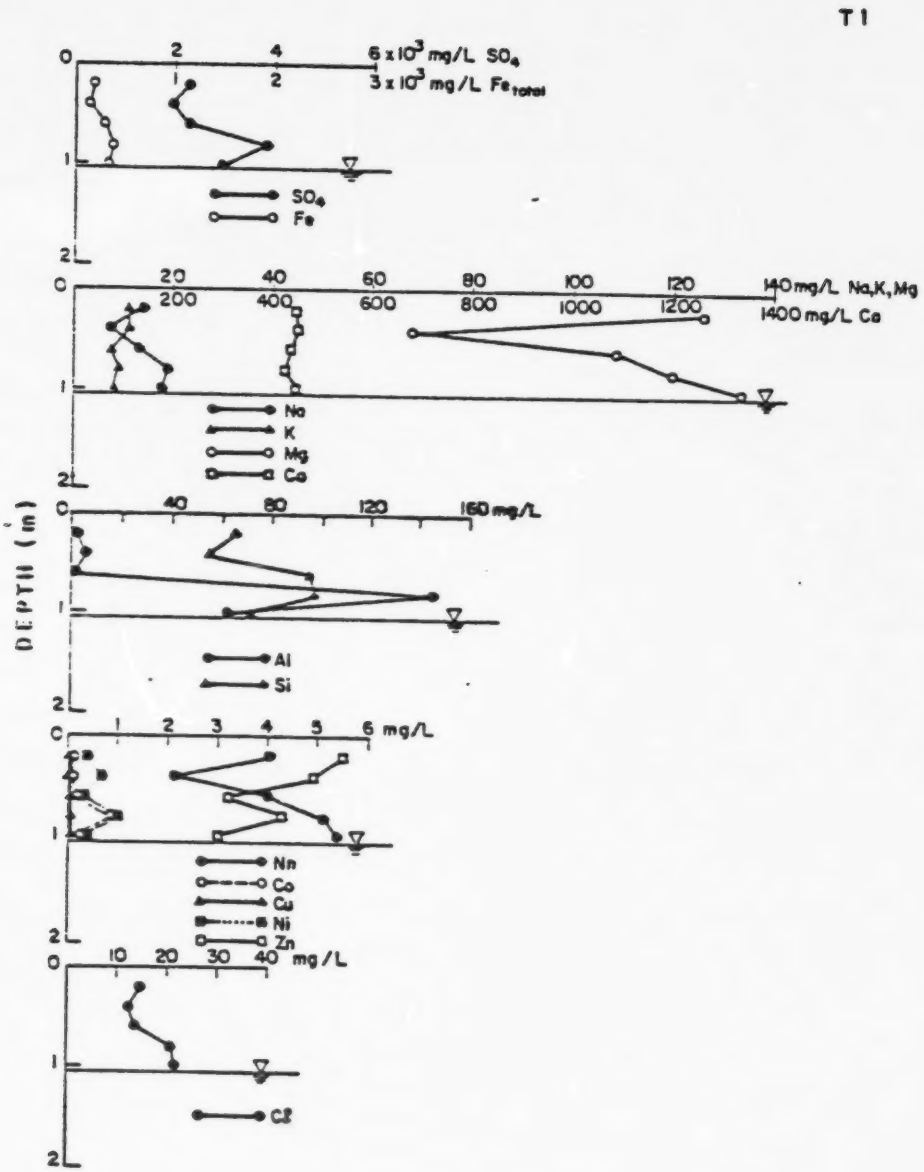

Figure 17a. Pore-water geochemistry at T1 in May, 1981.

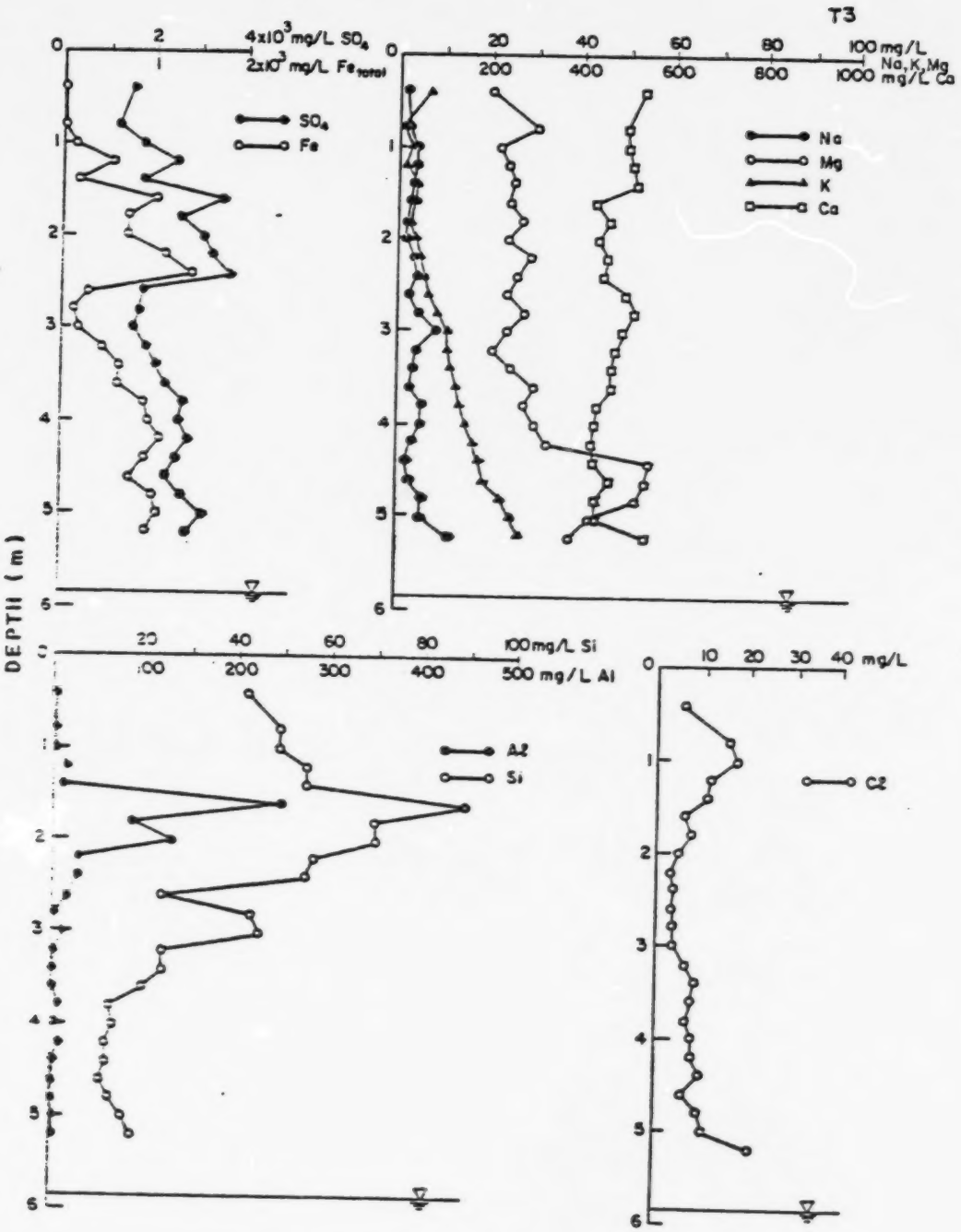

Figure 17b. Pore-water geochemistry at T3 in May, 1981 (SO_4, Fe(total), Na, K, Mg, Ca, Al, Si, Cl).

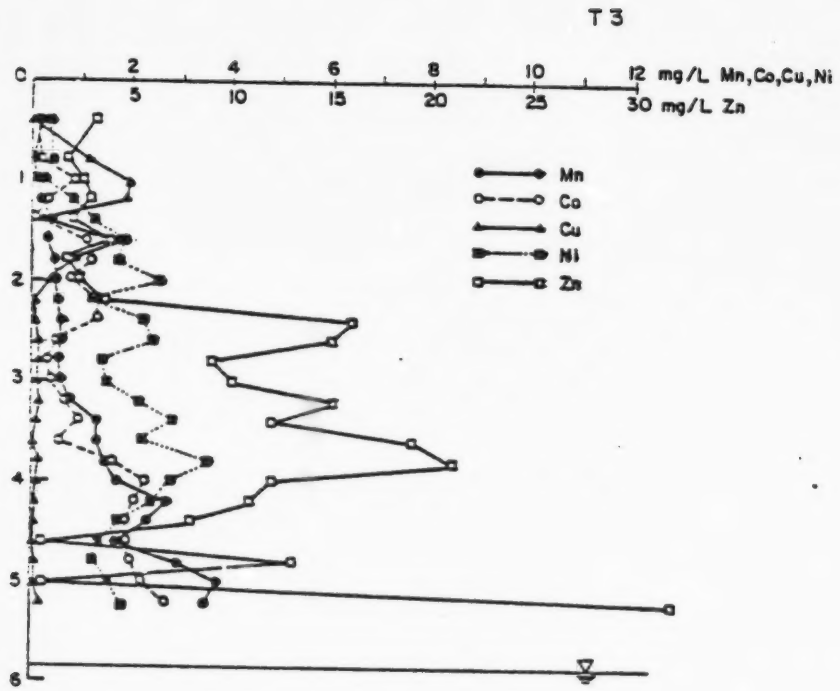

Figure 17c. Pore-water geochemistry at T3 in May, 1981 (Mn, Co, Cu, Ni, Zn).

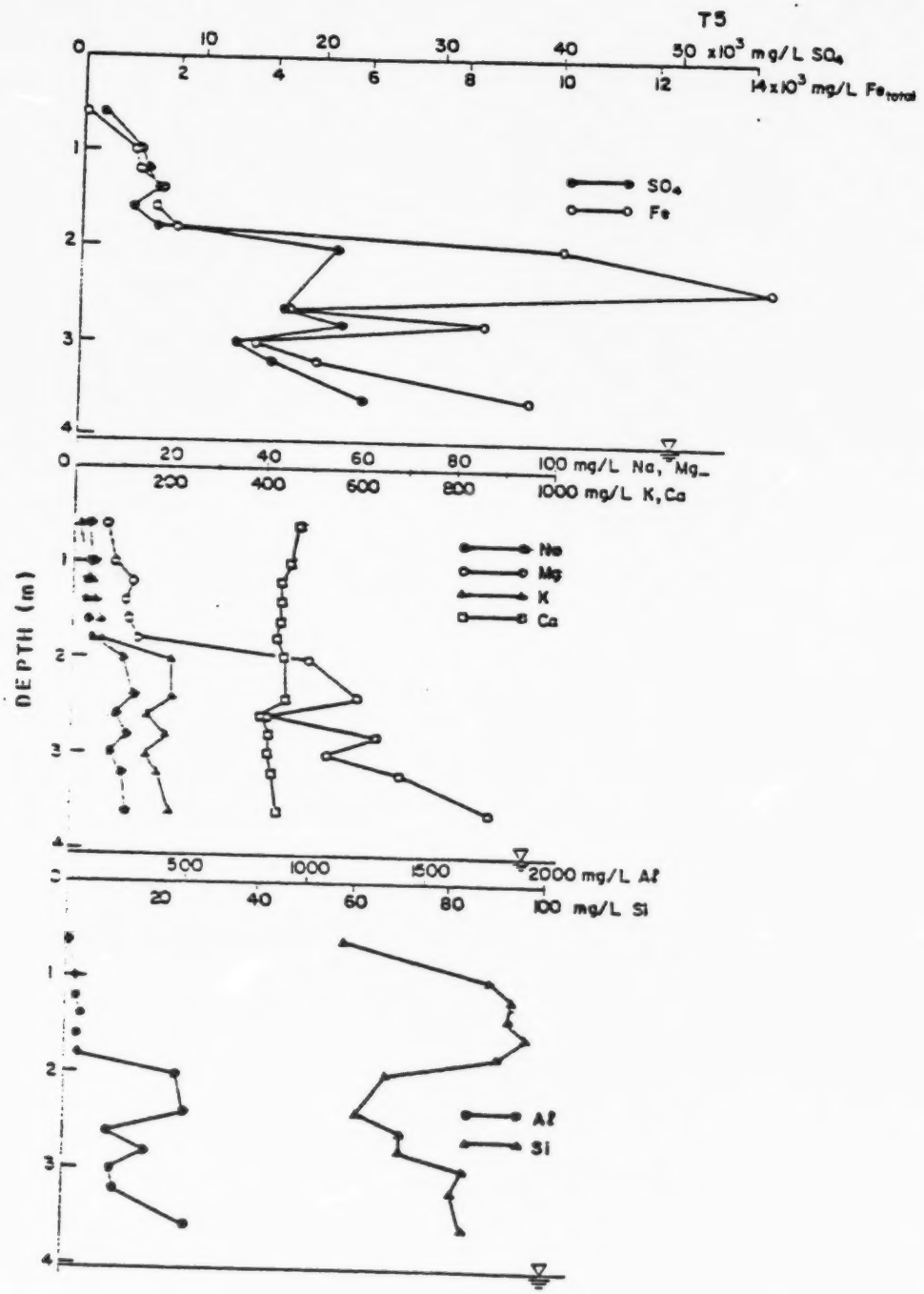

Figure 17d. Pore-water geochemistry at T5 in May, 1981 (SO_4, Fe(total), Na, K, Mg, Ca, Al, Si).

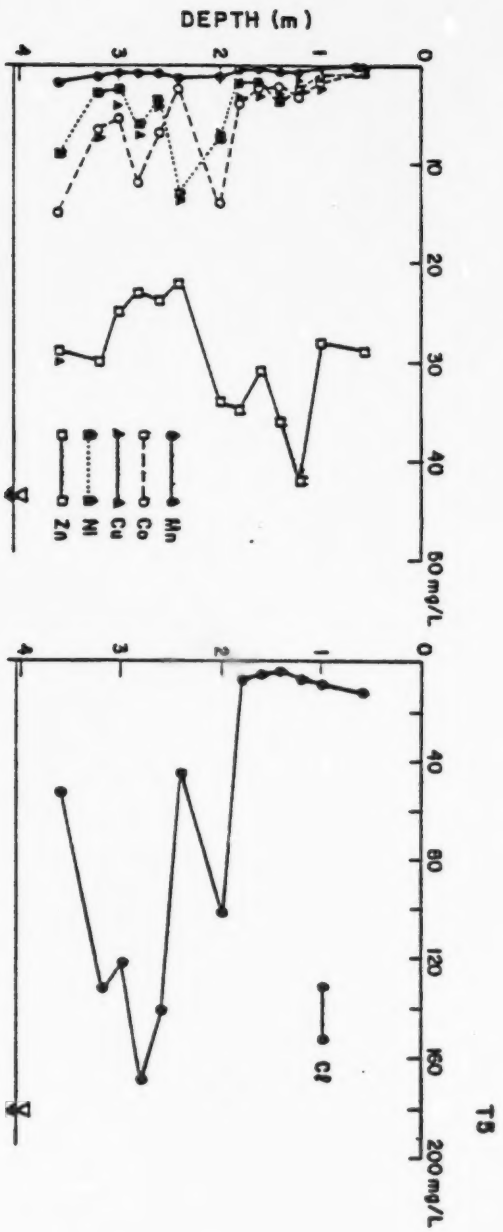

Figure17e. Pore-water geochemistry at T5 in May, 1981 (Mn, Co, Cu, Ni, Zn, Cl).

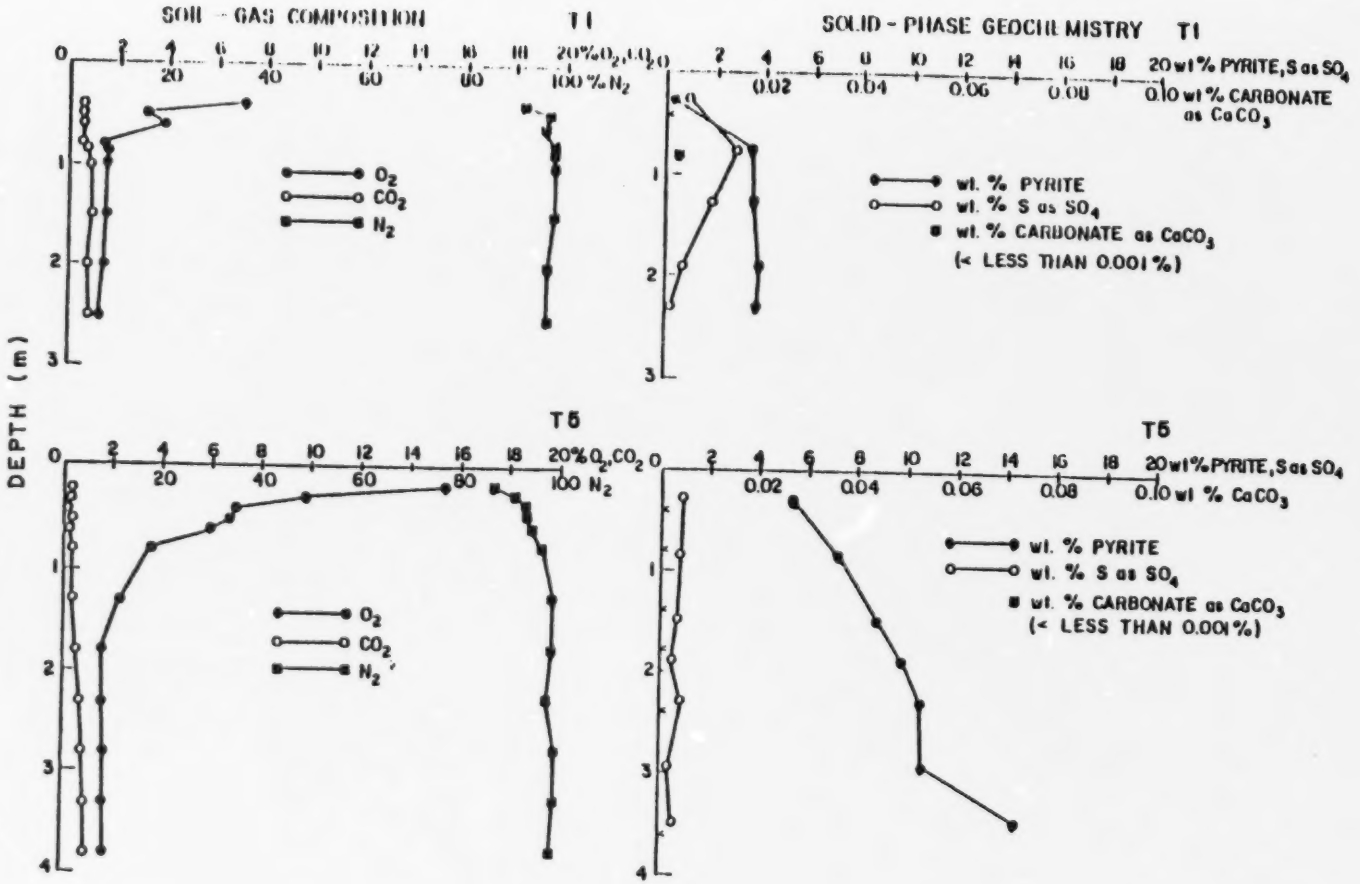
SOIL - GAS COMPOSITION T1
SOLID - PHASE GEOCHEMISTRY T1
DEPTH (m)
0 2 4 6 8 10 12 14 16 18 20% O2, CO2
20 40 60 80 100% N2
0.02 0.04 0.06 0.08 0.10 wt % CARBONATE as CaCO3
20 wt % PYRITE, S as SO4
O2
CO2
N2
wt. % PYRITE
wt. % S as SO4
wt. % CARBONATE as CaCO3
(< LESS THAN 0.001 %)
T5
T5

Figure 18a. Soil-gas composition and solid-phase geochemistry profiles at T1 and T5.

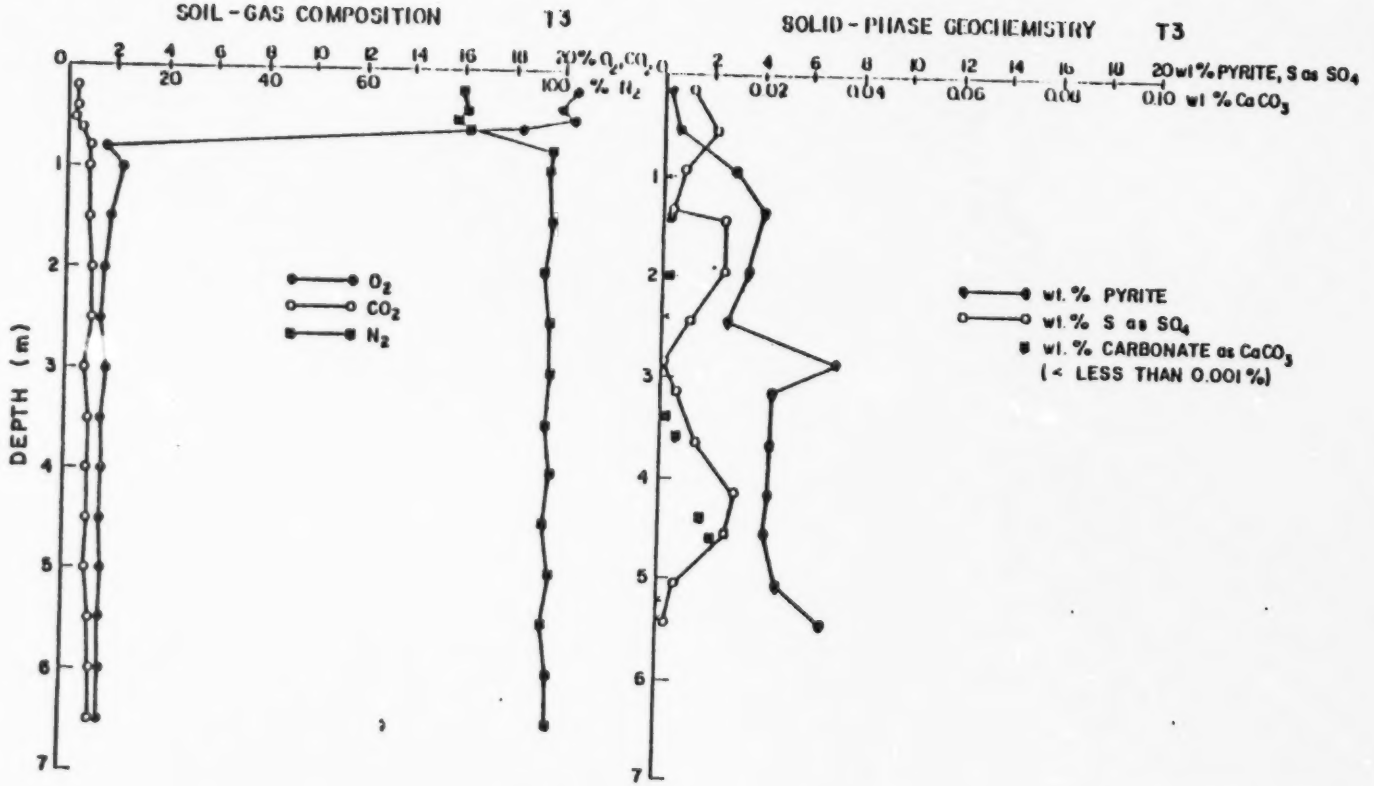

Figure 18b. Soil-gas composition and solid-phase geochemistry profiles at T3.

SATURATED ZONE GEOCHEMISTRY AND HYDROLOGY

Introduction

As outlined in Part 1 of this report, the most serious problem in the long-term management of Elliot Lake uranium tailings is the progressive acidification of pore water in the tailings due to pyrite oxidation. Pyrite, which is composed of reduced iron and sulfur, oxidizes in the presence of oxygen and water. When tailings deposition stops and tailings continue to drain, atmospheric oxygen moves down into the unsaturated zone. This creates a favourable environment for pyrite oxidation, and due to the fine grained nature of the pyrite, oxidation may take place rapidly. As pyrite oxidation proceeds, large amounts of ferrous iron, sulfate, and acidity are produced. In addition, the accompanying decrease in pH increases the solubility of heavy metals and most radionuclides. The oxidation products and associated soluble heavy metals are then displaced downward by infiltrating precipitation. Thus, although initially neutral, the pore water in the tailings mass becomes progressively more acidic as infiltrating precipitation replaces the original pore water.

Groundwater sampling in five of the inactive tailings in the Elliot Lake area has shown that acidification of pore waters has taken place to varying degrees. Moffet and Tellier (1978), who did the first study of tailings pore water in the Elliot Lake area, found that in the Nordic West Arm tailings impoundment much of the shallow groundwater has become acidic and

contains Fe^{2+}, SO_4^{2-}, heavy metals and most radionuclides far in excess of their concentrations in the original effluent from the mill. A similar condition exists in the adjacent Nordic Main tailings where, in addition to shallow acidification, a zone was found where pore waters in the entire tailings thickness have become acidic, and contaminated water is exiting the impoundment by seeping into the underlying aquifer (Blair et al., 1980; Blair, 1981; and Morin et al., 1982). Other inactive tailings impoundments where acidification of groundwater due to pyrite oxidation has occurred are the Lacnor tailings area (Cherry et al., 1980) and the William Lake and Stanrock tailings areas (Feenstra et al., 1981).

During the last several years the surfaces of three of the tailings areas have been vegetated as a preliminary means of reclamation. Recent sampling has shown that acidic conditions and high Fe^{2+} and SO_4^{2-} concentrations persist in the shallow groundwaters of these areas. Although previous studies of the Nordic Main and Nordic West Arm tailings areas have been reported on (Moffet and Tellier, 1978; Cherry et al., 1980; Blair, 1981; and Blackport and Cherry, 1980), a rigorous evaluation of the changes in groundwater chemistry since the establishment of the vegetation has not been done. There is a need for a more thorough description of how geochemical and hydrologic processes have interacted in the present mode of tailings reclamation to produce the groundwater conditions observed at present. This knowledge is the critical first step toward predicting future changes in the geochemistry of the tailings, and will in turn assist in the evaluation of alternative tailings management schemes.

Objectives and Scope

The objective of this study is to develop a detailed hydrogeochemical explanation for the extent and degree of acidification observed in the Nordic Main and Nordic West Arm tailings. The approach taken emphasizes the integration of hydrologic and geochemical factors to produce a unified picture of tailings processes. The tasks involved in achieving this goal are as follows:

1. Evaluate the influence that the physical hydrology exerts on the evolution of the tailings, with the emphasis on the transport of dissolved constituents in the absence of chemical reactions. It has been observed that piezometer nests on tailings areas with different hydrologic settings have vastly different groundwater chemical profiles. The flow system in the tailings and underlying aquifer will be described with the goal of defining chemical profile development as a function of such hydrologic factors as depth to water table, direction of groundwater flow, and rate of groundwater flow.

2. Document the mechanisms of acid production in the saturated and unsaturated zones of the tailings. Acid production is a complex process involving oxidation of pyrite by both organic and inorganic pathways (see Part III of this report). Definition of the primary oxidative pathways that have been important during the evolution of the observed geochemical conditions would be very useful in predicting future changes in the system.

3. Define the chemical processes that control the rate of migration of low pH water in the tailings, with particular attention to pH-modifying reactions involving Fe and Al solid phases. The production of H^+ and low pH by pyrite oxidation in the tailings has been offset to some degree by H^+

consumption by several geochemical processes. Maintenance of a high pH is desireable because heavy metals and some radionuclides are mobilized by low pH conditions. It is therefore critical to define the H^+ consuming processes in order to predict the degree of heavy metal and radionuclide mobilization that may occur in the tailings.

Methods

In order to monitor the hydrology of the tailings impoundments and underlying aquifer a network of piezometer nests was installed. The piezometers installed in the tailings are modified Casagrande drive-point type, consisting of a solid P.V.C. plastic drive point connected to 3.18 cm (1 1/4") diameter PVC pipe by a 15 cm length of perforated PVC pipe (Fig. 2.1). The intake screen consists of a section of porous polyethylene (vyon) fitted over the perforated PVC. The piezometers were installed by augering to the approximate depth desired, and then hand-driving the piezometer to the final depth in order to minimize the size of the disturbed zone around the screen.

Bundle piezometers were installed in the aquifer underlying the Nordic Main tailings. The bundles consisted of lengths of 1.27 cm (1/2") PVC pipe with up to 10 minipiezometers spaced along its length. Each mini piezometer was constructed by attaching a 10 cm length of nylon mesh screen to the end of a length of 0.95 cm (3/8") I.D. polyethylene tubing. (for more details on mini piezometer construction see Cherry et al., 1980b). The bundle piezometers were installed by insertion through the anulus of a hollow stem auger.

Filtered samples for analysis of the aqueous chemistry of the tailings groundwater were collected from the 3.18 cm piezometers by a syringe sampling technique (R.W. Gillham, 1982). This collection technique was chosen because it allowed down-hole filtering and did not subject the sample to pumping through long lengths of tubing. Samples for cation analysis were preserved by acidifying with HCl and refrigerating. The samples were analyzed for cations and trace metals using atomic adsorbtion by the Process and Development Laboratory of Rio Algom Limited, Elliot Lake, Ontario. Ferrous and total iron were determined by redox titration with potassium dichromate. Anion analyses were performed by the Geochemistry Laboratory of the University of Waterloo using column chromatography (Dionex ion analyzer), and dissolved silica was determined at the same laboratory by a photometric method on a Technicon Auto-Analyzer. Alkalinity titrations on filtered samples were performed in the field as soon as the sample was taken. The pH and pe of the unfiltered tailings groundwater were measured in a closed flow-through system maintained at groundwater temperature. Both were measured on Corning or Orion field meters using a sealed gel-type combination pH electrode (Canlab) and a platinum pe electrode (Orion 96-78). Electrical conductance of unfiltered samples of tailings groundwater was measured using a Corning electrical conductance meter.

Selected radionuclide contents of groundwater samples from two piezometer nests were analyzed by Monenco Analytical Laboratories, Calgary, Alberta. Activities of ^{228}Th, ^{230}Th, ^{232}Th, and ^{226}Ra were measured using alpha spectroscopy and ^{210}Pb activity was determined using beta spectroscopy. Total uranium was measured by colorimetry, additional analyses for ^{226}Ra were performed by the Elliot Lake Laboratory of CANMET.

Samples of porewaters from the zone above the water table were obtained by coring with 7.62 cm (3") ID. thin-walled aluminum tubing, and then removing the pore water by the methods described by D. Smyth (Section 1, this report).

Core of tailings solids for analysis of carbonate mineral content were collected from three sites on the tailings. This was done by augering to the water table with 7.62 cm hollow-stem augers, removing the augers, and then percussion driving a continuous section of 7.62 cm diameter thin-walled aluminum tube. A sediment trap was used to help keep the loose, cohesionless tailings from falling out of the sampling tube during recovery. Cores were immediately sealed with plastic end caps and silicon sealer, then wrapped with heavy-duty electrical tape. The sealed samples were cut open in the laboratory with a pipe cutter and a 20 to 30 gram sample quickly transferred to a buckner funnel. Samples were then vacuum washed with 3 successive 40 ml aliquots of methanol (see appendix C for details on method development). After air-drying the carbonate mineral content of the sample was determined by enclosing a weighed sample of tailings in a 50 ml syringe and evolving CO_2 gas by addition of concentration HCl. After the addition of helium as a carrier, the amount of CO_2 gas liberated by the sample was analyzed utilizing a Hewlett-Packard gas chromatograph with a TDC detector. A detailed description of the carbonate mineral detection method is presented by Barker and Chatten (in preparation).

Samples of aqueous sulfate for sulfur isotope analysis were collected by precipitating the sulfates as $BaSO_4$ by the addition of $BaCl_2$ to filtered water samples. Samples of sulfate in gypsum were obtained by first leaching the gypsum and then reprecipitating the sulfate as $BaSO_4$. The sulfur

isotopic composition of the sulfate was analyzed by the isotope laboratory at the University of Waterloo. The sulfate is decomposed to form sulfur dioxide by heating to approximately $1100^{0}C$, and the isotopic composition of the purified sulfur dioxide is determined using a mass spectrometer. Analysis of the pyrite is similar, except an oxidant is supplied to insure combustion to sulfur dioxide. A detailed description of the preparation on aqueous sulfate for sulfur isotopic analysis is given by in Feenstra (1980). Accuracy is on the level of $\pm$ $0.4^{0}/00$.

Physical Hydrology

A cross-section of the Nordic Main tailings area shows the stratigraphy to be comprised of 3 hydrologically important units: a sand aquifer, a layer of peat, and the tailings themselves (Fig. 2.2). The aquifer is made up of glaciofluvial sands that can be subdivided into an upper layer of 4 to 8 m of medium-grained sand, and a lower layer of very-fine-grained sand (Morin et al., 1982). Hydraulic conductivities of approximately 10^{-4} and 10^{-5} m/s for the upper and lower sand layers respectively were calculated from permeameter tests (Blair, 1981) and grainsize distribution curves (Morin et al., 1982). These values are corraborated by a value of 1.4 to 2.2 x 10^{-4} m/s for the hydraulic conductivity determined from pump test data in the aquifer underlying the Nordic West Arm tailings (Wardrop Associates Limited, 1978). A layer of peat up to 2 m in thickness overlies the aquifer over much of the tailings area. This peat has been removed by a dragline along the east and southeast edges of the tailings area for use as fill, and may also be missing from areas that were formerly topographic highs. No direct measurements of hydraulic conductivity have been made on the peat beneath

the Nordic Main tailings, but values between 5.5 to 6.4 x 10^{-9} m/s were calculated from rising head tests on piezometers installed in the peat layer underlying the adjacent Nordic West Arm tailings (Blackport and Cherry, 1980).

In the Nordic Main tailings hydraulic conductivities measured by rising head tests on piezometers range from 1 x 10^{-6} m/s to 3.1 x 10^{-8} m/s (Blair, 1981). These values are most representative of the range in horizontal hydraulic conductivity, and it is assumed that layering in the tailings produces a high degree of anisotropy, with horizontal to vertical hydraulic conductivity ratios of from 2.5 to 10 (Nelson et al., 1977; Kealy and Busch, 1971). In addition to the fine-scale anisotropy, the hydraulic conductivity of the tailings has been observed to decrease with increasing depth in the tailings (Blair, 1981; Blackport and Cherry, 1980). This decrease in hydraulic conductivity with depth has been attributed to grainsize segregation due to the deltaic style of deposition of the tailings (Blair, 1981), but may also indicate dewatering and compaction of initially underconsolidated slime layers under self weight (Conlin, 1980). There should also be a general tendency for decreasing hydraulic conductivity with increasing distance from the tailings discharge point due to loss of the coarser material by settling close to the discharge.

Data collected on water levels in the Nordic Main tailings area can be summarized in a map of depth-to-water table (Fig. 2.3). The depth to water table increases from less than a metre below ground surface near the northern limit of the area where the tailings are bounded by bedrock, to a depth of 6 to 10 metres along the southern edge where the tailings are bounded by a permeable dike and bedrock knobs. Seasonal changes in the

groundwater flow system are evident in the contrast between depths to static water levels measured in piezometers in December, 1979 and the water levels in July, 1980 (Fig. 2.4). Fall and spring recharge bring groundwater levels near to ground surface in the northern part of the tailings, and as much as 1.5 m higher than shown in Fig. 2.4 in the southern part.

Hydraulic gradients in the tailings and aquifer were determined by measuring static water levels in the piezometers in the tailings and bundle piezometers in the aquifer. Results for measurements on tailings piezometer nests (Fig. 2.4 and 2.4) indicate that vertical hydraulic gradients are highly variable, with gradients ranging from negligible to slightly upward (T4, T5 and T6), to a maximum of 0.21 downward (T3). Vertical gradients are downward at both T1 and T2, averaging approximately 0.066. The north-to-south horizontal gradient of the water table surface averages 0.011 between T1 and T7, and steepens southward to 0.04 between T7 and T8. The horizontal hydraulic gradient at the top of the sand aquifer measured between piezometer nests T1 and T8 is 0.008 to the south on the average; the gradient of 0.017 between T8C and T81, is significantly steeper. Data from bundle piezometers installed into the aquifer show low downward vertical gradients over most of the profiles at T5 and T7 (maximum of 0.004), locally high downward gradients at T3 (maximum of 0.04), and highly variable gradients at T4 (see appendix A for data). It is worth noting that at T3, T7 and T4, water elevations in the lowest piezometers indicate upward gradients. At T3 and T7 upward gradients can be attributed to a rising bedrock surface, but the cause of the upward gradient at T4 is unknown.

Resolution of specific flow directions in the tailings is difficult due to the heterogeneous and anisotropic nature of the tailings. In areas where vertical gradients are negligible, flow will be horizontal; however, even in areas where vertical gradients exceed horizontal gradients, flow may be dominantly horizontal due to the higher horizontal hydraulic conductivity. Over most of the tailings area the tailings and aquifer flow systems are separated by the low-permeability peat layer, as indicated by the large head loss across the peat at piezometer nests T1 and T2, and flux from the tailings in the aquifer is limited. In areas where the peat was removed or was not originally present the flux of tailings groundwater into the aquifer will be much greater. Downward flow of tailings groundwater into the aquifer is occurring in the area where peat is absent south of T3, and a contaminant plume currently under study (Morin et al., 1982) is thought to originate in this area.

In an effort to better define flow directions in the tailings a two dimensional finite element model of a cross-section of tailings between T1 and T8 was developed. After preparation of the grid, a calibration procedure was followed in which tailings hydraulic properties and boundary conditions were varied and the resulting potential field compared with known values until the combination of model parameters produced a flow system that closely portrayed heads measured in the field. Model results (Fig. 2.5) show a flow system with dominantly horizontal flow at shallow depth in the tailings and in the underlying aquifer, connected by a zone in which near vertical flow occurs across the lower tailings and peat layer. The model results are preliminary due to the low number of calibration points, and the resolution of the model will be improved in the future by expanding the field sampling network.

Aqueous Geochemistry

Hydrochemical Conditions

Pyrite in the tailings may be oxidized by oxygen or Fe^{3+}, as described by the two equations:

$$FeS_2 + 7/2\ O_2 + H_2O \Rightarrow Fe^{2+} + 2\ SO_4^{2-} + 2H^+ \quad (2.1)$$

$$FeS_2 + 14Fe^{3+} + 8H_2O \Rightarrow 15Fe^{2+} + 2SO_4^{2-} + 16H^+ \quad (2.2)$$

In both cases ferrous iron and sulfate are released in a 1:2 ratio. Additional H^+ will be generated if the iron released is subsequently oxidized and precipitated as ferric oxyhydroxide or as basic iron sulfate, as illustrated by the reactions:

$$FeS_2 + 15/4\ O_2 + 7/2\ H_2O \Rightarrow Fe(OH)_3 + 2SO_4^{2-} + 4H^+ \quad (2.3)$$

$$FeS_2 + 15/4\ O_2 + 5/2\ H_2O + 1/3\ K^+ \Rightarrow$$

$$1/3\ K\ Fe_3(SO_4)_2(OH)_6 + 4/3\ SO_4^{2-} + 3H^+ \quad (2.4)$$

Minimal H^+ production occurs if the Fe^{2+} is oxidized but does not precipitate:

$$FeS_2 + 15/4\ O_2 + 1/2\ H_2O \Rightarrow Fe^{3+} + 2SO_4^{2-} + H^+ \quad (2.5)$$

When these oxidation products are picked up by infiltrating precipitation, the result is a water with a low pH and high concentrations of Fe and SO_4^{2-}.

Profiles of the aqueous chemistry of the groundwater in the Nordic Main tailings show a two layer system in which recharging precipitation has moved downward into the tailings gradually displacing the original process water from the mill. Although detailed information on the chemistry of the effluent from the Nordic mill is unavailable, it was no doubt very similar to the process water currently being discharged from the Quirke Mill (Table 2.1). Effluent from the Quirke mill has a high pH and low concentrations of iron, aluminum and heavy metals. The dominant cation is calcium followed

by potassium and sodium, and the dominant anions are sulfate, nitrate, and chloride. Nordic mine effluent differred in that the pH was between 7 and 8 (Blair, 1981), and there is evidence that it contained more chloride.

Fig. 2.6 shows the profile of the aqueous chemistry for piezometer nest T6, which is representative of areas with shallow to moderately deep (5m) water table (see also Table 2.1). The water sample from the piezometer at 12 m is representative of process water that has been subject to a minor amount of pyrite oxidation. The pH is slightly below that at which it was discharged, and the sulfate and iron have increased. The profile of the aqueous chemistry shows that concentrations of iron and sulfate, products of pyrite oxidation, increase greatly at shallower depths in the tailing (Fig. 2.6). This sharp increase in concentration of these two constituents at 10 m approximately marks the boundary between downward-moving recharge and the underlying process water. The pH of the recharge water decreases at shallower depths in the tailings; however, the pH values are much higher than what would be predicted from the iron and sulfate concentrations and the stoichiometry of the pyrite oxidation reaction. This indicates that a significant amount of pH buffering has taken place, an important point that will be developed later in the text. Decrease in pH is accompanied by increasing pe, indicating more oxidizing conditions in the shallow, recharging groundwater. Elevated concentrations of aluminum and silica are found in the recharge water as a result of the dissolution of aluminosilicate minerals in the tailings due to the low pH condition. Cobalt concentrations in the recharge waters are much higher than in the process water and show a pattern typical of the heavy metals. The heavy metals are probably derived from oxidation of accessory sulfide minerals and mobilized by desorption by

the low pH. In general the concentration profiles of Co, Ni, and Zn in the tailings groundwaters are very similar, while the peak concentrations of Pb and Cu occur at shallower depths.

A limited amount of sampling was done in order to examine how radionuclides are mobilized in recharge water in the tailings. During the 1980 field season several of the piezometer nests on the Nordic Main tailings were sampled for ^{226}Ra; in addition water samples were analysed for lead-210 (^{210}Pb)., thorium-232 (^{232}Th), and uranium. Levels of ^{226}Ra in water currently discharged from Elliot Lake mills are about 1500 pCi/L, and it is believed that mill water discharged to the Nordic tailings impoundments had similar ^{226}Ra activity. Data collected from a piezometer nest installed in the new Quirke tailings area indicates that ^{226}Ra activity in the tailings water declines to a level of a few hundred pCi/L shortly after deposition. Water samples collected in August 1980, and analyzed by Rio Algom laboratories were found to contain 354 to 492 pCi/L of ^{226}Ra. Samples obtained from the same wells in February, 1981, contained ^{226}Ra activities of only about 200 pCi/L (A. Vivyurka, personal communication). None of the other chemical characteristics of the samples measured show significant differences between the two samples that can be related to the change in ^{226}Ra activity, and it is not known what reactions are responsible for the decrease in ^{226}Ra activity. Results of the sampling at T6 in the Nordic Main tailings show that the highest ^{226}Ra activity is found at 8.3 m depth in the recharge water (Fig. 2.6). Although ^{226}Ra activities are generally higher in the high-iron recharge water in all piezometer nests, the ^{226}Ra peak activity often occurs at slightly greater depth than the peak iron concentrations (Fig. 2.7).

Results of radionuclide analyses for T6 are shown in Table 2.2. The data show that U and ^{210}Pb occur in low concentrations at depths below 9 m, but in much higher concentrations in the high-iron waters at shallower depth, (Fig. 2.6). This distribution is very similar to that of the other heavy metals (Zn, Co, Cu, Ni) except that the peak U and ^{210}Pb concentrations occur at slightly shallower depth. This pattern of U and ^{210}Pb distribution agrees with observations made by Moffet and Tellier (1978) on radionuclide occurrence in the West Arm tailings. The heavy metals and radionuclides are probably mobilized by a combination of desorption due to increased Fe^{2+} concentration and decreased pH, and mineral dissolution. The observed concentrations of U and ^{210}Pb are in excess of accepted standards for drinking water (Moffet, 1976), and will constitute a health hazard if allowed to migrate from the disposal area.

The distribution of ^{228}Th, ^{230}Th, and ^{232}Th activities at T6 show no discernible trend (table 2.2). In addition, there apparently was error in the thorium analyses done by MONENCO on the 1980 samples, as major discrepancies were discovered between analyses done on split samples by MONENCO and the University of Waterloo Chemistry Department (K. Morin, Ph.D. thesis in progress). From the data available, no correlation can be made between high thorium activities and high iron concentrations.

The profile of groundwater geochemistry described above is typical of conditions in much of the Nordic Main tailings (for example at piezometer nests T1, T2, T4, T5 and T6); however, there are extreme variations in the depth to which recharge water has penetrated the tailings within the Nordic Main and Nordic West Arm tailings areas. This is due in large to the strong influence that physical hydrology exerts on the rate of downward movement

of recharge waters. Areas that have downward or horizontal gradients have developed hydrochemical profiles that show moderate depth of penetration of recharge waters. In contrast, acid recharge water has completely replaced the original process water throughout the entire tailings thickness in areas with high downward vertical hydraulic gradients. In the Nordic Main tailings recharge water with high iron concentrations has completely replaced original process water at piezometer nests T3, T7 and T8 (Fig. 2.8), and contaminated groundwater extends into the underlying aquifer at these sites.

Even lower pH values have been found in groundwater in areas of older tailings that have downward gradients. The most extreme case of groundwater acidification found is at piezometer nest UW14 in the Nordic West Arm tailings. The process of tailings acidification has been active 10 years longer than in the Nordic Main tailings, and the pH of the groundwater is below two throughout the tailings thickness (Fig. 2.8). The low pH indicates that at this location almost all of the acid neutralization capacity of the tailings has been spent and the pH has fallen to a level buffered by bisulfate formation via the reaction:

$$SO_4^{2-} + H^+ \; <==> \; HSO_4^- \quad K = 10^{+1,99} \qquad (2.6)$$

In the case of upward gradient in the tailings, neutral pH groundwater from the underlying flow system moves upward into the tailings and thereby limits the depth of penetration of acidic recharge water produced in the unsaturated zone. The geochemical profile of UW6 from the Nordic West Arm tailings shows the features of such a profile, with high iron water penetrating to only 3.5 m into the tailings (Fig. 2.8). However, areas with upward gradients constitute only a minor percentage of the total area of the Nordic and West Arm tailings areas.

Acid Production

Evidence has been accumulating that the production of acid by pyrite oxidation occurs at shallow depths in the unsaturated zone of the tailings. The rapid depletion of O_2 in the gas phase with increasing depth in the unsaturated zone is a clear indication of rapid oxidation (see Part I, this report). The concept of a shallow zone of acid production is also supported by data that indicates that tailings acidification has been less severe in areas where high water tables limit the amount of O_2 available.

The primary mechanism by which pyrite is oxidized under low pH (<4) conditions is oxidation by Fe^{3+}. Since the oxidation of Fe^{2+} to Fe^{3+} by oxygen is extremely slow in this pH range (Singer and Stumm, 1970) the amount of acid produced is strictly limited by the availability of Fe^{3+}. However, the iron-oxidizing bacteria, Thiobacillus ferroxidans, catalyzes the reaction, producing a rate 10^6 times faster than abiotic iron oxidation by oxygen. Thus, the bacteria insure an ample source of Fe^{3+} so long as oxygen is available. The oxidation of pyrite by Fe^{3+} and subsequent oxidation of the Fe^{2+} produced can be represented by the following schematic equation:

$$14Fe^{3+} + FeS_{2(s)} + 8H_2O \quad <=> \quad 15Fe^{2+} + 2SO_4^{2-} + 16H^+ \qquad (2.7)$$

The presence of iron oxidizing bacteria in low pH (<5) zones of the Elliot Lake tailings has been established (McCready 1976, and Silver and Taylor, 1981), and there is additional evidence of a narrow zone of high bacterial activity near the surface of the tailings (M. Silver, personal communication).

In addition to oxygen depletion, the above model predicts that Fe^{3+} may be abundant in solution where oxygen is present and bacterial action rapid;

but once all available oxygen is utilized Fe^{3+} will be reduced by pyrite oxidation and the dominant aqueous iron species will be Fe^{2+}. This hypothesis was tested by sampling and determining iron speciation in waters from the saturated and unsaturated zone at one location in the tailings. Results indicate that iron in samples from the zone above the water table at site T5 is up to 62% ferric, while iron in samples from directly below the water table were almost entirely Fe^{2+} (Fig. 2.9). While it is likely that much of the iron is lost from solution due to the precipitation of amorphous $Fe(OH)_3$ or basic iron sulfates such as jarosite ($K\ Fe_3(SO_4)_2(OH)_6$), molar ratios of Fe:S in solution in excess of the 1:2 ratio predicted by the stoichiometry of pyrite indicate that disproportionate amounts of iron have not been lost from solution. We conclude that the model of pyrite oxidation by Fe^{3+} mediated by bacterial oxidation of Fe^{2+} fits the available data.

It is known that some chemical reactions involving sulfur will show preference for either the lighter (^{32}S) or heavier (^{34}S) sulfur isotope, causing one isotope to be accumulated in the reactant and depleted in the product. Due to this phenomenon, the use of sulfur isotopic composition of solid tailings and associated pore waters was investigated as a potential tool for studying the mechanisms through which sulfide in tailings pyrite is oxidized to sulfate. Several different pyrite oxidation mechanisms have probably operated during the history of the tailings including oxidation by oxygen, oxidation by Fe^{3+}, and direct oxidation by bacteria. While there is no known fractionation effect in the first two mechanisms, there is both laboratory and field evidence indicating that SO_4^{2-} produced from pyrite through oxidation by Thiobacillus is depleted in the heavy isotopes of sulfur relative to the parent pyrite on the order of $-10^0/_{00}\delta^{34}S$ (Kaplan and Rittenberg, 1964; Nissenbaum

and Rafter, 1967). However, this effect may only be seen when the oxidation process is incomplete and partially oxidized sulfur species accumulate.

Sulfate in the tailings water comes from two sources: 'process sulfate' that was added as sulfuric acid during milling (a large portion of which was precipitated as gypsum during tailings neutralization with lime), and 'pyrite sulfate' derived by oxidation of sulfide in pyrite. If it is demonstrated that these two sulfate sources have distinctive isotopic compositions, then the original process water could be distinguished from recharge water. It was therefore hypothesized that if the sulfur isotopic composition of the sulfate in solution could be used to distinguish residual process water from recharge water, then the data would shed light on the specific mechanisms of pyrite oxidation that have been dominant in the tailings.

The results of sulfur isotopic analysis of samples from five of the piezometers at the T6 site on the Nordic Main tailings, as well as a water sample from the Quirke tailings area, a sample leached from Quirke tailings soids ('Quirke gypsum'), and a sample leached from Nordic Main solids ('Nordic Main gypsum'), are presented in Fig. 2.10. As expected, the aqueous sulfate in the Quirke tailings is somewhat depleted in ^{34}S relative to the gypsum in the Quirke tailings area, reflecting the slight preferential removal of the heavier isotope during gypsum precipitation. Similarity between the $\delta^{34}S$ of the gypsums at the Nordic Main and Quirke tailings areas indicates that the acid used in both mills had approximately the same sulfur isotopic composition.

It is interesting to note that the $\delta^{34}S$ of the water sample from the piezometer at 12 m is approximately +3 $^{0}/_{oo}$ enriched relative to the

$\delta^{34}S$ for the sample from the 10.5 m piezometer. This is probably due to preferential utilization of the lighter sulfur isotope by sulfate-reducing bacteria active in the peat layer underlying the tailings.

Most importantly, the $\delta^{34}S$ of the upper four piezometers at T6 are similar. Thus the sulfate in water at a depth of 10.5 m, thought to be residual process water, cannot be distinguished from the sulfate in the high Fe^{2+} recharge water found at shallower depths on the basis of sulfur isotopic composition. Pyrite from the Nordic Main tailings was found to have a $\delta^{34}S$ of 1 $^{0}/_{oo}$, and microbial fractionation should have produced aqueous SO_4^{2-} with a much reduced $\delta^{34}S$. One possible explanation for the lack of contrast in the $\delta^{34}S$ of the aqueous SO_4^{2-} is that no detectable sulfur isotopic fractionation occurred during pyrite oxidation. However, it is likely that any fractionation effect that may be occurring is obscured by rapid attainment of isotopic equilibrium between the aqueous sulfate and gypsum already present in the tailings. In either case the use of sulfur isotopes in the tailings as indicators of oxidation mechanisms is probably not possible due to the presence of large amounts of sulfate from the acid leach reagents.

Major Ion Geochemistry

In attempting to predict the migration of low pH conditions and toxic metals in the tailings it is important to have an understanding of the geochemistry of iron and aluminum in solution. This is because hydrolysis and precipitation/dissolution reactions of these metals act as strong pH buffers; both Al and Fe have found to be toxic to vegetation and fish life ; and it has been found that large quantities of radium (80,000 pCi/g) are

associated with the basic iron sulfate jarosite ($KFe_3 (SO_4)_2 OH)_2$) which has been identified in both fresh and weathered tailings (Kaimen, 1977, 1978).

Aqueous speciation of iron and aluminum is a function of the pH and availability of anions with which complexes may be formed such as F, Cl, and SO_4. Fe speciation is also a function of the redox potential of the water, expressed as pe (-log electron activity) and the ratio of Fe^{2+} to Fe^{3+} can be calculated from the relationship:

$$Fe^{2+} <==> Fe^{3+} + e^- \qquad K = 10^{-13,032} \tag{2.8}$$

Because of the interrelations of Fe activity, pH and pe, Fe speciation and solid phase stabilities are often illustrated by means of a pe-pH diagram. The progressive change in the pH and pe of groundwater at one site in the Nordic Main tailings is shown in Fig. 2.11. The data show that with increasing depth in the tailings, the increase in pH is coupled with a decrease in pe producing a trend parallel to the line defining a solution in equilibrium with amorphous ferric oxyhydroxide ($Fe(OH)_{3A}$.* A similar trend has been noted for groundwaters in sulfide tailings in New Brunswick (Boorman and Watson, 1976).

A more rigorous interpretation of the apparent equilibrium with $Fe(OH)_3$ is not possible without discussing the limitations of pe-pH diagrams. The diagram is constructed for one set of conditions, in this case total Fe = 5 mg/L and $pCO_2 = 10^{-2}$, and a change in these concentrations will alter the size of the stability fields. As each point plotted represents a water with a specific iron concentration and PCO_2, the proximity to equilibrium of the

---

* This diagram is constructed for a ferric oxyhydroxide pK of 38.5. The equilibrium constant for ferric oxyhydroxide has been found to be highly variable depending on the history of the water (Langmuir and Whittemore, 1971, Whittemore and Langmuir, 1975) and may be as high as 37.

individual samples must be examined by other methods. This comparison is facilitated by the calculation of ion activity products (IAP) and saturation indices (SI) where

$$SI = \log IAP/KSP \qquad (2.9)$$

A negative SI indicates undersaturation, while a positive SI indicates supersaturation. IAP's and SI's for the analytical data were calculated using the WATEQ2 chemical equilibrium program (Ball et al., 1979). Most of the IAPs for $Fe(OH)_{3A}$ calculated for analyses from 3 piezometer nests in the Nordic Main tailings fall between 36.3 and 40.4, indicating approximate equilibrium with amorphous $Fe(OH)_3$ (Langmuir and Whittemore, 1971; Whittemore and Langmuir, 1975) (table 2.3). While near-equilibrium is indicated, the calculation doesn't indicate whether equilibrium is being maintained by dissolution or precipitation of the solid phase. Equilibrium in the tailings groundwaters could be maintained by either process; $Fe(OH)_{3A}$ may be precipitating as the pH of high iron water increases due to H^+ - consuming reactions during downward flow; or $Fe(OH)_{3A}$ precipitated during tailings neutralization prior to deposition may be dissolving due to removal of Fe^{3+} from solution by pyrite oxidation. The removal of Fe^{3+} from solution by pyrite oxidation is a rapid reaction and the possibility that $Fe(OH)_{3A}$ may act as a source of Fe^{3+} for pyrite oxidation has been suggested elsewhere (Stumm and Morgan, 1970; van Breemen, 1972). Langmuir and Whittemore (1975) propose that high log IAP's (close to -37) suggest that water is actively precipitating $Fe(OH)_{3A}$ while lower values (-39 to -44) indicates that the water may be dissolving or in equilibrium with a more stable iron hydroxide. In view of the high log IAPs (average of 26 samples = -37.7), our present feeling is that $Fe(OH)_{3A}$ is being precipitated in the tailings due to pH increases caused by H^+ neutralization.

Equilibrium calculations also show that tailings groundwaters in the neutral pH range are supersaturated with respect to siderite ($FeCO_3$) with SI's ranging as high as 1.7 (Table 2.4). In addition a pe-pH diagram showing all measurements made in the Nordic Main, Nordic West Arm and Lacnor tailings areas indicates possible siderite control on iron concentration and pe (Fig. 2.12). Siderite supersaturation has been noted by other researchers in tailings seepage (Morin et al., 1982) and in a landfill leachate plume (Buszka, 1982). Supersaturation could be produced if pH-increasing reactions occur more rapidly than siderite precipitation can remove Fe^{2+} from solution, or if there is error in the equilibrium constant for siderite. K. Morin (personal communication) has pointed out that the K used for equilibrium calculations is for the precipitation of pure $FeCO_3$, and noting that naturally occurring siderite contains significant amounts of Ca^{2+} and Mn^{2+}, speculates that siderite rapidly precipitated from natural solutions has a higher solubility. It is believed that siderite precipitation is occurring in the neutral tailings groundwater on the basis of the SIs and the grouping of points along the siderite field boundary in Fig. 2.12.

The stability fields of the basic iron sulfate jarosite ($KFe_3(SO_4)_2(OH)_6$) for two water chemistries (high iron and sulfate, and low iron and sulfate concentrations) are shown in figure 2.12. The jarosite field was calculated using the pK for jarosite dissolution of 94.6 calculated by van Breemen (1976) from the experimental data of Brown (1970). Ball et al. (1979) dismissed Brown's results due to what they considered to be large uncertainties and use instead a pK of 98.80 $\pm$ 1.1 that is the average of the values derived from work by Zotov et al. (1973), Vlek et al. (1979), and Kashkai et al. (1975). I chose to follow the rationale of Miller (1979),

preferring the lower value because in Brown's experimental conditions equilibrium was approached from supersaturation, a condition likely to occur in the tailings. One is immediately struck by the large size of the jarosite stability field for typical K^+, SO_4^{2-} and Fe^{2+} activities found in the low-pH tailings waters, and all of the samples with a pH below approximately 5 are grossly supersaturated. High degrees of jarosite supersaturation in acid mine drainage have been reported by other researchers (Nordstrom et al. 1979; Miller, 1979) and it is suggested that jarosite may precipitate only in favourable microenvironments (Nordstrom et al. 1979). The 5 data points with the lowest pH in Fig. 2.12 come from a piezometer nest in the Nordic West Arm tailings. These points fall close to the line of jarosite equilibrium and it is possible that at this location jarosite solubility is effective at controlling solution composition. However, although jarosite has been identified in old tailings (Kaiman, 1977) and could be precipitating, equilibrium with jarosite is not realized in most tailings groundwater.

A different interpretation of the upper limit of pe values measured in groundwaters from pyritic tailings was made by Boorman and Watson (1976). They attribute the pe of their low-pH ("oxidation zone") samples to control by the O_2 - H_2O_2 redox couple as described by the reaction proposed by Sato (1960):

$$O_2 + 2H^+ + 2e^- \text{ <==> } H_2O_2 \qquad Eh^0 = 0.682 \qquad (2.10)$$

For waters with low oxygen partial pressures Sato (1960) assumes a lower limit of unity for the H_2O_2:O_2 ratio, producing the equation:

$$pe = 11.54 - pH \qquad (2.11)$$

which has been plotted on Fig. 2.12. Redox control by this mechanism has received support in the literature (Beck; 1974), and Langmuir (1970), noting

that the pe of oxygenated waters usually fall far below that predicted by the equation

$$1/2\ O_2 + 2H^+ + 2e^- \langle==\rangle H_2O. \qquad (2.12)$$

observes that Sato's proposed reaction is rapid enough to act as a pe control. Control by the O_2- H_2O_2 couple has been indirectly challenged by Whitfield (1974) who expressed doubt that H_2O_2 exists in sufficient quantities to act as a pe control in the reaction

$$H_2O_2 + e^- \langle==\rangle OH + OH^- \qquad (2.13)$$

$$Eh^0 = 0.835V \text{ (Ives and Janz, 1961)}$$

Whitfield contends that many past researchers were measuring potentials influenced by oxidation of the platinum electrode surface, which produces a platinum oxide coating that responds to pH as described by the equation

$$Eh = Eh^0 - 0.06\ pH \qquad Eh^0 = 0.88V \qquad (2.14)$$

The line for this equation plots well above the tailings pe-pH values, and it is believed that the field measurements are reflective of the solution redox conditions. In view of the high iron activities in the tailings groundwaters and the controversy regarding the importance of the O_2- H_2O_2 redox couple, it is concluded that the measured potentials are controlled by the Fe^{2+} - Fe^{3+} redox couple close to equilibrium with jarosite and $Fe(OH)_{3A}$ or jarosite alone.

The aqueous chemistry of aluminum is very similar to that of iron, except it has only one oxidation state, Al^{3+}. It's solubility is therefore not dependent on the pe of the groundwater. While the solubility of Al^{3+} in most natural waters is limited by amorphous or crystalline aluminum hydroxide, aluminum concentrations are often controlled by basic aluminum sulfates in acid sulfate waters (Nordstrom 1982, van Breemen 1973, van Breemen 1976).

Solid phase controls on aluminum concentration in the Al - OH - SO_4 system can be illustrated by plotting pAl + 3pOH versus 2pH + pSO_4 (Fig. 2.13 modified from Nordstrom, 1982). The lines describing equilibrium with respect to alunite ($KAl_3(SO_4)_2$ OH_6), basaluminite ($Al_4(SO_4)OH_{10}.5H_2O$) jurbanite ($AlSO_4OH.5H_2O$), amorphous aluminum hydroxide ($Al(OH)_{3A}$) and gibbsite ($Al(OH)_3$) are shown in the diagram. It can be seen from the figure and SIs (Table 2.5) that in the high pH range (pH > 5.5) the Al concentrations are close to equilibrium with $Al(OH)_{3A}$. Note that in these young waters with rapidly changing pH gibbsite is ineffective at limiting Al concentrations. The trend toward $(Al(OH)_{3A}$ saturation at high pH can be shown more clearly by plotting pH versus SI (Fig. 2.14). Basaluminite appears to be supersaturated in these waters, indicating that if basaluminite precipitation is occurring, it is not effective at limiting Al concentrations. Jurbanite is also near saturation in these waters. When evaluating SIs, caution must be exercised due to the large error in activity product that can be generated by small analytical errors when the activity of a component is raised to a large exponent. Thus the SI for basaluminite, which has an IAP = $[Al]^4$ $[SO_4][OH]^{10}$, will be highly sensitive by errors in pH and Al measurement. This is particularly true in the neutral groundwaters in the tailings, which have concentrations of aluminum approaching the detection limit (0.3 ppm reported, Rio Algom Lab).

The amorphous aluminosilicate allophane ($[Al(OH_3]_{1-x}$ $[SiO_2]_x$) is slightly supersaturated in the neutral tailings groundwater. Allophane precipitation is supported by the fact that SiO_2 concentrations are depressed below the solubility product of amorphous silica in waters in which allophane is supersaturated (Table 2.5), and amorphous silica undersaturation has been

observed in other waters actively precipitating allophane (Wells, Childs and Downes, 1977). At lower pH values, allophane is undersaturated and silica control by SiO_{2A} is indicated by slight supersaturation with respect to this phase. Slight SiO_{2A} supersaturation in groundwaters in acid-leach uranium tailings was also observed by Bush and Markos (1981). They suggest that the supersaturation may be due to slow kinetics of precipitation or unaccounted-for silica complexing with Fe^{3+}. Calculations using a log K = 9.8 ± 0.3 for the complex $Fe(H_3SiO_4)^{2+}$ (Reardon, 1979) indicate that this complex does not exceed 1 mg/L in the ground water of the Nordic Main tailings area. The existence of another silica complex, $H_4SiO_4SO_4^0$ ($K = 10^{+0,576}$) has been postulated (Marshall and Chen 1982). This complex could account for only up to 5.7 mg/L of the excess SiO_2 in the tailings water and the cause of slight supersaturation remain unknown.

At pH values below 5.5 the tailings waters are undersaturated with respect to $Al(OH)_{3A}$. SIs show that basaluminite and jurbanite are both close to saturation (Table 5) in these waters and it is not clear which of these two phases is influencing solution composition. In two of the low pH waters (T6-1, T5-1) basaluminite is undersaturated and jurbanite appears to be limiting Al concentrations in solution. This contention is supported by Fig. 2.13, that shows a cluster of data points near the junction of the two phases and a trend following jurbanite equilibrium with decreasing pH. In all of these waters alunite is highly supersaturated (Fig. 2.13), however, the kinetics of alunite precipitation are extremely slow (Nordstrom, 1982) and Al solubility control by alunite does not occur.

It is obvious from the data that the Al chemistry is complex and involves many solid phases. While the above discussion addresses the solid

phases one at a time, it is likely that multiple equilibrium between aqueous Al and several solid phases occurs. This is especially true for the near neutral -pH waters that are subject to rapid changes in pH during migration due to H^+ consuming reactions. In addition, it is likely that disequilibrium occurs locally due to the inability of precipitation/dissolution reactions to keep up with changes in pH. In spite of the cloudy picture, a tentative set of conclusions can be made.

1. Amorphous $Al(OH)_3$ and allophane are probably controlling Al concentrations in the neutral groundwaters (pH > 5.5) and basaluminite and jurbanite precipitation may be occurring slowing due to the high So_4 activities.
2. In moderately acid waters (pH 4-5.5) basaluminite and jurbanite are close to equilibrium with the waters and may be precipitating.
3. As pH decreases below 4, basaluminite becomes increasingly undersaturated and jurbanite limits Al concentrations.

This sequence of aluminum solubility controls was originally proposed by Nordstrom (1982) and describes the observed data well.

Acid Neutralizing Processes

A major objective of this study is the definition of chemical reactions in the tailings that neutralize acidity produced by pyrite oxidation. Production of acidic high Fe^{2+} pore waters in small localized zones could be tolerated if the acid neutralizing capacity of the enclosing materials is large enough to neutralize the groundwater before it migrates out of the tailings area. As the surface water in the Elliot Lake area has very low buffer capacity, it is important to prevent the migration of low pH, high Fe^{2+} waters from the

tailings. The oxidation of pyrite can be represented by the following equation:

$$FeS_2 + 7/2\ O_2 + H_2O \rightarrow Fe^{2+} + 2SO_4^{2-} + 2H^+ \qquad (2.15)$$

It follows that we can examine the relative rate of downward movement of the low pH (high H^+ activity) water by contrasting it with the depth to which the other pyrite oxidation products, Fe^{2+} and SO_4^{2-}, have penetrated the tailings. As mentioned above, the peak concentration of iron and sulfate are located at greater depths in the tailings than the low-pH condition, indicating the presence of H^+- consuming reactions. Several mechanisms are probably involved in the pH neutralization including dissolution of calcium carbonate; dissolution of aluminosilicate minerals; and sorption of the H^+ onto tailings solids. Neutralization by dissolution of calcium carbonate introduced to the tailings as impurities in the line added during tailing discharge has been suggested by other researchers (Blair, 1981). The consumption of H^+ by calcium carbonate dissolution is described by the reaction

$$2H^+ + CaCO_{3(s)} \leftrightarrows Ca^{2+} + H_2CO_3 \qquad (2.16)$$

The above equation shows that 1 mole of calcium carbonate will neutralize 2 moles of hydrogen ions. Attention was focussed on evaluating the importance of this mechanism because it has a rapid rate of reaction and because it can maintain a high pH.

Results of the analyses for carbonate mineral content for cores from three locations on the Nordic Main tailings appear in Fig. 2.15 (see also appendix C). The data show a similar pattern of distribution of solid carbonate mineral at each site with weight percent carbonate values (wt % $CaCO_3$) varying from below detection (<0.001) to 0.009 wt. % to depths of

7.5 to 9 metres followed by an abrupt increase to values as high as 0.056 wt. %. The highest values of wt. % $CaCO_3$ found at depth are similar to the average of 0.06 wt. % for samples from the Williams Lake tailings area (Feenstra et al., 1981), and the value of 0.048 wt. % for recent tailings from Rio Algom's Quirke mill (R. Nicholson, personal communication). Although there is a strong correlation between small grain-size and high carbonate content in the Quirke and Williams Lake samples, no such relationship was found for the samples from the Nordic Main tailings. This lack of correlation with grain-size is probably due to the overwhelming control of depth on carbonate mineral content shown in figure 2.15 .

The sharply reduced carbonate mineral contents of the tailings at shallower depths are interpreted as the result of dissolution of calcium carbonate from the tailings solids by low-pH infiltration. The reduced amounts of carbonate mineral that remain at shallower depths is attributed to preservation by precipitated coatings of gypsum, ferric oxyhydroxides, or aluminum hydroxides; or to incongruent dissolution of $CaCO_3$ causing precipitation of siderite ($FeCO_3$) via the reaction:

$$Fe^{2+} + CaCO_{3(s)} \rightarrow Ca^{2+} + FeCO_{3(s)} \qquad (2.17)$$

Siderite thus precipitated will persist in the tailings to a lower pH than calcite because the high concentrations of ferrous iron in solution maintain siderite saturation.

One indirect check on the hypothesis of low-pH retardation by calcium carbonate dissolution is to compare the amount of pH retardation observed in the field with the amount of retardation predicted by equation 1 for the levels of calcium carbonate found in the tailings. For this comparison the observed retardation factor (R) can be calculated as the ratio of the groundwater velocity to the velocity of the low-pH front:

$$R=(v_{gw}/v_{pH}) \qquad (2.18)$$

$$R=[\ 1 + 2mCaCO_3/mH^+_{total}\ ] \qquad (2.19)$$

As the velocities are approximated by the depths of penetration of the recharge water and the low pH condition respectively, these positions must be accurately located. The leading edge of peak iron and sulfate concentrations has been used to delimit recharge waters (Blair, 1981, Feenstra et al., 1981), but transport of these ions may also be retarded due to precipitation reactions. It was found, however, that the original process water can be easily recognized at sites T2, T4, T5, and T6 by the high concentrations of chloride derived from process reagents (Fig. 2.16). At T1 no high-chloride water was found, probably because of the lack of a properly situated sampling point, and at T3 all of the process water has been replaced by recharge waters. At all other sites the position of the high-iron and sulfate fronts coincide with decreasing chloride concentration, indicating that iron and sulfate are not retarded by geochemical reactions. The position of the low-pH front is taken as that depth at which pH drops below 4.5, as most of the available carbonate mineral will have been removed by dissolution at that point. The retardation factors calculated in this manner vary from 1.3 to greater than 3 where the depths of penetration must be estimated (table 6).

In order to calculate the retardation predicted by equation 2.19 for known calcium carbonate levels, we have to define the total hydrogen ion content of the input solution. For the tailings water, if it is assumed that no iron oxidation occurs and ferrous iron hydrolysis is negligible, then the sum of the important acid-forming species can be written:

$$mH^+ \text{ total} = (mH^+ + 3m\ Al^{3+} + mHSO_4^-) \qquad (2.20)$$

The coefficient of 3 on the aluminum is derived from the assumption that all aluminum will be precipitated as amorphous $Al(OH)_3$ or allophane. Estimation of a meaningful input solution composition is difficult because the pyrite oxidation rate which controls solution composition has not been constant in time. It is useful, however, to estimate the input solution as the lowest pH water found below the water table at each site. Input solution composition was estimated from unsaturated zone samples at sites where no groundwater with pH <4.5 occurs below the water table. The resulting total hydrogen ion contents of the groundwaters calculated using eq. 2.20 (table 7) show the major source of acid to be precipitation of aluminum solid phases.

Retardation factors calculated using equation 2.19 and a calcium carbonate value representative of the Nordic Main alkaline tailings (0.02 wt. %) are presented on table 6. Comparison of the R values shows that the Rs calculated from equation 2.19 are close to the retardation factors calculated from the relative positions of the low-pH and high chloride fronts. This suggests that calcium carbonate content of the neutral tailings is on the order of 0.02 wt. %, and that neutralization of low-pH recharge water by calcium carbonate can account for the observed pH and iron profiles in the tailings.

A more direct comparison between observed and predicted retardation can be made by rearranging equation 2.19 to solve for the amount of calcium carbonate necessary to produce the observed retardation, applying the same assumptions regarding input H^+ concentration. Fig. 2.17 shows the results schematically, with the calculated wt. % $CaCO_3$ shown next to the line marking the position of the low-pH front. The values of wt. % $CaCO_3$ generated are very similar to those found in the Nordic Main tailings, and

we conclude that the proposed neutralization reaction describes the pH profile in the Nordic Main tailings well.

Summary of Conclusions

The findings of this study can best be summarized by first describing the characteristics of the physical hydrology then developing a scenario for the geochemical evolution of the groundwater in the Nordic Main tailings since the deposition of tailing ceased in 1968. Grainsize segregation of the tailings during deposition by slurrying produced a tailings mass with extremely variable physical properties. The hydraulic conductivity of the tailings is highly anisotropic due to fine scale layering of slime and sand layers, and there is field evidence for a large-scale trend of decreasing hydraulic conductivity with increased depth and increased distance from discharge point. Although hydraulic gradients in the tailings are dominantly downward, preliminary results of a computer model of the tailings flow system indicates dominantly horizontal flow to the south in the shallow tailings becoming more vertical with increasing depth. Flow is essentially vertical across the peat layer and horizontal again in the underlying aquifer.

The groundwater present in the tailings immediately after deposition ceased was a calcium sulfate water with a high pH. As the tailings began to drain, atmospheric oxygen moved down into the unsaturated zone, creating an environment favourable for pyrite oxidation. Initially the pyrite oxidation was probably slow due to the high pH of the tailings. Although Fe and SO_4 were released during this stage, the pH of the porewater remained high due to H^+ consumption by the dissolution of small amounts of calcium carbonate in the tailings. Dissolution of calcium carbonate also resulted in the

precipitation of gypsum and possibly siderite due to the release of Ca and CO_3^{2-}. Thus the first water recharging the tailings had increased amounts of Fe and SO_4 but a neutral pH.

Acidity produced by continued oxidation eventually consumed all of the carbonate minerals present near the surface of the tailings, and a low-pH zone developed in the absence of this pH buffer. Pyrite oxidation rate then increased in the favourable low-pH environment due primarily to the action of Thiobacillus ferrooxidans and the increased solubility of Fe^{3+}. Sampling from the zone of active pyrite oxidation in the Nordic Main has confirmed the presence of high concentrations of ferric iron, and oxidation of pyrite by ferric iron has probably been the most important mechanism of pyrite oxidation in the history of the tailings. An evaluation of the feasibility of using the sulfur isotopic composition of aqueous sulfate in the tailings as a tool for further determining pyrite oxidation mechanisms concluded that the method is inapplicable in the Nordic Main tailings due to the large amounts of sulfate, derived from the sulfuric acid leach, already present both in solution and as gypsum.

As the pH in the carbonate-mineral free zone near the surface declined, aluminosilicate minerals such as sericite dissolved, consuming H^+ and producing high concentrations of Al and SiO_2 in solution. In addition, heavy metals and the radionuclides uranium and lead-210 were mobilized by a combination of mineral dissolution and desorption by the low pH. This low-pH groundwater with high concentrations of contaminants then migrated downward encountering calcium carbonate. The pH-neutralization that occurs where the low pH water encounters carbonate minerals results in the precipitation of amorphous ferric hydroxide, siderite, aluminum hydroxide,

and basic aluminum sulfates. The oxidation potential of the groundwater is controlled by the iron system, and removal of Fe^{3+} by ferric hydroxide precipitation causes the pe of the groundwater to decrease as the pH increases. The nature of the aluminum solid phase precipitated is dependent on the pH of the groundwater, and as the low-pH water is neutralized, there is evidence that the following sequence of precipitates occurs: jurbanite ($AlSO_4OH \cdot 5H_2O$) at pH less than 4, basaluminite ($Al_4(SO_4)(OH)_{10} \cdot 5H_2O$) at pH greater than 4 but less than 5.5, and amorphous $Al(OH)_3$ and allophane at pH greater than 5.5. These minerals are in turn dissolved as the pH of recharging water continues to decline. Neutralization of the migrating low-pH water also causes the removal of the heavy metals and radionuclides from solution by the processes of sorption and coprecipitation.

The thickness of the zone from which carbonate minerals have been removed increases over time, and the boundary separating highly contaminated low-pH groundwater from neutral pH groundwater moves downward. However, due to the retarding effect of the pH neutralization and attendant precipitation and sorption reactions on the rate of transport of the heavy metals, radionuclides, and low-pH, the depth of penetration of these constituents lags behind the leading edge of the recharge water which is defined by a decrease in Fe and SO_4 coincident with increased chloride concentrations. This sequence of processes has produced the zonation of groundwater geochemistry that we now observe is most of the instrumented tailings sites and shown in Fig. 2.6: groundwater with a high pH and low iron concentrations at the base of the tailings overlain and slowly being displaced by high-iron water with high pH, which is in turn overlain by low-pH recharge water with high iron, heavy metal and radionuclide concentrations.

The extent to which low pH recharge waters have penetrated into the tailings is highly variable in space. In areas with high downward gradients replacement has been extensive and in some cases complete. This has occurred in the SW area of the Nordic Main tailings due to the coarse grain size of tailings deposited along the tailings embankments and the absence of a peat layer in this area. In addition, sampling in two older tailings areas indicates that in time acid production can completely deplete the H^+ neutralizing capacity of the tailings and pH values of less than two can result.

In the future the rate of pyrite oxidation will probably decrease due to a number of factors including pyrite removal from shallow depth and the formation of grain surface coatings. Indeed, at most sites in the Nordic Main tailings the peak concentrations of iron in groundwater is found well below the water table, and the iron concentrations in water recharging the water table are declining. This indicates that the period of most rapid pyrite oxidation is past and the rate of pyrite oxidation has been decreasing recently. However, the data show that even reduced rates of pyrite oxidation will cause serious water quality degradation when the pH buffer capacity of the tailings is depleted. While H^+ consumption by carbonate mineral dissolution and it's affect on contaminant transport in the tailings is fairly well understood, much work remains to be done on pH^+ neutralization by the dissolution of aluminosilicate minerals and secondary aluminum and iron solid phases before the advanced stages of tailings acidification will be understood.

List of Tables in Chapter 2

Table

2.1 Chemical analyses of water samples from the Nordic tailings (piezometer nest T6) and Quirke tailings area.

2.2 Results of radionuclide analyses for water samples from piezometer nest T6, Nordic Main tailings area.

2.3 Calculated ion activity products (IAP) of $Fe(OH)_3$ for water samples from the Nordic Main tailings area.

2.4 Siderite saturation indicies for water samples from three piezometer nests on the Nordic Main tailings.

2.5 Saturation indicies for selected Al and Si-bearing minerals at piezometer nests T4, T5 and T6, Nordic Main tailings.

2.6 Comparison of observed and calculated retardation factors.

2.7 Calculation of H^+_{total} for hypothetical input solution.

List of Figures in Chapter 2

Figure

2.1 Design of piezometer tips used in tailings.

2.2A Schematic cross-section of the Nordic Main tailings.

2.2B Location map and monitoring sites at the Nordic Main and Nordic West Arm tailings.

2.3 Map of depth-to-water table, Nordic Main tailings.

2.4 Depth to static water level in piezometer nests in the Nordic Main tailings.

2.5 Cross sections of the Nordic Main tailings showing A) stratification and permeabilities, B) finite element grid, and C) potential field generated by the computer model.

2.6 Profile of groundwater geochemistry at piezometer next T6, Nordic Main tailings.

2.7 Profiles of ^{226}Ra activity in groundwaters from piezometer nests T1, T2, T4 and T5, Nordic Main tailings.

2.8 Profiles of groundwater geochemistry at piezometer nests T3, UW14 and UW6 showing pH and concentrations of cobalt, iron and sulfate.

2.9 Profile of pore water geochemistry at piezometer nest

T5 showing the change in iron speciation with depth.

2.10 Sulfur isotopes for pore water at piezometer nest T6, Nordic Main tailings.

2.11 pe-pH plot for iron speciation in groundwaters from piezometer nest T6, drawn for [Fe] = $10^{-4,05}$ iron, PCO_2 of 10^{-2}, pK of $Fe(OH)_3$ = 38.5.

2.12 pe-pH plot for iron species and solid phases for groundwaters from the Nordic Main, Nordic West Arm, and Lacnor tailings.

2.13 Values of (pAl + 3pOH) plotted versus (2 pH + pSO_4) for 21 analyses of ground waters from the Nordic Main tailings shown in relation to the solubility curves of several Al containing solid phases.

2.14 Plot of pH versus saturation index for amorphous aluminum hydroxide (pK = 31.61).

2.15 Profiles of carbonate mineral content in tailings solids at T1, T5, and T6, Nordic Main tailings.

2.16 Concentration of Cl in pore waters at piezometer nests T1 through T6, Nordic Main tailings.

2.17 Schematic of piezometer nests T1, T5, and T6 showing depth of penetration of the recharge front depth of penetration of the low-pH condition, and the weight percent

calcium carbonate predicted for the observed retardation. Predicted position of the pH front for a representative wt. % $CaCO_3$=0.02 shown as a dotted line.

Tables in Chapter 2

Table 2.1

Chemical analyses of water samples from the Nordic Main tailings (piezometer nest T6) and Quirke tailings area (neutralized tailings) (all analyses mg/L except pH and pe, or as noted)

	lab	Neutralized Tailings*	T6 12 m	T6 8.3 m	T6 4.6 m
pH	field	10.9	6.5	5.66	3.99
pe	field	-	1.64	5.52	7.69
Fe total	2	1.4	290	6,030	1,710
Al	2	< 3.0	0.3	41	116
SiO_2	1	-	13.8	51.5	125
Ca	2	612	450	388	432
Mg	2	0.35	488	286	24
Na	2	36	69	16	2.9
K	2	142	156	206	31
SO_4	1	1325	3905	14,100	4,800**
PO_4	1	-	< 2.0	< 2.0	< 2.0
Cl	1	14	136	32.3	4.2
F	1	-	2.9	32.4	2.6
Cu	2	0.06	< 0.01	< 0.01	0.02
Zn	2	0.04	0.1	8.0	0.52
Ni	2	< 0.09	0.39	9.1	1.4
Co	2	< 0.09	0.13	7.1	1.6
Pb	2	< 0.17	0.1	0.49	2.6
Mn	2	0.04	4.4	8.0	0.54
Alk (as HCO_3^-)	field	-	662	95	-
Ra TOTAL pCi/L		1679[2]	117[3]	412[3]	95[3]
NO_3		575	-	-	-

** SO_4 value adjusted to achieve charge balance

* analysis done by Rio Algom Laboratory, March 1977, A.J. Vivyurka, written communication

1. University of Waterloo laboratory
2. Rio Algom Environmental Control laboratory
3. ^{226}Ra, Monenco Analytical laboratory

Table 2.2

Results of radionuclide analyses for water samples from piezometer nest T6, Nordic Main Tailings area (all results are activities except uranium which is expressed in µg/L; precision represented as ± 1 standard deviation).

Piezometer Depth m	Pb^{210} ±10%	Th^{228}	Th^{230}	Th^{232}	Ra^{226}	µg/L Uranium
4.6	1708.	6.±2.	19.±5.	4.±2.	95.±7.	1360.
6.3	1265.	2.±1.	6.±2.	≤0.5	67.±4.	5000.
7.1	2746.	6.±2.	3.±1.	≤0.5	135.±3.	5200.
8.3	203.	22.±5.	6.±2.	1.±0.5	412.±4.	440.
9.3	37.	9.±3.	1.±0.5	≤0.5	111.±7.	78.
10.6	63.	6.±2.	13.±4.	4.±2.	129.±5.	36.
12.0	55.	5.±2.	4.±2.	1.±0.5	117.±5.	44.
13.3	51.	8.±2.	1.±0.5	≤0.5	100.±5.	48.

Table 2.3

Calculated ion activity products (IAP) of $Fe(OH)_3$ for water samples from the Nordic Main tailings area.

Piezometer Nest and Depth (m)	activity Fe^{3+}	activity OH^-	-log IAP
T4- 1.7	4.79×10^{-10}	1.70×10^{-10}	38.6
- 2.0	2.61×10^{-8}	6.97×10^{-11}	38.1
- 3.2	1.17×10^{-9}	1.59×10^{-10}	38.3
- 4.0	8.13×10^{-14}	2.36×10^{-9}	39.0
- 5.2	1.85×10^{-8}	4.87×10^{-9}	32.7
- 6.0	8.98×10^{-14}	2.62×10^{-9}	38.8
- 7.0	4.97×10^{-15}	1.23×10^{-8}	38.0
- 8.8	2.10×10^{-11}	4.20×10^{-9}	35.8
-10.0	1.12×10^{-15}	3.90×10^{-8}	37.2
-13.2	1.18×10^{-17}	3.59×10^{-7}	36.3
-18.0	2.54×10^{-15}	1.64×10^{-8}	38.0
T5- 4.7	1.22×10^{-7}	3.24×10^{-11}	40.4
- 5.6	5.06×10^{-6}	2.00×10^{-12}	38.4
- 8.0	1.35×10^{-11}	3.09×10^{-9}	36.4
- 9.1	2.91×10^{-13}	1.16×10^{-9}	37.6
- 9.9	8.21×10^{-15}	5.50×10^{-9}	38.9
-12	1.37×10^{-12}	3.57×10^{-9}	37.2
-14	3.71×10^{-17}	3.35×10^{-8}	38.9
T6- 4.6	1.70×10^{-8}	4.49×10^{-11}	38.8
- 6.3	3.38×10^{-8}	3.73×10^{-11}	38.8
- 7.1	3.03×10^{-8}	7.16×10^{-11}	38.0
- 8.3	2.64×10^{-10}	1.78×10^{-9}	35.8
- 9.3	4.60×10^{-13}	5.00×10^{-9}	37.3
-10.6	1.04×10^{-14}	2.67×10^{-8}	36.7
-12.0	2.11×10^{-16}	2.21×10^{-8}	38.6
-13.3	9.51×10^{-15}	1.59×10^{-8}	37.4

Table 2.4

Siderite saturation indices for water samples from three piezometer nests on the Nordic Main tailings (all depths in metres)

T4		T5		T6	
Depth	SI	Depth	SI	Depth	SI
4.0	1.111	8.0	1.728	8.3	0.881
6.0	1.218	9.0	0.916	9.3	1.423
7.0	0.338	9.9	1.746	10.6	0.978
8.8	1.056	12.0	1.245	12.0	1.602
10.0	0.809	14.0	1.136	13.3	1.521
13.2	0.815				
18.0	1.497				

Table 2.5 Saturation indices for selected Al and Si - bearing minerals at piezometer nests T4, T5, and T6 (arranged by pH).

	Depth (m)	pH	Jurbanite $AlSO_4OH$ pK = 17.23[1]	Basaluminite $Al_4(SO_4)(OH)_{10}$ pK = 117.3[2]	Amorphous $Al(OH)_3$ pK = 31.611[3]	Amorphous SiO_2 pK = 2.71[4]	Allophane $[Al(OH)_3]_{1-x}[SiO_2]_x$ pK^5
T4	2.0	4.06	1.40	0.25	-2.57	0.09	-0.44
	3.2	4.40	1.32	1.70	-2.02	-- NO SiO_2 ANALYZED --	
	1.7	4.55	0.80	1.39	-2.20	0.02	-0.38
	4.0	5.80	0.67	7.29	-0.40	-0.33	0.39
	6.0	5.90	0.62	7.44	-0.44	-0.23	0.49
	8.8	6.05	0.28	7.24	-0.29	-0.51	0.44
	7.0	6.50	-0.78	6.36	-0.19	-0.70	0.52
	9.4	6.85	-1.24	5.73	-0.07	-0.52	0.60
	10.0	7.09	-1.81	5.42	-0.34	-0.88	0.66
	13.2	8.00	-3.49	4.36	-0.03	-0.57	1.17
T5	5.6	2.31	0.89	-10.96	-6.55	0.51	-0.33
	4.7	3.85	1.84	0.07	-3.02	0.10	-0.48
	8.0	5.49	0.29	5.00	-0.86	-0.27	0.10
	12.0	5.98	0.56	8.04	-0.11	-0.37	-0.58
T6	6.3	3.91	1.88	0.56	-2.87	0.15	-0.42
	4.6	3.99	1.36	-0.32	-2.99	0.16	-0.46
	7.1	4.30	2.11	3.74	-2.10	0.14	-0.19
	8.3	5.66	2.05	11.50	0.58	-0.18	0.94
	9.3	5.90	-0.39	3.15	-0.97	-0.29	-0.10
	12.0	6.51	-1.80	2.26	-0.72	-0.86	-0.16

1. Rawajfih, 1975
2. Singh, 1969
3. Latimer, 1952
4. Morey et al., 1965
5. log K = -5.71 + 1.68 pH, Paces, 1975

Table 2.6

Comparison of observed and calculated retardation factors

Piezometer Nest	Depth to high Cl water (m)	Depth to low pH water (<4.5), m	R, Ratio of Depths	R, calculated for 0.02 wt % $CaCO_3$
T1	< 7.5 [1]	2.5 [2]	3+	1.54
T3	< 9 [1]	3.0 [2]	3+	2.04
T4	6	3.5	1.7	1.87
T5	12	7	1.7	1.10
T6	10	7.5	1.3	1.17

[1] minimum depth of penetration; no high Cl water encountered

[2] estimated from unsaturated zone data of D. Smythe, Part I, this report.

Table 2.7

Calculation of H^+ TOTAL for hypothetical input solution (on a per litre basis)

	mH^+	$3mAl^{3+}$	$mHSO_4^-$	mH^+ TOTAL
T1*	0.0003	0.020	0.001	0.0213
T3*	0.001	0.009	0.001	0.011
T4	0.0001	0.0129	0.0001	0.0131
T5	0.002	0.107	0.005	0.114
T6	0.0001	0.066	0.0001	0.0662

* At these sites there was no ground water with a pH < 4.5 below the water table, so an input solution chemistry was estimated from the analyses of unsaturated zone samples from D. Smythe, part I of this report.

Figures in Chapter 2

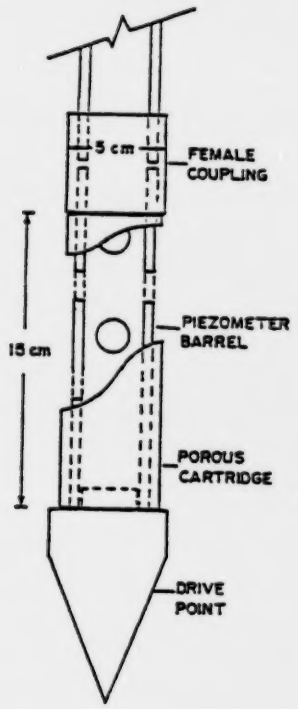

Figure 21- Design of piezometer tips used in tailings (Blair et al, 1980).

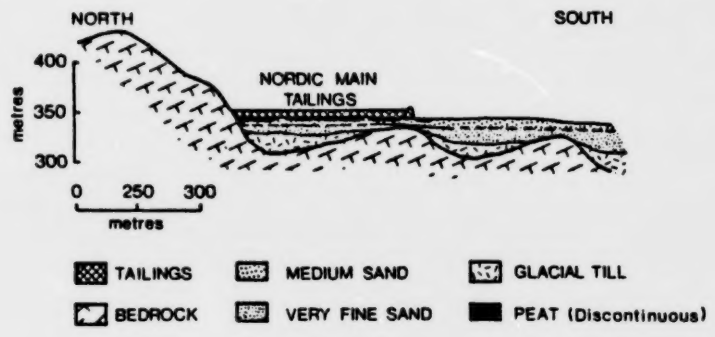

Fig. 2.2A Schematic cross-section of the Nordic Main tailings

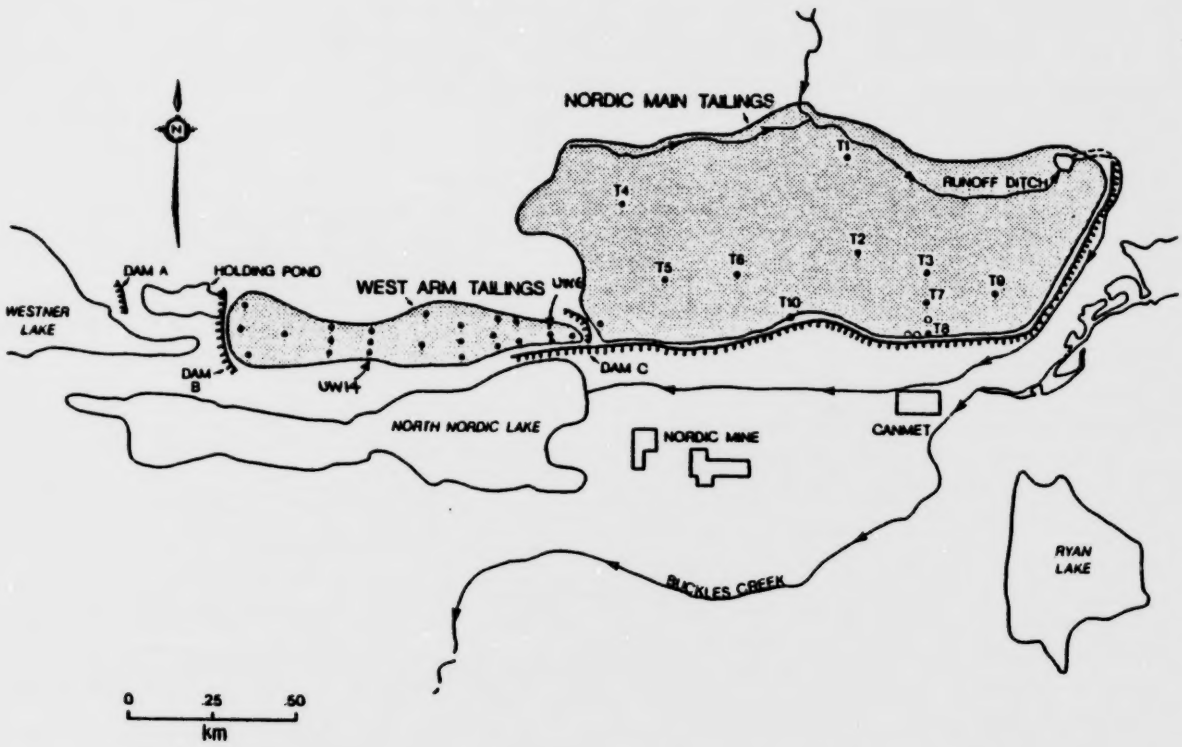

Fig. 2.2B Location map and monitoring sites at the Nordic Main and Nordic West Arm tailings.

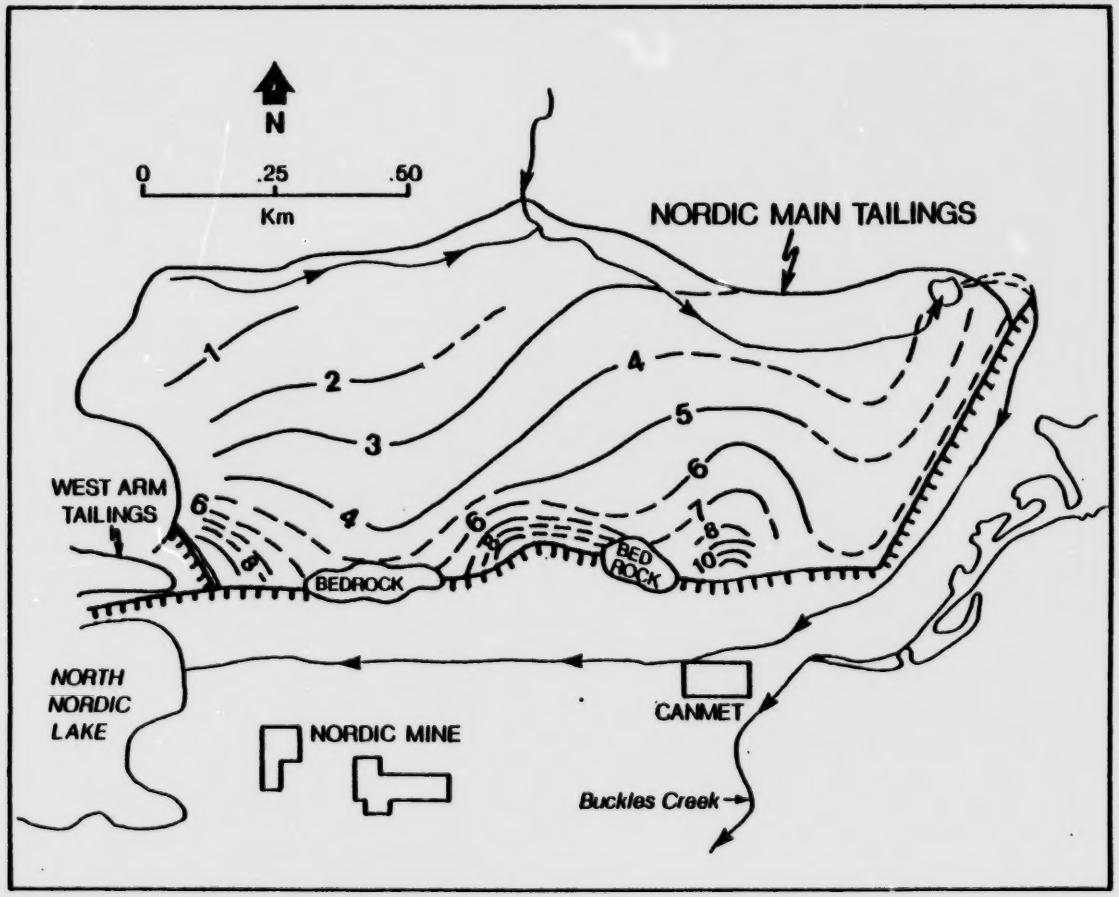

Fig.2.3 Map of depth-to-water table: Nordic Main tailings (contour interval one metre).

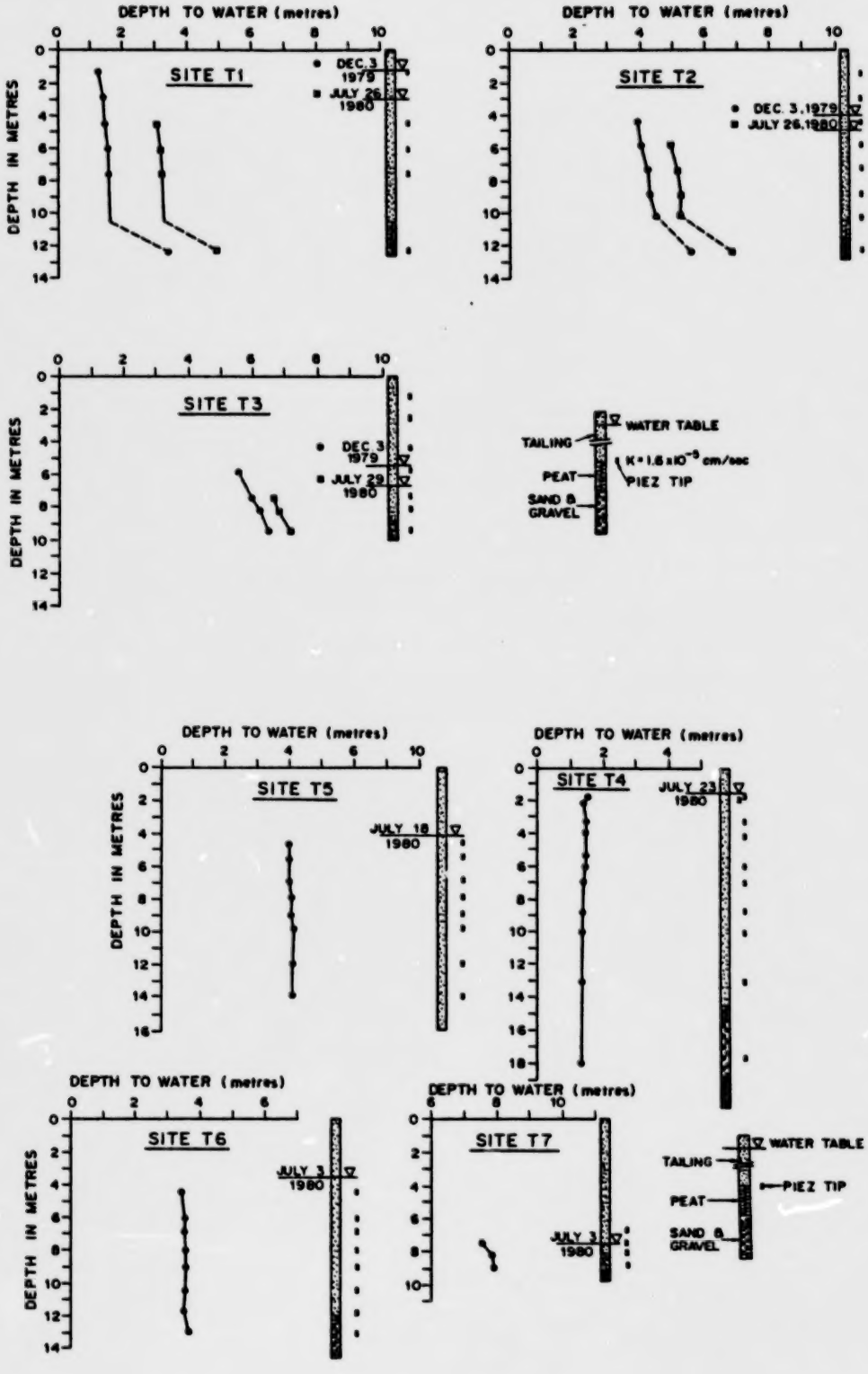

Fig. 2.4 Depth to static water level in piezometer nests in the Nordic Main tailings

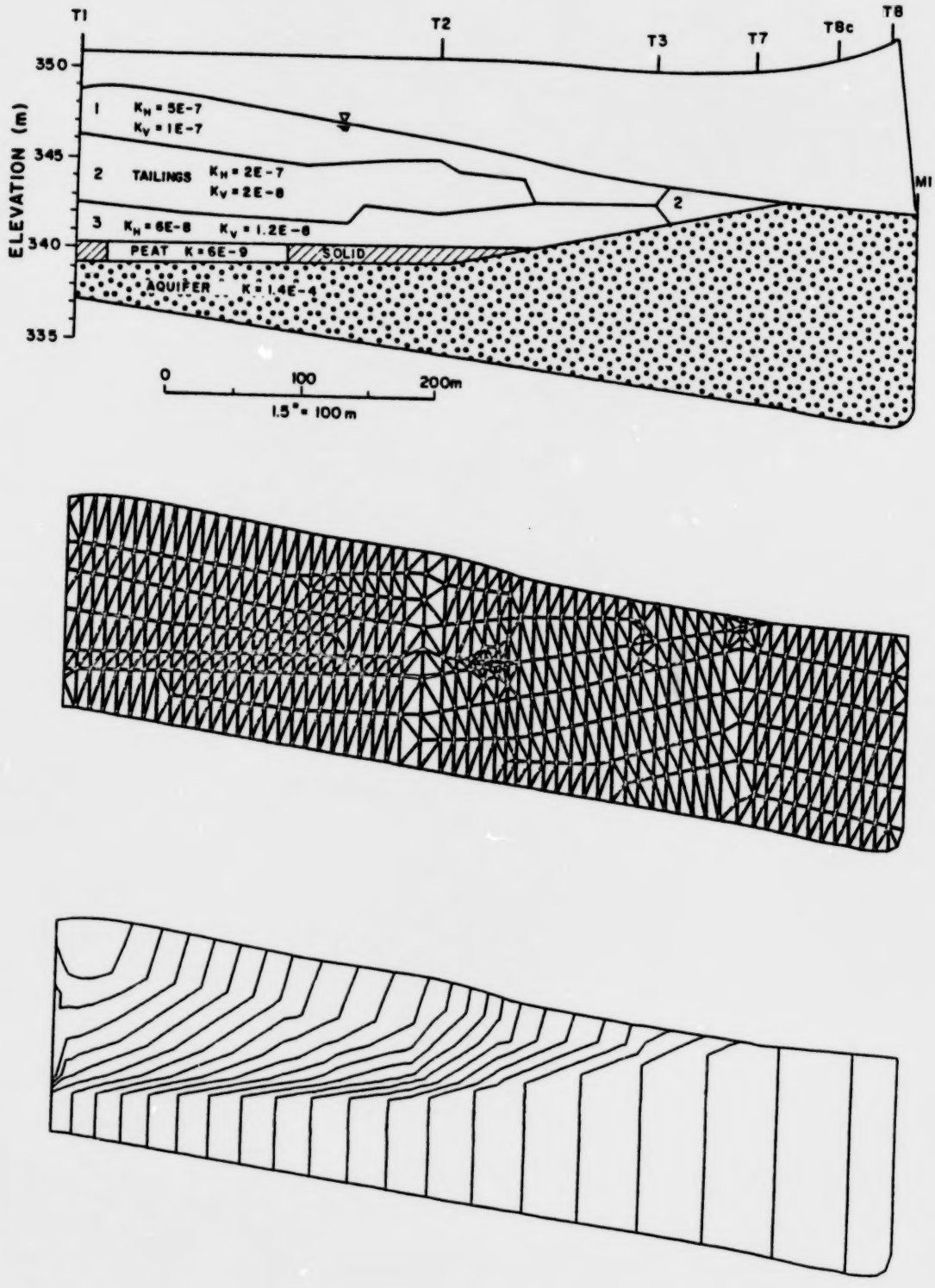

Fig. 2.5 Cross sections of the Nordic Main tailings showing A) stratification and permeabilities, B) finite element grid, and C) potential field generated by the computer model.

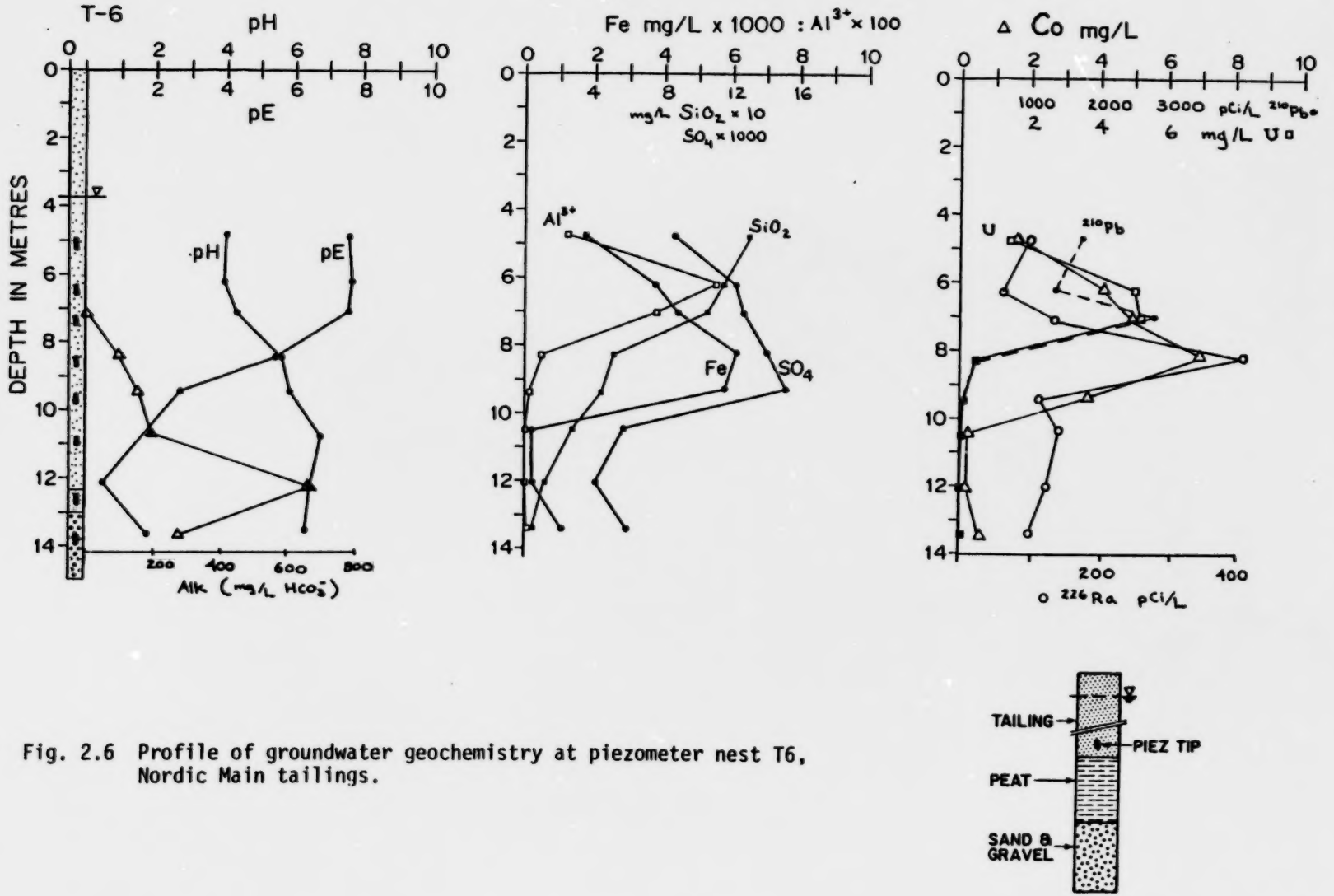

Fig. 2.6 Profile of groundwater geochemistry at piezometer nest T6, Nordic Main tailings.

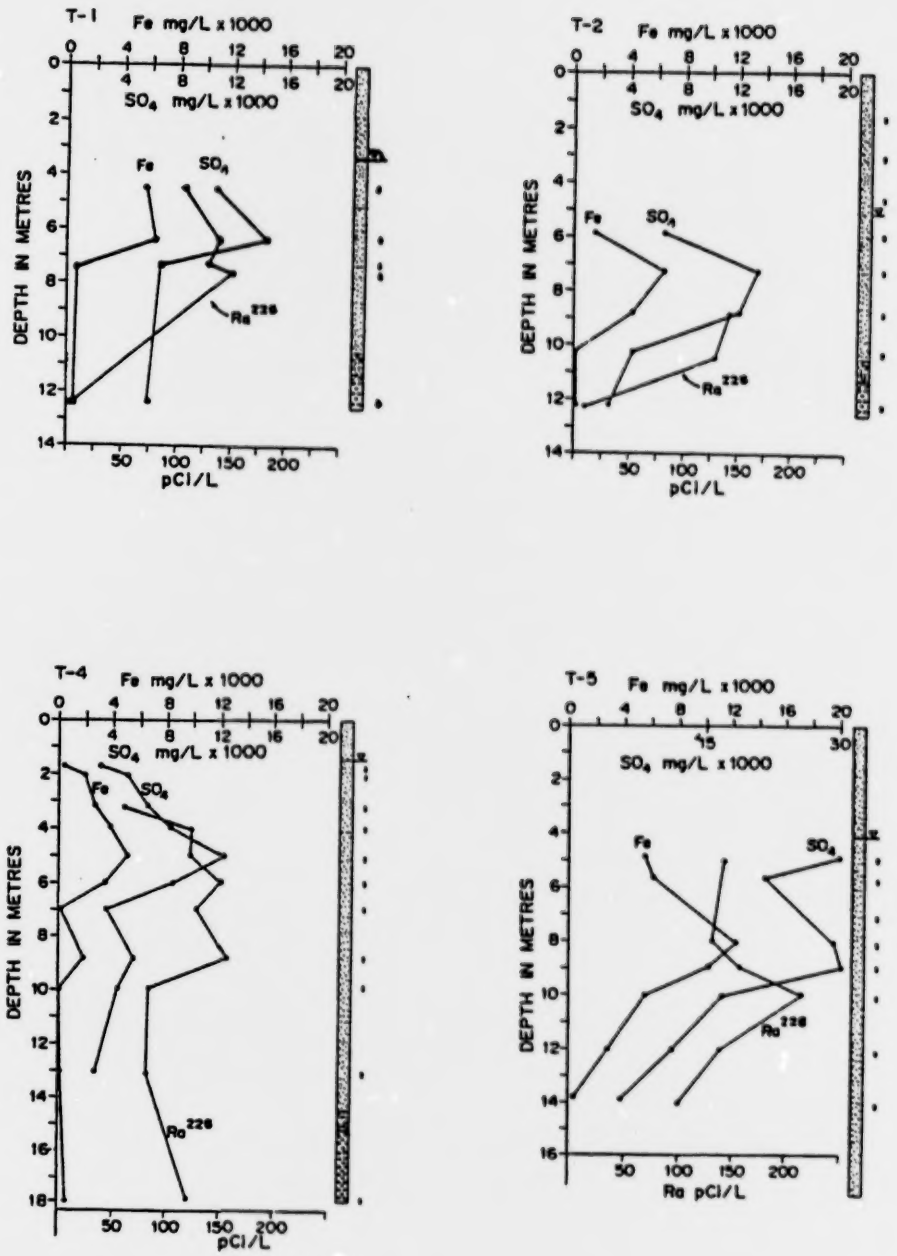

Fig. 2.7 Profiles of ^{226}Ra activity in groundwaters from piezometer nests T1, T2, T4, and T5, Nordic Main tailings.

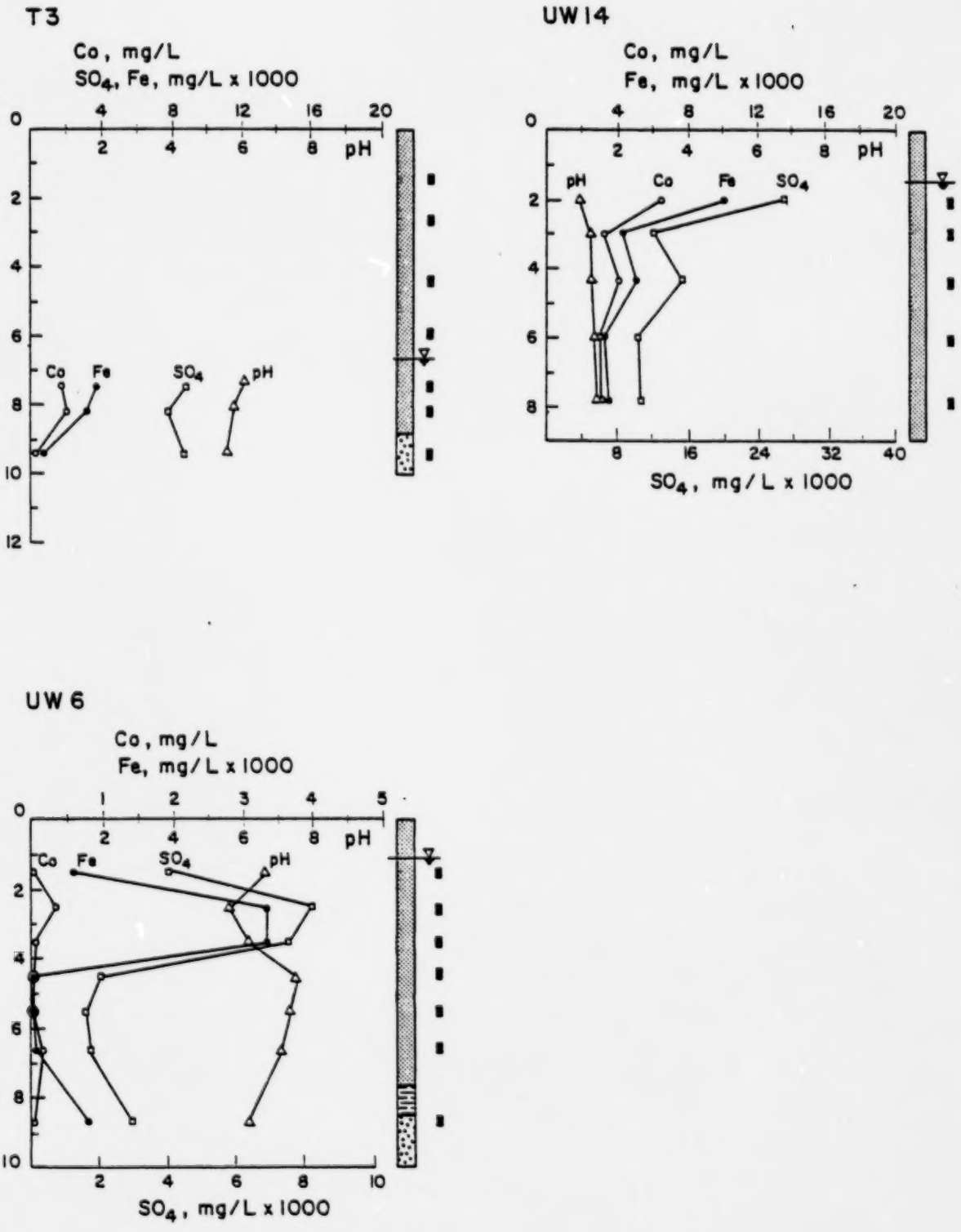

Fig. 2.8 Profiles of groundwater geochemistry at piezometer nests T3, UW14, and UW 6 showing pH and concentrations of cobalt, iron and sulfate.

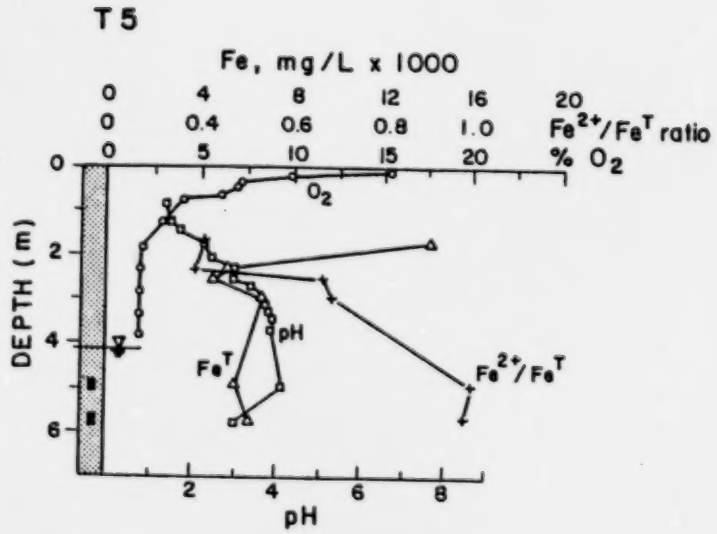

Fig. 2.9 Profile of pore water geochemistry of piezometer nest T5 showing the change in iron speciation with depth.

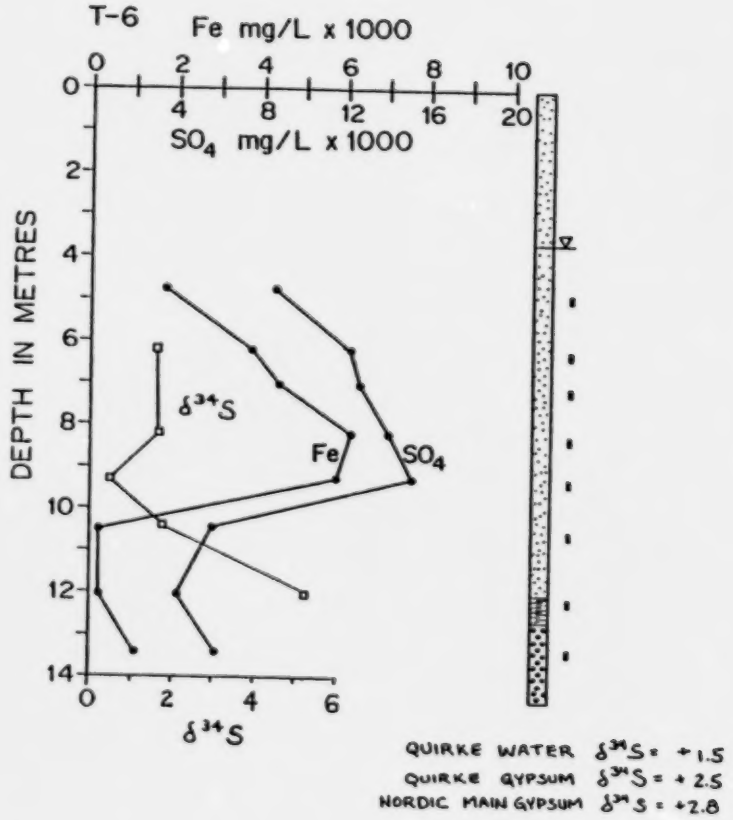

Fig. 2.10 Sulfur isotopes for pore water at piezometer nest T6, Nordic Main tailings

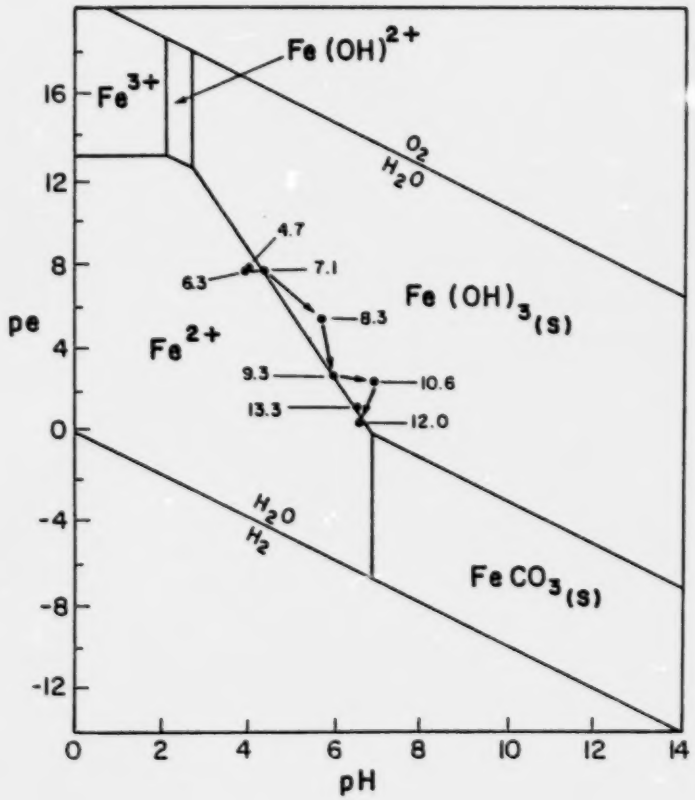

Fig. 2.11 pe-pH plot for iron speciation in groundwater from piezometer nest T6, drawn for [Fe] = $10^{-4.05}$ iron, PCO_2 of 10^{-2}, pK of $Fe(OH)_3$ = 38.5

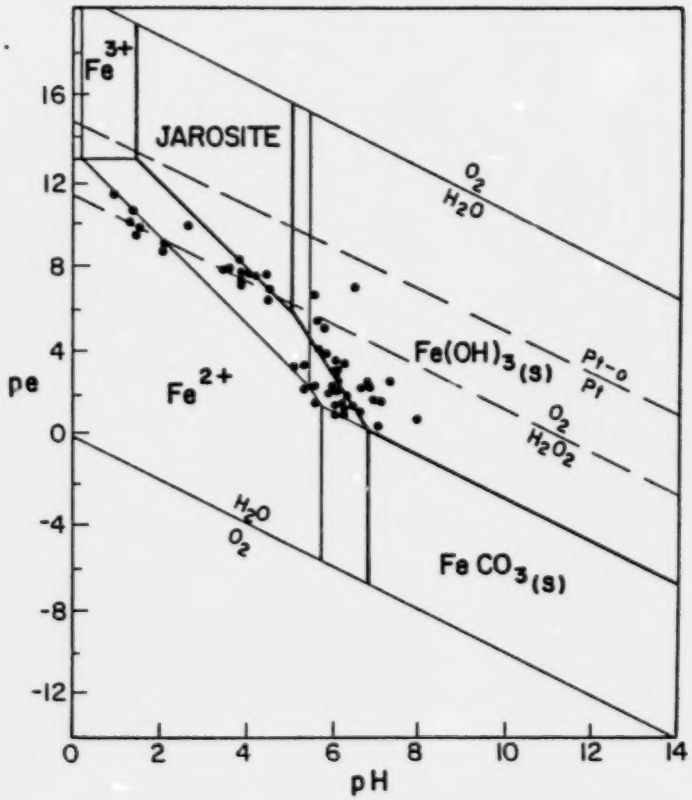

Fig. 2.12 pe-pH plot for iron species and solid phases for groundwaters from the Nordic Main, Nordic West Arm, and Lacnor tailings. Heavy line defines fields drawn for [Fe] = $10^{-4.05}$, [K] = 10^{-3}, [SO_4^{2-}] = 10^{-2}, pK of $Fe(OH)_3$ = 38; thin line [Fe] = $10^{-1.79}$, [K] = $10^{-2.5}$, [SO_4] = $10^{-1.8}$, pK of $Fe(OH)_3$ = 38.

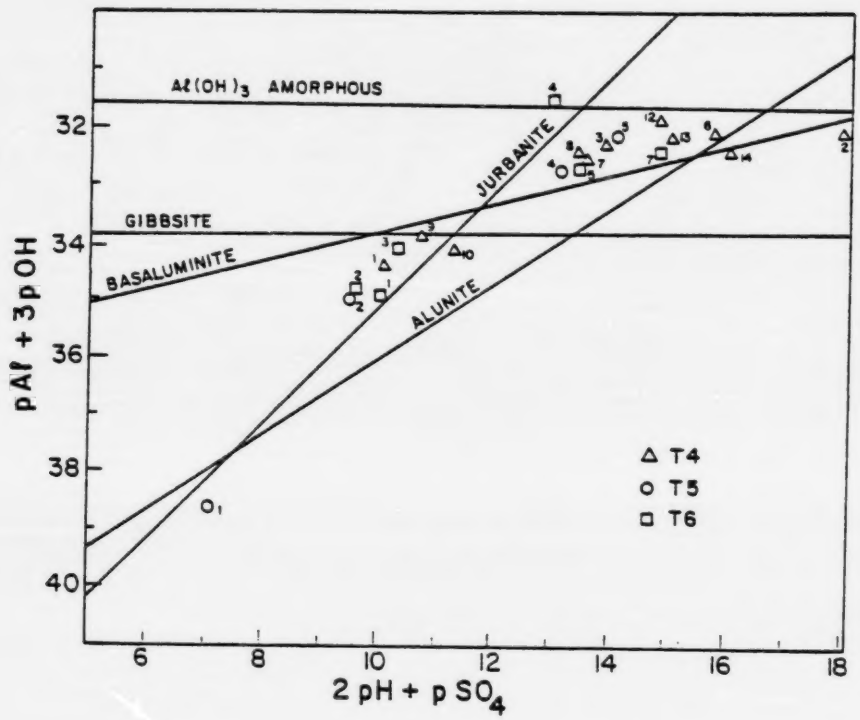

Fig. 2.13 Values of ($_p$Al + 3pOH) plotted versus (2pH + pSO_4) for 21 analyses of ground waters from the Nordic Main tailings, shown in relation to the solubility curves of several Al containing solid phases (modified from van Breeman, 1972). Equilibrium constants used: $pKAl(OH)_3$ = 31.611; pK Gibbsite = 33.9; pK Alunite = 85.4, Adams and Rawajfoh (1977); pK Basaluminite = 117.3, Singh and Brydon, 1970; pK Jurbanite = 17.23, van Breeman 1973.

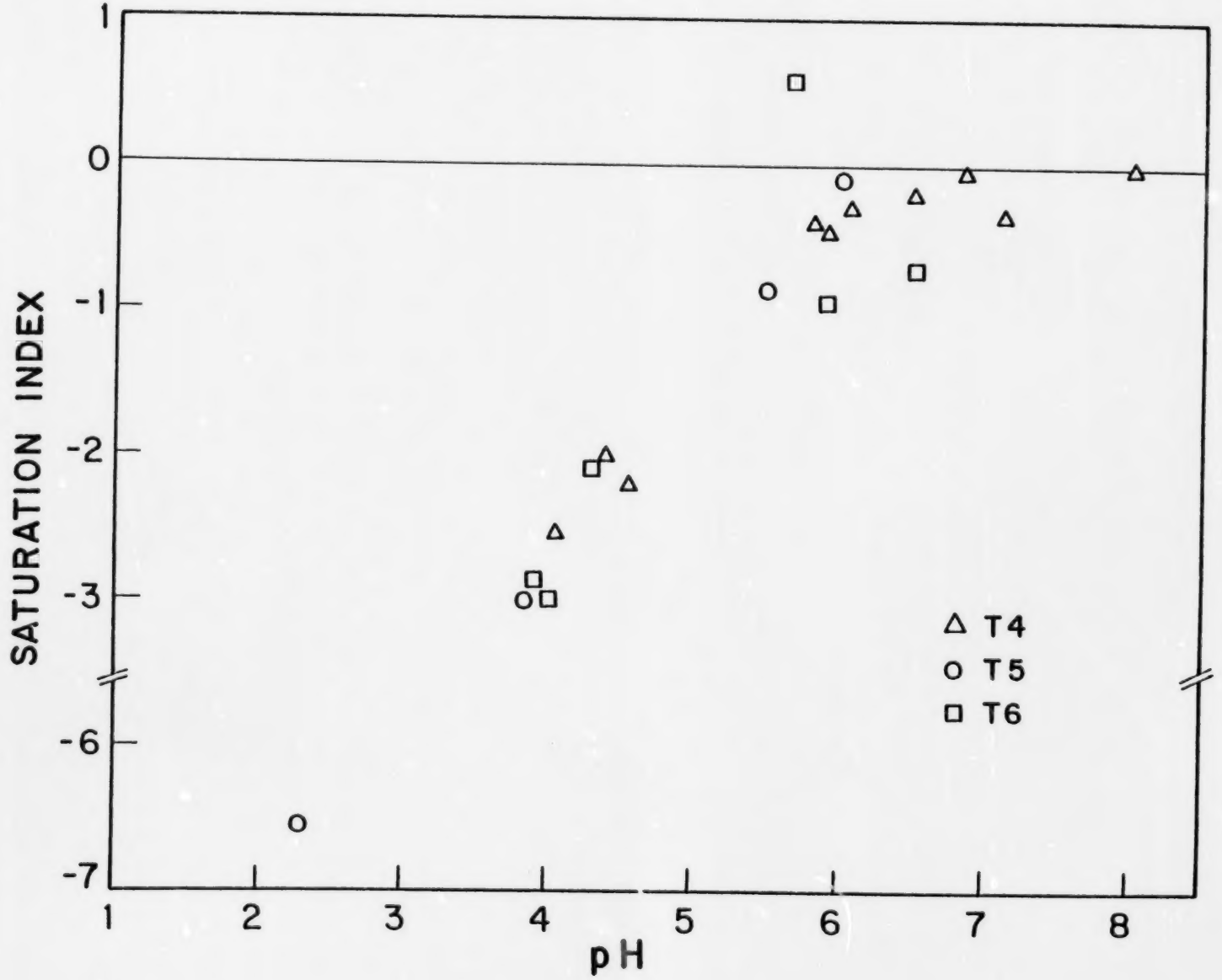

Fig. 2.14 Plot of pH versus saturation index for amorphous aluminum hydroxide (pK = 31.61)

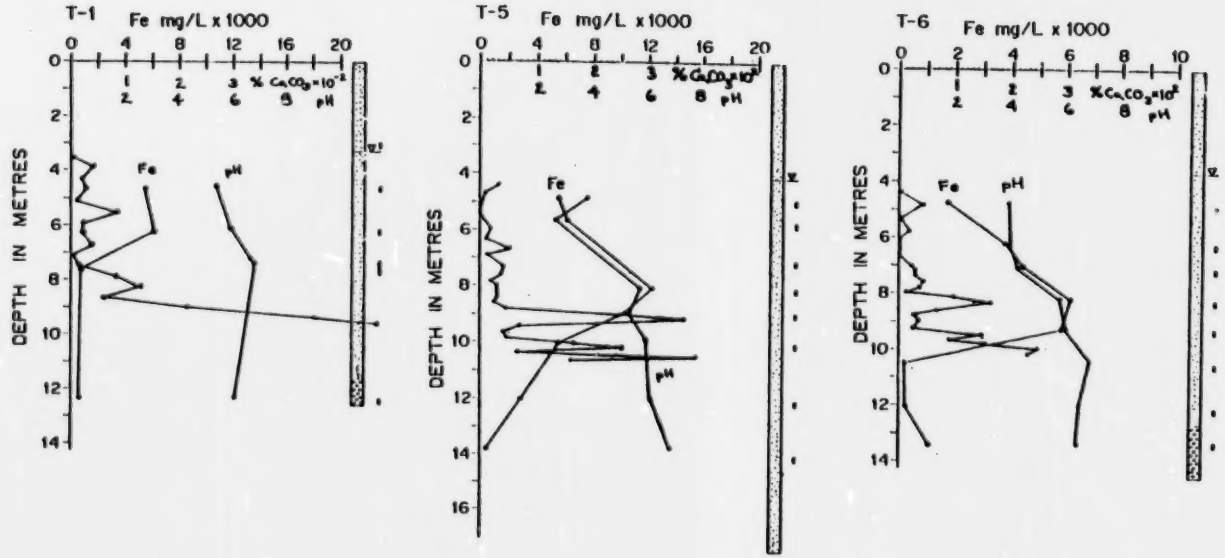

Fig. 2.15 Profiles of carbonate mineral content in tailings solids at T1, T5, and T6, Nordic Main tailings.

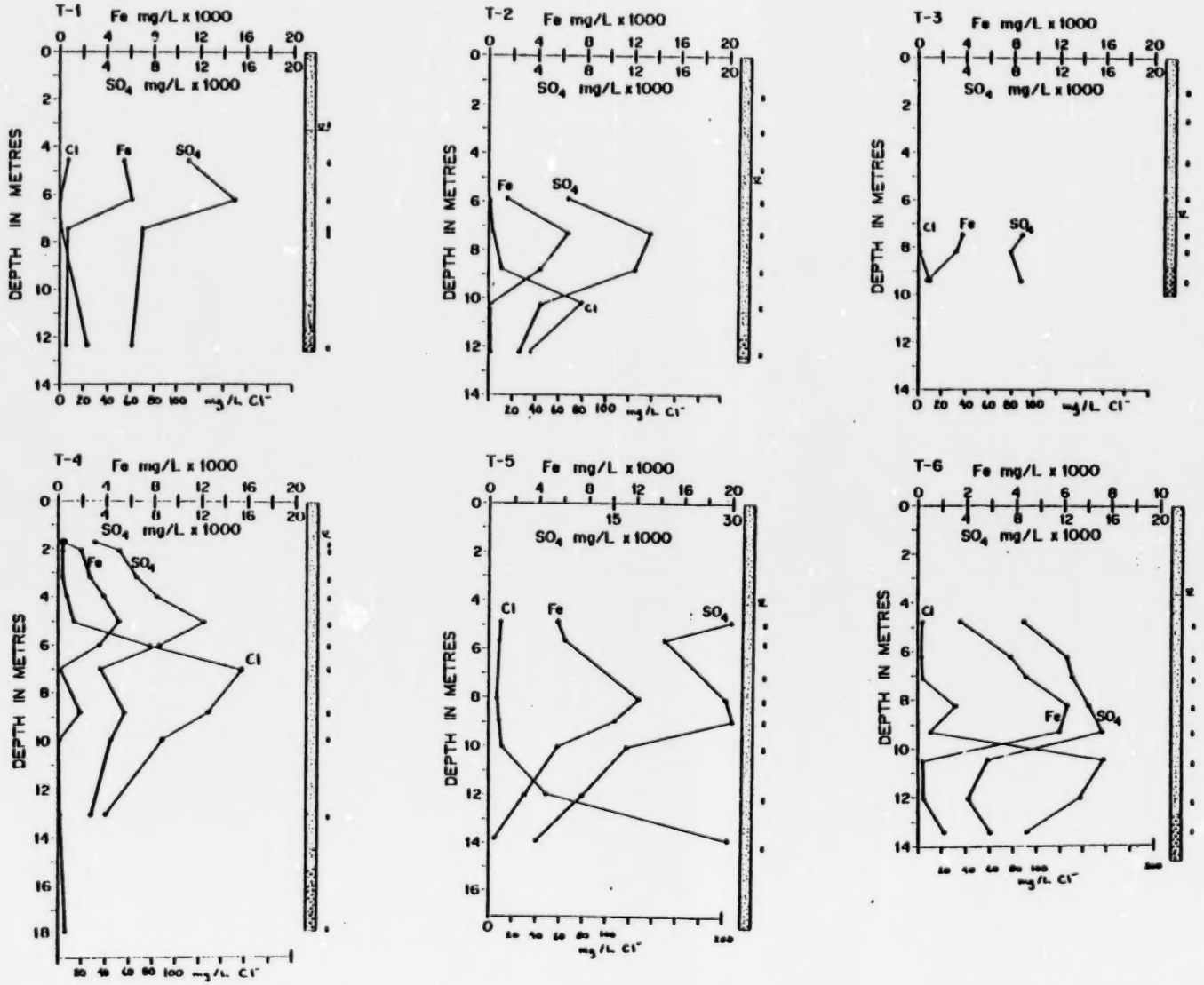

Fig. 2.16 Concentration of Cl^- in pore waters at piezometer nests T1 through T6, Nordic Main tailings.

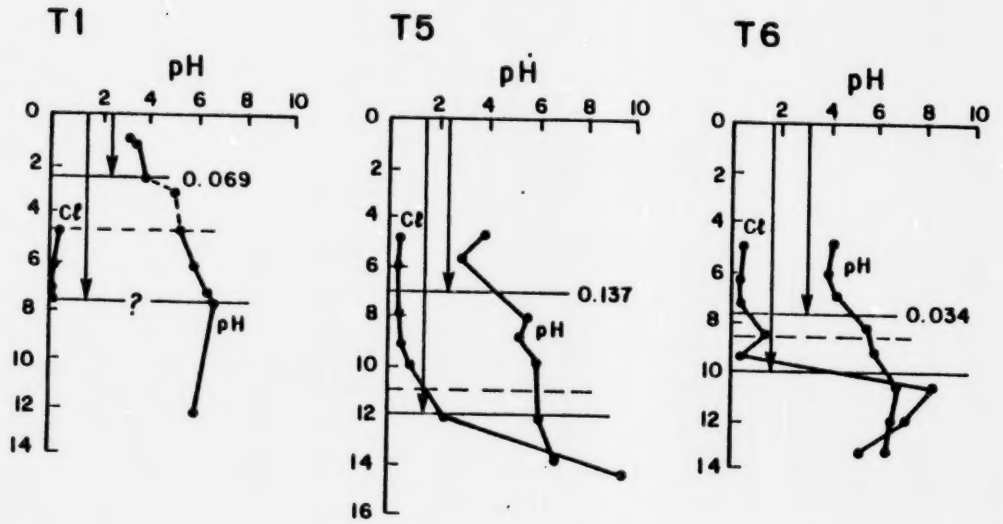

Fig. 2.17 Schematic of piezometer nests T1, T5, and T6 showing depth of penetration of the recharge front, depth of penetration of the low-pH condition, and the weight percent calcium carbonate predicted for the observed retardation. Predicted position of pH front for a representative wt. % $CaCO_3$ = 0.02 shown as dotted line.

LABORATORY INVESTIGATION OF FACTORS AFFECTING PYRITE OXIDATION

Introduction

Preliminary investigations of the uranium tailings impoundments at Elliot Lake indicated that oxidation of milled pyrite was responsible for acidification of the pore water in the shallow subsurface . Significant pyrite oxidation was found to occur in the uppermost one-half to one metre of tailings where the pH values of the pore water was as low as 0.9 . Because acid production and accompanying elevated concentrations of sulphate, iron and other metals in the infiltrating pore water are detrimental to groundwater and surface-water quality in the region, study of the pyrite oxidation process was extended.

Information gathered in a literature search of pyrite oxidation and related topics has shown that a number of critical variables control the rate at which pyrite is oxidized when exposed to near earth-surface conditions. Because pyrite is thermodynamically unstable under these conditions and will decompose spontaneously, it is only the rate factor that determines the extent of oxidation. The nature of the pyrite oxidation process and the effects of important variables on the reaction rates are discussed below.

Literature Review

Evidence presented in chapters 1 and 2 of this report and by Cherry et al. (1980) suggest that pyrite oxidation occurs within about 50 cm. of the surface of the tailings. Gas phase sampling indicated that, within probable sampling error, oxygen was depleted in the soil gas across an interval as small as 10 cm. in the first one-half to one metre depth. Results in chapter 1 show CO_2 gas increases relative to N_2 with depth in the tialings where the CO_2 is likely generated by the dissolution of residual carbonate material that originated in the lime slurry added to the tailings prior to disposal. Tailings pore water pH values as low as 0.9 were observed within tens of centimetres of the surface.

Pyrite oxidation can occur in a number of ways including, 1: Inorganic with a) oxygen and b) ferric iron, and 2: Microbial a) direct and b) indirect. Inorganic oxidation of pyrite by oxygen can be summarized by the stoichiometric reaction;

$$FeS_2(s) + 7/2\ O_2 + H_2O \Longrightarrow Fe^{2+} + 2SO_4^{2-} + 2H^+ \qquad (3.1)$$

(Singer and Stumm, 1970) The mechanisms of this reaction are not known but the overall stoichiometry is consistent with equation 3.1. Inorganic pyrite oxidation by ferric iron is only significant at low pH values due to the strong dependence of ferric-ion solubility on pH. The reaction may be written aerobically as

$$FeS_2(s) + 2Fe^{3+} + 2H_2O + 3O_2 \Longrightarrow 3Fe^{2+} + 2SO_4^{2-} + 4H^+ \qquad (3.2)$$

or anaerobically as

$$FeS_2(s) + 2Fe^{3+} \Longrightarrow 3Fe^{2+} + 2S^0 \qquad (3.3)$$

(Lundgren and Silver, 1980)

Singer and Stumm (1970) present experimental evidence that suggests the anaerobic oxidation of FeS_2 by Fe^{3+} follows the stoichiometry of eq. 3.4.

$$FeS_2(s) + 14Fe^{3+} + 8H_2O \Longrightarrow 15Fe^{2+} + 2SO_4^{2-} + 16H^+ \qquad (3.4)$$

Microbial catalysis of pyrite oxidation is regarded as direct if the bacteria act at the surface of the sulphide and result in oxidation of the ferrous iron and sulphur in the pyrite. Indirect microbial catalysis refers to the ability of the bacteria to accelerate the oxidation of aqueous ferrous iron and hence further pyrite oxidation through equations 3.2 or 3.3. Because inorganic oxidation rates for ferrous to ferric ions is slow in acid media, Singer and Stumm (1970) suggested that this was the rate limiting step in pyrite-related acid mine drainage formation. These authors noted that the ferrous oxidizing bacteria break the kinetic barrier of this reaction and therefore are largely responsible for the production of large quantities of acid over relatively short periods.

Regardless of whether inorganic or microbial pathways are followed for pyrite oxidation, oxygen is necessary to initiate the reactions. In a review of the literature related to coal reclamation studies, Shumate et al. (1971) found that oxygen availability was the most critical factor in the pyrite oxidation reaction. These authors stressed the importance of oxygen transport in the subsurface environment and demonstrated the possible oxidation-rate limitations by diffusion controlled transport through water. Because the diffusion of O_2 in air is 10^4 times that in water, pyrite oxidation rates would be significantly reduced by increasing the thickness of the water layer in contact with the pyrite and the atmosphere. These authors developed a rate equation that utilizes diffusion coefficients for

oxygen in both gas and liquid phases as well as the simple rate constant for pyrite oxidation (see Table 3.1) but they did not indicate what rate constant should be used. In a subsequent section of that report, a reaction rate for the inorganic oxidation of pyrite is given in terms of a rate constant as well as adsorption constants for gaseous O_2 and other competing gases (see Table 3.1). In a study of a sulphidic mill tailings empoundment in New Brunswick, Boorman and Watson (1976) suggested that oxygen transport in the topmost one meter of tailings was the most important factor in sulphide oxidation processes. These authors noted that the oxidation front was confined to a narrow zone probably because deeper oxygen penetration was limited by uptake during oxidation and by the lower permeability of the tailings caused by precipitation of iron oxides and other metal oxide minerals.

Although oxygen has been identified as a critical parameter in pyrite oxidation, there is uncertainty as to the quantitative role it plays in reaction rate equations. Shumate et al. (1971) cited studies in which the reaction rate order of oxygen was found to be zero. In other terms, this indicates a constant oxidation rate independent of oxygen concentration. Another study cited in the same review indicated that the rate order has a value of one at low oxygen concentrations. Yet another study cited in a review by van Breeman (1972) found the rate order of oxygen to be 2/3. Each of these rate orders would result in significantly different pyrite oxidation rates and therefore would effect the prediction of acid generation rates.

Bacterially mediated oxidation of pyrite and other sulphide minerals is well documented in both field and laboratory studies. A recent review of microbial leaching of sulphide ores shows that this process has been widely used in the economic recovery of metals (Lundgren and Silver, 1980).

Although a number of bacteria are present in sulphidic acid media, (Zajic, 1969), the one most commonly associated with sulphide-mineral oxidation is Thiobacillus ferrooxidans, an acidophillic chemoautotroph that utilizes CO_2 as a carbon source and derives energy from Fe^{2+}, S^0 and $FeS_2(s)$ oxidation. These bacteria have been found in acid mine drainage (Shumate et al., 1971; Nordstrom, 1977 and Nordstrom, 1982), acid sulphate soils (van Breeman, 1972) and sulphide mill tailings (Boorman and Watson, 1976). More recently, significant numbers of iron oxidizing bacteria were identified in shallow subsurface samples of Nordic Main tailings at Elliot Lake (Silver and Taylor, 1981).

It is known that these bacteria are most active in the pH range of 1.0 to 2.5 but are viable over a much greater range of values. Kleinman (1979) has shown that inoculation of pyritic coal samples with iron oxidizing bacteria results in accelerated rates of oxidation even when the initial pH was as high as 7. It has been suggested previously that other non-Thiobacillus bacteria were responsible for initiating oxidation at high pH values (Walsh, 1972). This author also suggested that a succession of pH-specific bacteria became active in the oxidation reactions when the pH declined during this process. Kleinman's results, however, suggest that T. ferrooxidans and other closely related organisms in the culture are able to initiate the oxidation reaction at high initial pH values.

Bacteria can attach directly to the mineral surface (Kelly and Jones, 1978), and it is possible that they can develop localized conditions of low pH in order to carry out energy yielding oxidation. Arkesteyn (1979) has shown that oxidation of Fe^{2+} and $FeS_2(s)$ yields less energy with increasing pH whereas oxidation of S^0 by this organism is unaffected in the pH range of 3

to 5. This may indicate that T. ferrooxidans or related organisms initiate the oxidation process by attacking residual sulphur that may be produced during the partial oxidation of the sulphur moiety of pyrite. Bacterial populations on solid samples from field sites have shown that approximately 50% of each sample is composed of T. ferrooxidans and the other 50% are T. thiooxidans (D.K. Nordstrom, pers. comm. 1982). Bloomfield (1978) has suggested that T. thiooxidans utilizes S^0 as an energy source that is produced during oxidation of pyrite by Fe^{3+}. These types of relationships may indicate that microbial mediation can occur over a range of pH values. It is known that other members of the Thiobacillus genus are responsible for the oxidation of various reduced sulphur compounds at alkaline pH (Lundgren et al. 1971). What is not known, however, is whether these bacteria can mediate the oxidation of crystalline pyrite at high pH levels, as would occur in the tailings beneath an alkaline surface cover.

Eh values between 200 and 500 mV have been observed in sulphide oxidizing systems, however, Shumate et al. (1971) suggest that these potentials result from the near steady-state ferric-ferrous ratios that develop during the cyclic oxidation of pyrite by bacteria. Nutrients required by these organisms include NH_4, SO_4, K, PO_4, Mg and Ca plus other trace substances that are normally available in a heterogeneous system.

Torma et al. (1972) found that the concentrations of carbon dioxide played an imporant role in oxidation rates of zinc sulphides by Thiobacillus ferrooxidans. Kelly and Jones (1978), however, showed that reduced rates of oxidation upon CO_2 depletion were caused by arrest in population growth that resulted in linear oxidation kinetics of ferrous iron. These researchers found that growth was unaffected by excess CO_2 in the microbial system for batch tests.

Although Lundgren and Silver state that only O_2 is utilized as an electron acceptor, Arkesteyn (1980) suggests that ferric iron can be substituted for this role. This may not be critical because inorganic oxidation of pyrite by ferric iron is relatively rapid. Sensitivities to Ag, Hg and Mo have been documented and some intolerance to Se, As and Te have been observed. In batch experiments, Kelly and Jones (1978) found that high ferric iron concentrations inhibit bacterial action and further that ferrous iron concentrations greater than 0.5 M show similar inhibitory effects.

In field situations, it is expected that oxidation products such as ferric and ferrous iron would be removed periodically by flushing of infiltrating precipitation. However, because the bacteria can remain attached to the pyrite surface (Berry and Murr, 1978), the microbial population could readily establish itself after flushing has occurred. In the Elliot Lake area where precipitation is on the order of 0.8 m per year (Blair, 1981), inhibition of these bacteria caused by product buildup is unlikely to occur except during prolonged dry spells in the summer months. Because near-optimal conditions occur in the tailings masses at Elliot Lake it is not surprising that bacteria were observed in shallow cores of oxidized tailings (Silver and Taylor, 1981). Although these observations of iron oxidizing bacteria do not prove that these organisms are responsible for significant pyrite oxidation, other evidence can be cited to support this hypothesis.

Indirect evidence of microbial catalysis of ferrous iron oxidation, in the presence of pyrite, can be obtained from ferric/ferrous ratios. Because ferric iron is not thermodynamically stable in the presence of pyrite, and because the rate of pyrite oxidation by Fe^{3+} is rapid at low pH (Singer and Stumm, 1970), high Fe(III)/Fe(II) ratios suggest that catalytic oxidation of

Fe(II) is occurring. High ferric iron concentrations have been observed in near surface pore water on the Nordic tailings site at Elliot Lake (Chapter 2, this report). This suggests that microbial mediation of pyrite oxidation is occurring in this environment and hence acid generation may be controlled by the factors noted above that are critical to microbial growth. In a laboratory study of pyrite oxidation, Singer and Stumm (1970) found that microbially assisted oxidation rates were about 10^6 times as fast as inorganic rates. Hence, if bacteria were present under favourable conditions, catalysis by bacteria would be the determining factor in pyrite oxidation. It should be noted, however, that if a strong neutralizing agent is present in the pyritic material, microbial activity may not be as significant as under acidic conditions and it is likely that inorganic oxidation would become increasingly important.

Surface area is another important factor in the rate of pyrite oxidation. Although Carrucio (1975) suggested that only framboidal or sulphur ball pyrite was reactive, it was shown that the very high surface areas of this form of pyrite was responsible for this observation (Shumate et al. 1971). In studies of microbial ore leaching, Torma et al. (1972) showed that oxidation rates are proportional to surface area. In a review of acid-sulphate-soil studies, van Breeman (1972) cited numerous studies that indicated pyrite surface area as an important factor in oxidation rates. Framboidal pyrite with a mean particle diameter of 30 microns may have surface areas as high as 10^5 cm^2/g whereas ground crystalline pyrite of the same particle diameter would have surface areas on the order of 5×10^2 cm^2/g. Nonetheless, it was observed that even in tailings with well crystallized crushed pyrite derived from uranium ore at Elliot Lake, oxidation results in pH values as

low as 0.9 and Fe and SO_4 concentrations of many thousands of mg/L in the shallow subsurface (Chapter 1, this report). This indicates that although surface area of pyrite is an important factor in rate controls, the relatively large particle diameters observed in uranium mill tailings does not prevent oxidation of this mineral.

It is known that moist unbuffered aerated pyrite will oxidize and result in acidic conditions over periods of weeks to months. Much less is known, however, about the oxidation rates of pyrite in neutral-buffered systems. This process has not had much attention mainly because acidic conditions do not develop in such natural systems and high sulphate concentrations are the only deliterious effects observed. In systems with limited carbonate alkalinity, however, the rate of acid production and subsequent titration of alkalinity becomes important.

In laboratory experiments on pyritic soils, it was shown that significant oxidation of pyrite occurred in the calcite-buffered soils when compared with unbuffered soils (Arkesteyn, 1980). Over a 55 day incubation period, the buffered soils produced up to 60% of the oxidation products of the unbuffered microbially active soils. This rate was slightly higher than that of the sterile unbuffered soils. It was also observed in this experiment that whereas inoculation of the unbuffered soils doubled the oxidation rate, the oxidation rate in the carbonate soils was unaffected. Arkesteyn took special precautions to assure the purity of the T. ferrooxidans inoculum and therefore it is not known whether a mixed culture would have had an effect on the oxidation rates of the buffered soils. A study of sulphide weathering on tailings samples showed emperically that a specific excess of carbonate was needed to avoid acidification of liquid effluent (Jongejan, 1973). These

studies did not, however, deal with the rate of pyrite oxidation under carbonate buffered conditions.

Temperature can also influence the rate of pyrite oxidation. Shumate et al. (1971) cite studies indicating that the oxidation rate doubles with a 10^0C rise in temperature suggesting conformation with Arrhenius behavior. Presumably this relationship refers to abiotic oxidation reactions. However, microbial mediation of the oxidation reaction implies that optimum temperatures are in the rate of 25 to 40^0C (Lundgren and Silver, 1980).

Although no mention of pyrite content in relation to oxidation rates is made in the literature, it is possible that the autocatalytic nature of the reaction may be affected by the degree to which pyrite is dispersed throughout the granular media. The pyrite content may also warrant a practical consideration due to the lower limit of pyrite attainable by floatation or other seperation processes. If depyritized tailing were used as part of the tailings-cover options, the effects of low pyrite contents should be investigated.

After reviewing the literature, it is apparent that most of the research dealing with pyrite oxidation or sulphide-mineral oxidation invokes bacterial catalysis, usually with Thiobacillus ferroxidans. The research involving this microorganism usually falls into two categories. The first emphasizes oxidation rates of Fe(II) in solution under optimal conditions and the second deals with metalurgical applications of bacterial leaching in ore slurries under optimal conditions. Very little work has been published on the effects of limiting oxygen concentrations or the dynamics in systems where continual outward flux of products occurs. With the exception of Arkesteyn's (1979) study, few results have been published on the rates of oxidation over a range

of pH values. Such studies would be necessary to evaluate the relative importance of inorganic versus microbial oxidation in the presence of various buffering agents. Aspects of pyrite oxidation not found in the literature concern microbial versus inorganic oxidation rates at elevated pH values. This can be critical if neutralizing agents such as added limestone or naturally occurring Al hydroxides act as buffers in the tailings system. Most studies of reaction rates are applied only to laboratory conditions. Field studies that have dealt with pyrite oxidation often reveal complex results that are difficult to interpret. Conditions expected in tailings management plans and evidence given in the literature indicate a number of variables that play important roles in the oxidation rates of pyrite. These variables can be summarized as 1) oxygen content, 2) microbial mediation, 3) surface area, 4) carbonate buffering, 5) temperature and 6) pyrite content.

Research Rationale

The above mentioned variables involved in pyrite oxidation have been identified in the literature, however, little is known regarding their relative importance. In addition, no overall rate equation has been developed to account for these variables and their role in pyrite oxidation. For instance, although it is known that oxygen is necessary for initiation of the oxidation reaction, the effects of low oxygen concentrations are not known. Also, little is known about the rate of pyrite oxidation at neutral to alkaline pH levels resulting from limestone dissolution. The questions become important in the context of probable close-out options of the uranium tailings impoundments.

In this investigation, an attempt was made to determine the relative importance of each of the above mentioned variables. Because of the large number of variables and the difficulty in experimental determination of reaction-rate parameters, each of the variables was selected to have only two levels in this experiment. The levels were chosen at high and low values that conform either to probable limits in the field environment or to those technically feasible in the laboratory. This experimental design is referred to as a 2^n factorial and is used to determine important differences in the effects of variables and possible interactions involved between them. The data were analysed statistically to determine the significance of these differences. In order to reduce the number of samples and maintain the strength of statistical inferences, a one-half replicate modification was used. This resulted in the study of 32 samples in place of the original 64. Although the effects of higher order interactions are lost, these combinations were considered to be insignificant. A more detailed description of the statistical design of this experiment may be obtained from Cochran and Cox (1957, p.279).

Experimental Methods

The investigation of critical variables on pyrite oxidation rates was designed as a preliminary laboratory experiment of which the results could be used in the planning of more detailed reaction-rate studies. The methods used in this experiment were chosen to reflect some conditions observed in the field environment, yet relatively simple enough to maintain good control on the factors involved in this complex process. The experiments were static in that only one moisture application was made during the oxidation

period. The initial moisture content was selected to allow free gas-phase flow in the tailings samples and gas phase compositions and temperatures were maintained at constant values.

Experimental Design

The reconstituted pyritic tailings were characterized by two levels of the six variables noted above (Table 3.2). These samples were placed in specially designed oxidation cups that maintain atmospheric contact at the top and bottom of the tailings. The moisture content was selected so that gas-filled pore space was continuous in the samples. Thirty-two primary samples and eight semi-random replicates were prepared for the main experiment. The replicates provide a better estimate of random error. This series of samples was designated as ST1 denoting static-oxidation series one. In addition to this series, a supplementary 2^3 design was constructed in order to determine the effects of sample preparation on freshly crushed pyrite. Carbonate buffer, microbial activity and xanthate floatation treatment were the three variables investigated in this experiment (Table 3.3). Fresh museum-grade pyrite was crushed, sieved and otherwise treated similarly to the tailings pyrite. Crushed and sieved silica sand was used as the granular matrix for these oxidation experiments. All of these samples were incubated at room temperature with a 20% oxygen atmosphere and a pyrite content of 7%. This experiment was designed as ST2 series denoting static-oxidation series two.

The samples were prepared as outlined below and were placed in the appropriate incubators for a period of 56 days. When the samples were removed, they were leached and the leachate was collected quantitatively so

that soluble sulphate could be analysed and the total sulphate mass determined. The sulphate totals are an estimate of the extent of pyrite oxidation. These values were then used in the statistical analysis to determine significant differences in the quantity of pyrite oxidized during the experiment.

Sample Preparation

A thirty kilogram sample of fresh Quirk Lake tailings was obtained from the Rio Algom mill at Elliot Lake. Initial analyses of this material indicated 80% of the grains, by weight, passed the 180 micron mesh sieve (Fig. 3.1). Sulphur analyses on the different size fractions, however, revealed that pyrite contents of greater than 1% occurred only in the less than 125 micron fractions. For this reason, the largest grain-size fraction used was the -125 + 95 micron fraction. The smallest sieve pan for practical use was 45 micron mesh and therefore the smallest grain-size used in this study was the -63 + 45 micron fraction. Significant quantities of gypsum and detectable amounts of calcite were also present in the different-size fractions (Table 3.4).

The thirty kilograms of tailings were first dry sieved into appropriate size fractions in 1/2 phi intervals. Because the size-ranges to be used in the experiment comprised only small fractions of the total, another fifty kilograms of whole tailings was obtained and sieved. After sieving, the tailings were washed in deionized water to remove excess gypsum and were ultrasonically cleaned to remove fines that adhere to the larger grains. Pyrite was then separated from the tailings by floatation in a Denver Equipment bench-top floatation unit using potassium xanthate (0.2 g/kg

tailings) as a surfactant and pine oil (0.2 g/kg tailings) as a carrier. Sulphur analyses on the depyritized tailings indicated virtually total removal of pyrite.

Because the presence of surfactant on pyrite surfaces is inhibitory to oxidation and other surface-related phenomena, the potassium xanthate was removed by a procedure outlined in Rao (1971). After floatation, each 100 g of pyrite was treated with 2 ml of 1N NaOH and 1 ml of 30% H_2O_2 and allowed to react for about four hours. The depyritized tailings were also treated to remove residual xanthate. These fractions were then acidified with 0.05 N HCl, washed and ultrasonically cleaned in deionized water. When the pyrite concentrates were resieved, it was found that significant quantities passed the original size-limiting pans, indicating that sample treatment either resulted in grinding or aided in better separation of grain sizes. Because the pyrite concentrates contained other sulphide minerals in small quantities and because many sulphides oxidize more rapidly than pyrite, it was attempted to remove these minerals electromagnetically. After removal of magnetite with a hand magnet, the pyrite concentrates were passed slowly through a Franz electromagnetic separator at amperage settings of 0.1, 0.3, 0.7 and 1.4 for a total of four runs.

The pyrite concentrate fractions were divided into appropriate weight aliquots with a Soil Test sample splitter in preparation of the high and low pyrite content tailings. Pyrite and/or ground calcite were then added to the selected samples of depyritized tailings. The reconstituted tailings were then mixed in small plastic containers by gentle shaking and rolling by hand. These samples were placed in the oxidation cups and autoclaved once on each of two consecutive days.

The microbial inoculum used in this experiment was initiated from a near-surface oxidized sample of Nordic tailings. The oxidized tialings were observed to harbour bacillus-type bacteria under a UV fluorescent microscope. The genus and species were not determined but subsequent culture growth in a specialized medium suggested that the iron oxidizing Thiobacillus ferrooxidans was present. Three grams of oxidized tailings were transferred to 150 ml of 9K culture medium (Silverman and Lundgren, 1959) on September 14, 1981. After six weeks, a subjective microbial count was conducted with a NIKON LABOPHOT fluorescent microscope using NH_4 ANS (3 mg/ml) as a staining agent. A rough estimate of bacteria suggested that the cultures contained at least 10^5 cells per ml. On October 27, a 10% by volume transfer of this culture was completed using a modified culture medium. The modified medium consisted of only 4 g of $FeSO_4 * 7H_2O$ per litre plus 5 g of finely crushed pyrite per 100 ml. This medium was used to ensure that the microbial population would maintain the ability to catalyze the oxidation of crystalline pyrite. A second transfer of culture material was performed on November 11 after completing another subjective microbial count. On December 22, following another count, the culture was transferred to 500 ml of modified medium containing 20 g of fine freshly ground pyrite. The culture resulting from this third transfer was used to prepare the inoculum for the experiment reported herein.

Observations of the bacterial culture prior to processing revealed that the cells commonly adhered to pyrite surfaces but that a large proportion of cells remained in suspension throughout the medium. In order to inoculate the selected tailings samples and avoid added contamination by pyrite and excess dissolved sulphate and iron, it was necessary to separate the

Thiobacillus cells from the pyrite and iron-sulphate-rich medium. After a number of techniques had been tested, the inoculum was prepared by consecutive filtration through different pore-size filters. Initially, the culture medium was blended for two minutes to dislodge the cells that were observed adhering to pyrite surfaces. The culture was then filtered through a double layer of hardened No. 5 Whattman filter paper that has pore diameters in the tens of microns range. The solids were retained and rewashed with 0.05 N H_2SO_4. This slurry was then refiltered in the same manner as above. The clear filtrates were combined and the resulting solution was vacuum filtered through a 0.22 micron millipore membrane. The millipore membrane was rinsed with weak sulphuric acid to remove the iron-sulphate-rich culture medium. The membrane was then removed from the filter apparatus and wiped gently with a rubber policeman and washed with weak sulphuric acid to remove the bacterial cell cake. This washed material was then added to the deionized water used to moisten the selected tailings samples.

After moistening the 100 g reconstituted tailings samples with either sterile or inoculated deionized water, they were placed in the selected incubators. Two of the incubators were maintained at near-room temperature and two were placed in a modified domestic freezer and maintained about 5^0C. One each of the temperature-paired incubators was fed a gas mixture containing 20% oxygen and the other 0.5% oxygen. One percent CO_2 and a balance of N_2 gas was common to all gas mixtures. The pyritiferous tailings remained in the incubators for 56 days.

The incubators consisted of plastic squaroid desicators fitted with gas inlet and outlet recepticles. Circulation fans were installed in the desicators

to prevent gas stagnation and subsequent limitation of oxygen transport to the tailings moisture. The gas mixtures were humidified prior to entering the incubators by passing through a porous glass bubler under a 30 cm column of water. The gas outlet tubes were placed under 5 cm of water to maintain a positive pressure in the incubators. The pressure differential minimized the possibility of atmospheric contamination in the incubators.

Sample Processing

At the end of the oxidation period, the tailings samples were removed from the oxidation cups and placed in two syringe-filter units. These syringes were fitted with 0.1 micron filter membranes sealed with rubber O-rings. Twenty ml of deionized water were then added to each syringe and allowed to infiltrate the tailings sample. The syringe assembly was centrifuged for five minutes at 1200 rpm and the filtrate was collected in plastic scintillation vials below the syringe. This process was repeated five times in order to remove all soluble sulphate. This filtrate was collected in a 250 ml volumetric flask. Fifteen ml of 1N HCl were then added to each syringe unit and allowed to infiltrate the tailings. The leachate produced from three such treatments was collected in a 100 ml volumetric flask. The acid leaching was performed in order to dissolve any acid-sulphate minerals that may have formed in small quantities during pyrite oxidation. The solid tailings were then rinsed with four aliquots of deionized water, removed and dried. The contents of the two volumetric flasks were analysed for sulphate and the total sulphate leached from the tailings was determined. Because some sulphate was present in the initial moisture, the total soluble sulphate content of the tailings was corrected by this amount.

Statistical Treatment

A 2^n factorial design was used for both the ST1 and ST2 series experiments. The advantages of this approach are the relatively small number of samples needed to investigate a large number of variables as well as the inferences regarding possible interaction among variables. This factorial design provides a means of testing for the presence of an effect due to a variable and also the relative significance of those effects.

The ST1 experiment included six variables at two levels each. This experiment was run, however, as a 1/2 balanced replicate in order to reduce the number of tailings samples needed. The experiment was therefore comprised of 32 tailings samples. In addition, eight of the samples were duplicated in order to obtain a better estimate of the experimental error. Because most of the variables are expected to have additive effects, the level of interaction (or non-additive effects) among the variables was expected to be limited. For this reason, all three-factor interactions were pooled and used as an error term resulting in 10 degrees of freedom for error.

The statistical analysis involved the construction of a contrast table in which the contrast sums of squares were computed for each effect. The sum of squares were then summarized in an ANOVA table and the F-ratios were determined. (see Cochran and Cox, 1957) The significant factors at the $p = 0.05$ level are those with F-ratio values greater than $F(1,10) = 4.96$.

The ST2 experiment included three variables at two levels each. This results in the processing of eight pyritic quartz-sand samples. In this experiment, however, there is only one three-factor interaction available for the error term and hence the statistical analysis and inferences regarding this experiment are limited.

Results and Discussion

The ST1 series experiment was initiated on March 8, 1982 at 1700 hours. The ST2 series experiment was initiated on March 9 at 0930 hours. The internal temperatures of the incubators were recorded twice daily and are listed in Appendix D. The refrigerated incubators remained at about 4.8^{0}C. The internal gas compositions were also monitored periodically and the results shown in Appendix E indicate that virtually no change in oxygen or carbon dioxide contents occurred throughout the experiment.

On the eighth day of the oxidation run, it was discovered that one sample in close proximity to the circulation fan in the high-temperature low-oxygen desicator had become dry and much of the sample had been blown throughout the desicab. All samples in this desicab (D4) were then removed, the destroyed sample was replaced with a new one and the remaining samples were freed of contamination, leached in HCl and resterilized in the autoclave. The oxidation run was restarted on this set of samples on March 19.

After 56 days, ST1 and ST2 series samples were removed from the desicabs. These samples were found to be dry and only some displayed an oxidized appearance. This dryness was unexpected because preliminary oxidation runs had indicated no loss of moisture over a period of about 60 days. The addition of the circulation fans, however, created an increase in temperature of about 2.0 degrees above that outside the desicab. Because the influent gas was humidified outside the desicab, the higher internal temperature decreased the relative humidity to below 100% and therefore induced evaporation in the samples. The time needed to dry the samples is not known but because all but one sample in D-4 contained moisture after

eight days, it is expected that total drying of the tailings occurred only after at least one or two weeks. Because the internal and external temperature differences for all desicabs was about the same (2.0^0C), it is probable that drying of samples in all desicabs occurred over similar time intervals. If this is true then the pyrite oxidation reaction, that requires moisture, would have occurred to a similar extent for all samples. In this respect, the relative amounts of sulphate produced in each sample may be a valid indicator of the extent of oxidation under the set conditions.

The tailings samples were found to have produced between 2 and 71 mg of SO_4 during the oxidation period (Tables 3.5 and 3.6). This amount of SO_4 is comparable to the 14 to 50 mg of SO_4 produced by moist tailing of a similar pyrite content over a 58 day period in preliminary studies. This suggested that significant oxidation did occur even though samples became dry during the oxidation period. More than 95% of the total leached sulphate was accounted for in the deionized-water-leach fraction indicating that the water leach was sufficient to remove the sulphate produced by pyrite oxidation.

The results of the ST1 series experiment were analysed statistically. The error mean square was derived as noted above and a summary ANOVA table is given in Table 3.7. The effects having F-ratios greater than 4.96 are significant at the 5% probability level. The results indicate that temperature (F) is the most significant factor, pyrite content (E) is also significant and grain size (B) (surface area) is of marginal significance. Upon closer inspection, however, it is noted that all other variables are nested within the various levels of oxygen content (A) and temperature (F). This nesting of variables was necessitated by the number of desicab units available for the

experiment. Because only four of these units were used and because these comprise a whole experiment within the main study, a whole plot anaysis of the four desicabs should be made. Because this is a split plot design, the error term for "between" desicabs is expected to be larger than that for "within" desicab variability (Cox, 1958) and hence the error term for the main analysis should not be used here. Therefore, there is no error term available for this analysis. However, a visual inspection of the 2 x 2 contingency table (Table 3.8) suggests that the significant effects due to temperature (F) are consistent across the levels of oxygen content (A). In this table, 1 signifies the low level and the lower case letter, the high level of the respective variables. Although it is thought that reprocessing of D4 tailings samples may have had an effect on the sulphate produced, the consistent increase of yield from low to high temperature (F) at both levels of oxygen suggests that any such effects are insignificant. This data suggests therefore that temperature is most likely a significant factor, resulting in greater yields of sulphate at the high level.

The significance of pyrite content as a factor in pyrite oxidation is somewhat surprising. It was expected that surface area effects would be more pronounced for this surface-controlled reaction. On closer inspection, it is observed that pyrite content (E) and surface area (B) are not independent variables. As pyrite content increases, so does the available surface area even though the grain size remains constant. This suggests that the pyrite content and surface area variables should be analysed separately in order to better understand the combined effects of each. It should be remembered here that pyrite content (E) was found to be significant while surface area (B) was marginally significant in the preliminary analysis.

Inspection of the 2 x 2 contingency table (Table 3.9) of surface area (B) versus pyrite content (E) indicates that the largest and most outstanding yield occurs at high levels of both B and E. Statistical comparison of the yields by contrasts indicates that the yield of the low levels of both (1) is significantly different from the yield at the high levels of both (be) variables. Further analysis indicates that be is significantly different from the other three yields at the $p = 0.01$ probability level. All other comparisons are not significant. In this table, the yield of the low levels of both variables represents the smallest surface area while e and b represent intermediate values and be represents the greatest surface area samples. The results here indicate that all significance shown by factors B and E in the main analysis (Table 3.7) is due to the effect of surface area only and that pyrite content is not in itself a significant variable.

Statistical analysis of the results from the ST2 series experiment was not definitive. The ANOVA table (Table 3.10) indicates that all mean square values except XZ and XYZ interactions are in the same range. In this case, however, if only three-factor interactions are taken for the error term, only one degree of freedom remains for error. Because the XYZ mean square is extremely different from other mean square values and it is also in great contrast with the error mean square from the previous ST1 results, it does not appear to be a reliable estimate of the error in this case. The error term may be estimated from the previous ST1 series experiment but this may be an over estimate due to the lack of "between" desicab variability in this experiment. In any case, significance of any variables in the ST2 experiment is doubtful due to their close correspondence in mean square values. This suggests that the xanthate treatment given to the pyritic

tailings did not significantly affect the degree of oxidation of pyrite in the main experiment.

The results of this analysis suggests that the three other variables (i.e. oxygen content, microbial activity and carbonate buffering) at the specified levels did not affect the sulphate yield under these experimental conditions. The reasons for the lack of effect of these variables on the pyrite oxidation rate are not known but some possible explanations are listed below.

Oxygen content was cited in the literature as having zero, first and a fraction order rate control on pyrite oxidation. It is not known whether these discrepancies are due to experimental conditions or if they reflect different oxygen concentration ranges used. If the rate order of oxygen is concentration dependent, it is possible that the low level of oxygen used in this experiment (0.5%) was not sufficiently low to affect oxidation rates. Even this result is significant, however, in that it illustrates that oxygen concentrations as low as 0.5% may be capable of sustaining significant pyrite oxidation in the abandoned tailings.

Microbial activity is one variable that is known to have significant effects on pyrite oxidation rates. The lack of significance between inoculated and sterile sulphate yields here suggests that the microbial culture did not develop sufficiently. This may have been due to the innoculation technique but it is more likely a function of the experimental conditions. Although the samples remained in the incubator for about 60 days, the tailings sample had probably become dry much sooner. During Thiobacillus culture preparation, it was observed that two to five weeks were necessary for newly transferred cultures to become established in the fresh culture medium. If this length of time is required for significant microbial growth

under ideal conditions, it is not surprising that the culture did not become productive in a shorter period under less than ideal conditions. If the tailings samples had remained moist during the entire 60 day incubation period, it is likely that microbial innoculation would have had an effect.

There is little known about the effects of carbonate buffering on pyrite oxidation rates, therefore it is not surprising that this factor had no significant effect on sulphate yield. The results here suggest that the production of sulphate from pyrite oxidation is similar whether the system is buffered or not. This may only be true when sterile oxidation rates are compared because it is likely that microbial mediation was not significant under the experimental conditions.

These results raise important questions, however. If temperature is indeed the most significant factor, can its effects be predicted by Arrhenius behavior? Although the role of surface area in pyrite oxidation rates seems obvious, what rate order is involved? At what low level of oxygen content is there an effect on oxidation rates? And finally, does carbonate buffering affect oxidation rates in systems that are microbially active? These questions should be answered during subsequent separate experiments if a rate model of pyrite oxidation is to be developed.

Summary of Conclusions

A review of the literature indicated that six variables likely affect the pyrite oxidation rates in near-earth-surface environments. There was considerable uncertainty, however, with regard to the relative importance of these variables to reaction rates. Because a relatively large number of variables are involved, it is necessary to focus on those factors that exhibit

the greatest influence on the reaction rates. In this context, then, a factorial experiment was designed to determine the significant differences in pyrite oxidation due to these variables.

The main experiment (ST1) was comprised of 32 tailings samples of 100 g, each set at a specified combination of the high and low levels of the six variables. A supplementary experiment (ST2) using freshly crushed quartz sand and pyrite was designed similar to the main study but contained only three variables, one of which was the xanthate floatation treatment applied to the tailings samples. The samples were moistened and subjected to the various levels oxygen content and temperature in incubators. After 56 days had elapsed, the tailings samples were removed from the incubators and quantitatively leached of SO_4. The sulphate was analysed and the total amount of SO_4 released by pyrite oxidation was determined. Even though the tailings samples were discovered to be dry when removed from the incubators, it is probable that valid comparisons among variables for short reaction periods can be made.

Statistical analysis of the sulphate yields suggested that temperature differences (between 5 and 28^0C.) significantly affected pyrite oxidation rates during the experimental period. Because of experimental conditions, the temperature and oxygen content factors were actually designed as a complete experiment in which the other four variables were nested. This nesting resulted in no degrees of freedom for error in the temperature-oxygen content analysis but visual inspection of the 2 x 2 table of yields indicates that the results are consistent with the results of the main analysis.

Pyrite content was also found to be significant and surface area displayed marginal significance. Upon further analysis, however, it was

discovered that all of the significance was due to the increase of surface area in the various combinations of these two variables. No other variables were found to have a significant affect on pyrite oxidation at the levels chosen for this experiment and no interaction (or non additive) effects were observed.

The results of the experiment suggest that pyrite oxidation can be sustained at sufficient levels even when the oxygen content of the gas phase is as low as 0.5%. Microbial mediation did not affect sulphate production probably because the bacterial population did not have sufficient time to establish itself before the tailings became dry. Carbonate buffering did not significantly affect inorganic oxidation rates within the oxidation period.

List of Tables in Chapter 3

Table

3.1 Summary of pyrite oxidation rate models cited in the literature.

3.2 Summary of selected factors and their levels in the ST1 experiment.

3.3 Summary of selected factors and their levels in the ST2 experiment.

3.4 Summary of selected properties determined on the size fractions of fresh Quirke Lake tailings.

3.5 Sample numbers, sulphate yield and treatments applied to tailings in experiment ST1.

3.6 Sample numbers and treatments applied to tailings in experiment ST2.

3.7 ANOVA table for results of the ST1 experiment.

3.8 2 x 2 contingency table of the oxygen content (A) and temperature (F) factors.

3.9 2 x 2 contingency table of surface area (B) and pyrite content (E) factors.

3.10 ANOVA table for the results of the ST2 experiments.

List of Figures in Chapter 3

3.1 Grain size distribution of fresh Quirke Lake tailings.

Tables in Chapter 3

Table 3.1 Summary of pyrite oxidation rate models cited in the literature

EQUATION	PARAMETER IDENTIFICATION	REFERENCE
$R_r = [1/1/_{Km} + 1/_{K_1}]C_1$ $K_m = (1/\frac{L}{D_1} + \frac{X}{D_2})$	R_r = reaction rate D_1 = diffusivity of O_2 in porous media D_2 = diffusivity of O_2 in air L = length of diffusion path in porous medium X = diffusion path in water film K_1 = reaction rate constant C_1 = concentration of O_2 at L + X	Shumate et al. (1971)
$R = (kO_2/(1 + K_1O_2 + K_2I))$	k = reaction rate constant O_2 = concentration of O_2 K_1 = adsorption equilibrium constant for O_2 on pyrite K_2 = adsorption equilibrium constant for competing gas on pyrite I = concentration of competing gas	cited in Shumate et al. (1971)
$R = [K\ Fe^{2+}/Fe^{3+}/\ 1 + Fe^{3+}$ $K_1 + K_2Fe^{2+}/Fe^{3+}]$	k = reaction rate constant K_1 = adsorption equilibrium constant for Fe^{3+} on pyrite K_2 = adsorption equilibrium constant for Fe^{2+} on pyrite	cited in Shumate et al. (1971)

Table 3.1 cont'd

EQUATION	PARAMETER IDENTIFICATION	REFERENCE
$-\frac{d[Fe^{3+}]}{dt} = k[Fe^{3+}][FeS_2]$	k = reaction rate constant - varies from 0.4 to 17.4 day^{-1} $[FeS_2]$ = molar concentration of pyrite	Singer and Stumm (1969) cited in Nordstrom (1980)

Table 3.2 Summary of selected factors and their levels in the ST1 experiment.

Factor	Description	Level	
		High	Low
A	Oxygen Content (%)	20	0.5
B	Surface Area (Diam. μ)	(54)	(200)
C	Microbial Activity	(+)	(-)
D	Carbonate Buffer	(+)	(-)
E	Pyrite Content (%)	7	1
F	Temperature (°C)	28	5

Table 3.3 Summary of selected factors and their levels in the ST2 experiments.

Factor	Description	Level	
		High	Low
X	Carbonate Buffer	(+)	(-)
Y	Xanthate Treatment	(+)	(-)
Z	Microbial Activity	(+)	(-)

Table 3.4 Summary of selected properties determined on the size fractions of fresh Quirke Lake tailings

GRAIN SIZE (μ)	SPECIFIC GRAVITY	BULK DENSITY (g/ml)	PECENT GYPSUM	PERCENT CALCITE	TOTAL SULPHUR (%)
-15	2.83	1.19	6.76	0.16	6.71
-63 + 45	2.87	1.41	1.30	0.11	6.22
-90 + 63	2.78	1.43	0.58	0.07	3.84
-125 + 90	2.73	1.43	0.43	0.03	1.88
-180 +125	2.73	1.42	0.25	0.02	0.65
-250 +180	2.73	1.38	0.18	0.01	0.27
-355 +230	2.71	1.40	0.15	0.01	0.18
-425 +355	2.70	1.34	0.35	0.01	0.18
+425	2.70	1.32	1.01	0.02	0.29

Table 3.5 Sample numbers, sulphate yield and treatments applied to tailings in experiment ST1

SAMPLE NO.	SULPHATE YIELD (mg/L)	OXYGEN CONTENT		PARTICLE DIAMETER		BACTERIAL INNOCULATION		CARBONATE BUFFER		PYRITE CONTENT		TEMPERATURE	
		20	0.5	54	200	YES	NO	YES	NO	7	1	28	5
ST1-1	3		+		+		+		+		+		+
-2	22	+		+			+		+		+		+
-3	2	+			+	+			+		+		+
-4	6		+	+		+			+		+		+
-5	3	+			+		+	+			+		+
-6	11		+	+			+	+			+		+
-7	2		+		+	+		+			+		+
-8	13	+		+		+		+			+		+
-9	12	+			+		+		+	+			+
-10	9		+	+			+		+	+			+
-11	4		+		+	+			+	+			+
-12	13	+		+		+			+	+			+
-13	11		+		+		+	+		+			+
-14	44	+		+			+	+		+			+
-15	12	+			+	+		+		+			+
-16	13		+	+		+		+		+			+
-17*	7	+			+		+		+		+	+	
-18	31		+	+			+		+		+	+	
-19*	39		+		+	+			+		+	+	
-20	21	+		+		+			+		+	+	
-21*	23		+		+		+	+			+	+	
-22	21	+		+			+	+			+	+	
-23*	36	+			+	+		+			+	+	
-24	11		+	+		+		+			+	+	
-25*	4		+		+		+		+	+			+
-26	47	+		+			+		+	+			+
-27*	48	+			+	+			+	+			+
-28*	51	+			+		+	+		+			+
-29	71		+	+		+			+	+			+
-30	50		+	+			+	+		+			+
-31*	22		+		+	+		+		+			+
-32	56	+		+		+		+		+			+

*Denotes sample with replicate

Table 3.6 Sample numbers and treatments applied to tailings in experiment ST2

SAMPLE NO.	SULPHATE YIELD	XANTHATE TREATMENT		CARBONATE BUFFER		BACTERIAL INNOCULATION	
		YES	NO	YES	NO	YES	NO
ST2-1	56	+		+		+	
-2	22	+		+			+
-3	39	+			+	+	
-4	34	+			+		+
-5	52		+	+			+
-6	25		+	+			+
-7	10		+		+	+	
-8	14		+		+		+

Table 3.7 ANOVA table for the results of the STI experiment

EFFECT	MEAN SQUARE	d.f.	F-Ratio	Level of Significance
A	300.	1	1.7	
B	800.	1	4.4	(Marginal)
C	12.5	1	0.1	
D	50.	1	0.3	
E	1458.	1	8.0	$0.01 < p < 0.05$
F	4005.	1	22.1	$p << 0.01$
AB	24.5	1	0.1	
AC	32.	1	0.2	
BC	210.	1	1.2	
AD	242.	1	1.3	
BD	55.	1	0.3	
CD	435.	1	2.4	
AE	312.	1	1.7	
BE	435.	1	2.4	
CE	0.1	1	0.0	
DE	120.	1	0.7	
AF	21.	1	0.1	
BF	0.	1	0.0	
CF	450.	1	2.5	
DF	40.	1	0.2	
EF	338.	1	1.9	
Error (all 3 factor)	181.25	10	-	

Error Terms	Mean SQUARE
ABC	28.125
ABD	45.125
ACD	465.125
NVF	72.
ABE	325.125
ACE	253.125
BCE	162.
ADE	10.125
BDE	32.
CDE	420.5
	1812.5

Table 3.8 2 x 2 contingency table of the oxygen content (A) and temperature (F) factors.

F \ A	1	a
1	7.375	15.125
f	31.375	35.875

Table 3.9 2 x 2 contingency table of surface area (B) and pyrite content (E) factors

E \ B	1	b
1	14.375	17.000
e	20.500	37.875

Table 3.10 ANOVA table for the results of ST2 experiment.

EFFECT	MEAN SQUARE	d.f.
X	312.7	1
Y	420.5	1
Z	480.5	1
XY	288.	1
XZ	32.	1
YZ	450.	1
XYZ	0.5	1

Figures in Chapter 3

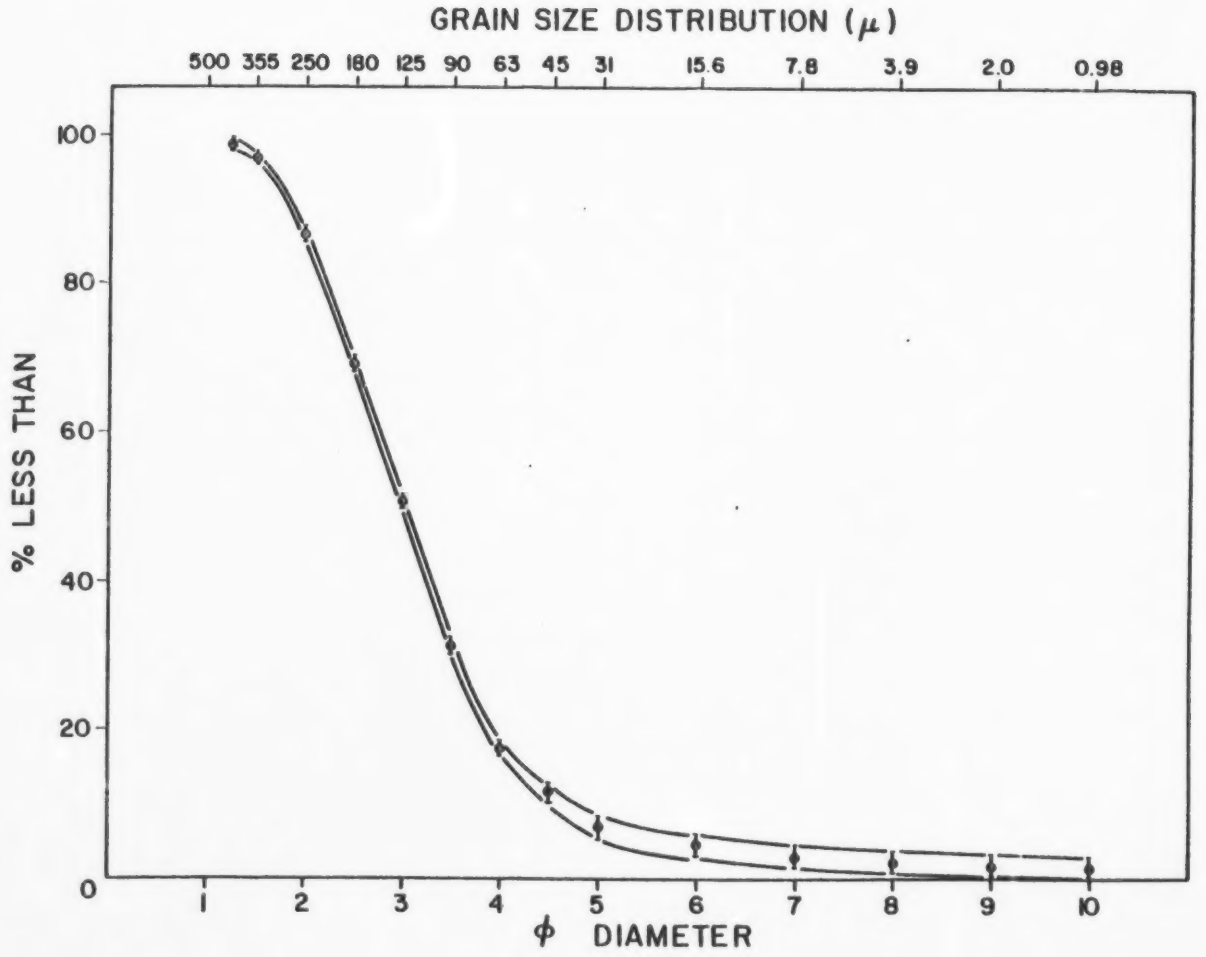

Figure 3.1 Grain size distribution of fresh Quirke Lake tailings.

REFERENCES

Arkesteyn, G.J.M.W., 1979. Pyrite oxidation by Thiobacillus ferrooxidans with special reference to the sulphur moiety of the mineral, Antonie van Laeurvenhoek (Microbiology), 45: 423-435.

Arkesteyn, G.J.M.W., 1980. Pyrite oxidation in acid sulphate soils: The role of microorganisms, Plant and Soil, 54: 119-134.

Ball, J.W., Nordstorm, D.K. and Jenne, E.A. 1980. Additional and revised thermochemical data and computer code for WATEQ2 - A computerized chemical model for trace and major element speciation and mineral equilibria of natural waters. U.S. Geological Survey - Water-Resources Investigations 78-116, 109 p.

Ball, J.W., Jenne, E.A. and Nordstrom, D.K., 1979. WATEQ2 - A computerized chemical model for trace and major element speciation and mineral equilibria of Natural Waters. In E.A. Jenne ed., Chemical Modeling in Aqueous Systems, American Chemical Society Symp. Series 93, pp. 815-835.

Beck, W.G., 1974. In The Sea, Vol. 5, E.D. Goldberg, Ed., Wiley-Interscience N.Y., p. 153.

Berry, V.K. and Murr, L.E., 1978. Direct observations of bacteria and quantitative studies of their catalytic role in the leaching of low grade, copper-bearing waste. In L.E. Murr, A.E. Torma, and J.A. Brierly (eds.) Metallurgical Applications of Bacterial Leaching and Related Microbiological Phenomena, Academic Press, p. 103-136.

Blackport, R. and Cherry, J.A., 1980. Patterns of groundwater flow, pH, and electrical conductance in the Nordic West Arm tailings, Elliot Lake, Ontario. Waterloo Research Institute Project No. 007-10.

Blair, R.D., 1981. Hydrogeochemistry of an Inactive Pyritic Uranium Tailings Basin, Nordic Mine, Elliot Lake, Ontario. University of Waterloo, unpublished Master of Science thesis, 79 p.

Blair, R.D., Cherry, J.A., Lim, T.P. and Vivyurka, A.J. 1980. Groundwater monitoring and contaminant occurrence at an abandoned tailings area, Elliot Lake, Ontario. In Brawner, C. (ed.), Proc. First Intern. Conf. on Uranium Mine Waste Disposal, Soc. Mining Engineers of AIME.

Bloomfield, C., 1972. The oxidation of iron sulfides in soils in relation to the formation of acid sulphate soils. J. Soil Sci., 23: 1-16.

Boorman, R.S. and Watson, D.M., 1976. Chemical processes in abandoned sulphide tailings dump and environmental implications for northeastern New Brunswick, CIM Bulletin, Aug., 86-96.

Breemen N. van 1976. The genesis and solution chemistry of acid sulphate soils in Thailand. Ph.D. Thesis, Centre for Agric. Pub. and Doc., Wageningen, The Netherlands. 263 p.

Breemen, N. van, 1972. Soil forming processes in acid sulfate soils. p. 66-130. IN H. Dost, (ed.) Acid Sulfate Soils. Publ. 18(1), Internat. Inst. for Land Recl. and Improv., Wageningen, the Netherlands.

Brown, J.B., 1970. A chemical study of some synthetic potassium-hydronium jarosites. Can. Min. 10: 696-703.

Bush, K.J. and Markos, G., 1981. Evidence for the instability of silicate minerals in acid leach uranium mill tailings. Symp. on Uranium Mill Tailings Management, Fort Collins, Colorado. Geotech. Eng. Prog. Civil Eng. Dept., Colorado State U., p. 473-486.

Buszka, P., 1981. Hydrogeochemistry of Contaminated Groundwater in Sand Aquifers at a Landfill Near North Bay, Ontario. Unpublished M.Sc. Project, University of Waterloo.

Caruccio, F.T., 1975. Estimating the acid potential of coal mine refuse. In M.J. Chadwich and G.T. Goodman, eds., The Ecology of Resource Degradation and Renewal. Blackwell Scientific Publ., p. 197-205.

Chapman, L.J. and Thomas, M.K. 1968. The Climate of Northern Ontario. Department of Transport Meteorological Branch, Toronto, Ontario, 58 p.

Cherry, J.A., Blackport, R.J., Dubrovsky, N., Gillham, R.W., Lim, T.P., Murray, D., Reardon, E.J., and Smyth, D.J.A., 1980. Subsurface hydrology and geochemical evolution of inactive pyritic tailings in the Elliot Lake Uranium District, Canada. Uranium Mill Tailings Management, Proceedings of the Third Symposium, November 24-25, 1980, Geotechnical Engineering Program, Civil Engineering Department, Colorado State University.

Cherry, J.A., Gillham, R.W., Anderson, F.G. and Johnson, P.E., 1980b. Hydrogeological studies of a sandy aquifer at an abandoned landfill: Part 2, monitoring devices. In CFB Borden landfill study, Vol. 1. Waterloo Research Institute, Waterloo, Ontario.

Cochran, W.G. and Cox, G.M., 1957. Experimental Design (2nd Ed.), Wiley Publ. Co.

Conlin, B.H., 1980. Design considerations for earthquake-resistant mine tailings impoundment structures in northern Ontario. Unpublished M.Sc. Thesis, Department of Civil Engineering, University of Toronto.

Cox, D.R., 1958. Planning of Experiments, John Wiley and Sons, New York, N.Y., 308 p.

Dugan, P.R. and Apel, W.W., 1978. Microbiological desulfurization of coal. In L.E. Murr, A.E. Torman and J.A. Brierly (eds.) Metallurgical Applications of Bacterial Leaching and Related Phenomena, Academic Press, p. 223-250.

Feenstra, S., 1980. The Isotopic Evolution of Sulfate in a Shallow Groundwater Flow System on the Canadian Shield. University of Waterloo, unpublished Master of Science thesis, 152 p.

Feenstra, S., Blair, R.D., Cherry, J.A., Chakravatti, J.L., and LaRocque, E., 1981. Hydrogeochemical Investigations of two inactive tailings areas in the Elliot Lake Uranium District, Ontario, Canada. Uranium Mill Tailings Management, Proceedings of the Fourth Symposium, November, 1981, Geotechnical Engineering Program, Civil Engineering Department, Colorado State University.

Folk, R.L., 1974. Petrology of Sedimentary Rocks. Hemphill Publishing Company, Austin, Texas, 182 p.

Gillham, R.W., 1982. Syringe devices for ground-water sampling. Ground Water Monitoring Review 2, (2): 36-39.

Hawley, J.R., 1972. The Problem of Acid Mine Drainage in the Province of Ontario. Ministry of the Environment, Industrial Wastes Branch, Toronto, 338 p.

Ives, D.J.G. and Janz, G.J., 1961. Reference electrodes. Theory and Practice. Academic Press.

Jongejan, A., 1973. An experimental study of the weathering of mill tailings in connection with water pollution Part 4: The effect of tailings samples from various Canadian mining companies on the composition of water. EMR, Mines Br. Invest. Rept. IR 73-55, 65 p.

Kaiman, S., 1977. Mineralogical examination of old tailings from the Nordic Lake mine, Elliot Lake, Ontario. CANMET, Energy, Mines, and Resources Canada. Report ERP/MSL 77-190 (IR).

Kaiman, S., 1978. Mineralogical examination of current Elliot Lake uranium tailings. CANMET, Energy, Mines, and Resources, Canada. Report MRP/MSL 78-85 (IR).

Kaplan, I.R., and Rittenberg, S.C., 1964. Microbiological fractionation of sulfur isotopes. Journal of General Microbiology, 34: pp. 195-212.

Kashkai, C., Borovskaya, Y.B. and Babozade, M.A., 1975. G_f, 298 determination of synthetic jarosite and its sulfate analogues. Geokhimya 5: 778-784.

Kealy, C.D. and Busch, R.A., 1971. Determining seepage characteristics of mill tailings dams by the finite element method. U.S. Bureau of Mines RI 7477.

Kelly, D.P. and Jones, C.A., 1978. Factors affecting metabolism and ferrous iron oxidation in suspensions and bath cultures of Thiobacillus ferrooxidans: Relevance to ferric iron leach solutions generation. In L.E. Murr, A.E. Torma and J.A. Brierly (eds.) Metallurgical Applications of Bacterial Leaching and Related Microbiological Phenomena, Academic Press, 19-44.

Kirk, B.W., 1981. Eriometry as a dust measurement technique for use in underground mines. Division Report MRP/MRL 81-(OP), CANMET, Energy, Mines and Resources Canada, 21 p.

Kleinmann, R.L., 1979. The Biogeochemistry of Acid Mine Drainage and a Method to Control Acid Formation. Unpublished Ph.D. Thesis, Princeton University, 104 p.

Lai, Sung-Ho, Tiedja, J.M. and Erickson, A.E., 1976. In situ measurements of gas diffusion in soils. Soil Science Society of America. 76: p. 3-6.

Langmuir, D., 1970. Eh-pH Determination, in Methods of Sedimentary Petrology, R.E. Carrier, Ed., Wiley-Interscience, N.Y., p. 597-635.

Langmuir, D. and Whittemore, D.O., 1971. Variations in the stability of precipitated ferric oxyhydroxides. in. J.D. Hem ed, Nonequilibrium systems in Natural Water Chemistry, Adv. Chem. Ser. 106.

Latimer, W.M., 1952. Oxidation potentials (2nd ed.): Pentrice-Hall Chemical Series, 296 p. Englewood, N.J.

Lindsay, W.L., 1979. Chemical Equilibria in Soils. John Wiley and Sons, New York, 449 p.

Lundgren, D.G. and Silver, M., 1980. Ore leaching by bacteria. Ann. Rev. Microbiol., 34: 263-83.

Lundgren, D.G., Vestal, J.R. and Tabita, F.R., 1971. The Microbiology of mine drainage pollution. IN R. Mitchell (ed.) Water Pollution Microbiology, Wiley-Interscience, New York. p. 69-88.

Marshall, W.L., and Chen, C.T.A., 1982. Amorphous silica solubilities - VI. Postulated sulfate-silicic acid solution complex. Cosmochim Acta 46: 367-370.

Miller, S.D., 1979. Chemistry of a pyrite strip-mine spoil. Ph.D. Dissertation, Yale University, New Haven, 189 p.

Millington, R.J., 1959. Gas diffusion in porous media. Science, 130, p. 100-102.

Moffet, D. 1976. The Disposal of Solid Wastes and Liquid Effluents from the Milling of Uranium Ores. CANMET, Energy, Mines and Resources, Canada, Scientific Bulletin 76-19, 76 pp.

Moffet, D. and Tellier, M. 1978. Radiological investigations of an abandoned uranium tailings area. Journal of Environmental Quality, v. 7, no. 3,

Morey, G.W., Fourner, R.O. and Rowe, J.J., 1964. Solubility of amorphous SiO_2 at 25°C; Journal of Geophysical Research, 69: 1995-2001.

Morin, K.A., Cherry, J.A., Lim, T.P. and Vivyurka, A.J. 1982. Contaminant migration in a sand aquifer near an inactive uranium tailings impoundment, Elliot Lake, Ontario. Can. Geotechnical Jour., 19, no. 1.

Murray, D. and Moffett, D., 1977. Vegetating the uranium mine tailings at Elliot Lake, Ontario. Journal of Soil and Water Conservation 32, July-August, p. 171-174. pp. 49-62.

Nelson, J.D., Shepard, T.A., and Charlie, W.A., 1977. Parameters affecting stabilities of tailings dams. Proc. Conf. on Geotech. Practice for Disposal of Solid Waste Materials, Ann Arbor, Mich., June 1977, pp. 444-460.

Nissenbaum, A., and Rafter, T.A., 1967. Sulfur isotopes in altered pyritic concretions from Israel. Journal of Sediment. Petrol. 37, pp. 961-962.

Nordstrom, D.K., 1982. The effect of sulfate on aluminum concentrations in natural waters: some stability relations in the system Al_2O_3 - SO_3 - H_2O at 298K. Geochim. Cosmochim. Acta, 46: 681-692.

Nordstrom, D.K., 1977. Hydrogeochemical and Microbiological Factors Affecting the Heavy Metal Chemistry of an Acid Mine Drainage System. Unpublished Ph.D. Thesis, Stanford University, 210 p.

Nordstrom, D.K., 1980. Aqueous pyrite oxidation and the formation of secondary iron sulphate and iron oxide/hydroxide minerals. Acid Sulphate Weathering Symp., Soil Sc. Soc. Am., Annual Meeting, Ft. Collins, Colorado.

Nordstrom, D.K., Jenne, E.A. and Ball, J.W., 1979. Redox equilibria of iron in acid mine waters. In Jenne, E.A. (ed.) Chemical Modelling in Aqueous Systems: Speciation, Sorption, Solubility and Kinetics. Symp. Series 93, American Chemical Society, p. 51-80.

Ontario Ministry of the Environment, 1978. Water Management Goals, Policies, Objective and Implementation - Procedures of the Ministry of the Environment, 67 p.

Paces, T., 1973. Steady-state kinetics and equilibrium between ground water and granitic rock, Geochim Cosmochim Acta, 37: 2541-2563.

Papendick, R.I. and Runkles, J.R., 1965. Transient state oxygen diffusion in soil: I. The case when rate of oxygen consumption is constant. Soil Science 100, p. 251-261.

Patterson, R.J., Frape, S.K., Dykes, L.S. and McLeod, R.A. 1978. A coring and squeezing technique for the detailed study of subsurface water chemistry. Canadian Journal of Earth Scences 15, p. 162-169.

Raicevic, D., 1979. Decontamination of Elliot Lake uranium tailings. CIM. Bulletin, August 1979, p. 109-115.

Rao, S.R., 1971. Xanthates and Other Related Compounds, Marcel Dekker Inc., New York, 504 p.

Rawajfih, Z., 1975. The solubilities of aluminum-hydroxy-sulfate compounds as a possible mechanism of sulfate retention by soils: Ph.D. Dissertation, Aurburn University, 91 p.

Reardon, E.J., 1979. Complexing of silica by iron (III) in natural waters. Chemical Geology 25: 339-345.

Reardon, E.J., Allison, G.B. and Fritz, P., 1979. Seasonal chemical and isotopic variations of soil CO_2 at Trout Creek, Ontario. Journal of Hydrology 43, p. 355-371.

Robertson, J.A. 1968. Geology of Township 149 and Township 150. Geological Report 57, Ontario Department of Mines, 162 p.

Sato, M., 1960. Oxidation of sulfide ore bodies. I. Oxidation mechanisms of sulfide minerals at 25°C. Econ. Geol. 55: 1202-1231.

Shumate, K.S., Smith, E.E., Dugan, P.R., Brant, R.A., Randles, C.I., 1971. Acid Mine Drainage and Abatement. EPA Water Quality Office, Water Pollution Control Research Series DAST-42, 14010 FPR 04/71.

Silver, M. and Talor, J.B., 1981. Assessment of the microbiological populations in field and test pit experiments at Elliot Lake, Ontario, Canada. CANMET Rept. MRP/MSL 81-17 (TR), 31 p.

Silverman, M.P. and Lundgren, D.G., 1959. Studies on the chemoautotraphic iron bacterium Ferrobacillus ferrooxidans 1: An improved medium and a harvesting procedure for securing high cell yields. J. Bacteriol, 77: 642-647.

Singer, P.C. and Stumm, W., 1970. Acid mine drainage; the rate determining step. Science, 167: 1121-1123.

Singh, S.S., 1969. Basic aluminum sulfate formed as a metastable phase and its transformation to gibbsite: Canadian Journal of Soil Science, 49:: 383-388.

Stumm, W. and Morgan, J.J., 1970. Aquatic Chemistry, Wiley-Interscience, New York, 583.

Torma, A.E., Walden, C.C., Duncan, D.W. and Branion, R.M.R., 1972. The effect of carbon dioxide and particle surface area on the microbiological leaching of a zinc sulfide concentrate. Biotechnol. Bioeng., 14: 777-786.

Truesdell, A.H. and Jones, B.F., 1964. WATEQ, a computer program for calculating chemical equilibria of natural waters. Journal of Research U.S. Geological Survey 2, p. 233-248.

Vlek, P.L.G., Blom, Th.J.M., Beek, J. and Lindsay, W.L., 1974. Determination of the solubility product of various iron hydroxides and jarosite by the chelation method. Soil Si/ Soc. Amer. Proc. 38: 429-432.

Walsh, F., 1972. Biological control of mine drainage IN R. Mitchell (ed.) Water Pollution Microbiology, V. 2, Wiley-Interscience, New York, 377-389.

Wardrop Associates Limited, 1978, unpublished pump test conducted for CANMET, Elliot Lake Laboratory.

Whitfield, M., 1974. Thermodynamic limitations of the use of the platinum electrode in Eh measurements. Limnol. Oceanogr. 19: 857-865.

Whittemore, D.O., and Langmuir, D., 1975. The solubility of ferric oxyhydroxides in natural water. Groundwater, vol. 13, pp. 360-365.

Zajic, J.E., 1969. Microbial Biogeochemistry. Academic Press, New York, 345 p.

Zotov, A.V., Mironova, G.D., Rusinov, V.L., 1973. Determination of the Gibbs free energy $F_{f,298}$ of jarosite synthesized from a natural solution. Geokhimiya, 739-745.

Appendix A

DATA ON PHYSICAL HYDROLOGY

Table A 1 Tailings piezometer depths and hydraulic head

Piezometer Number	Datum	Piezometer tip depth below datum (m)	Elevation of Piezometer top (m)	Elevation of Piezometer point (m)	Hydraulic Head (m) June 27, 1980	July 26, 1980	June 13, 1981
T1-1	351.84	13.09	351.83	338.74	347.48	345.95	346.48
2		8.52	351.84	343.32	348.44	347.61	348.34
3		8.44	351.84	343.40	348.44	347.61	348.33
4		7.09	351.84	344.79	348.43	347.67	348.40
5		5.52	351.84	346.32	346.63	348.78	348.55
6		3.94	351.84	347.88	348.79	dry	348.68
7		2.40	351.84	350.44	dry	dry	dry
T2-1	352.00	12.65	352.00	339.35	June 21/80 344.74	July 26/80 344.44	June 13/81 344.76
2		10.96	352.00	341.04	346.01	345.79	-
3		9.82	351.99	342.17	346.10	345.63	346.13
4		8.30	352.00	343.70	346.20	345.83	346.23
5		6.86	351.99	345.13	346.38	346.03	346.45
6		5.82	351.99	346.53	346.45	dry	dry
7		5.46	352.00	346.01	dry	dry	dry
8		3.99	352.01	349.51	dry	dry	dry
T3-1	351.42	10.54	351.42	340.88	June 21/80 343.58	July 29/80 343.23	June 13/81 343.49
2		9.10	351.46	342.32	344.00	343.70	344.00
3		8.62	351.37	342.80	344.09	343.79	344.08
4		6.96	351.42	344.46	dry	dry	dry
5		5.57	351.38	345.85	dry	dry	dry
6		4.21	351.42	347.21	dry	dry	dry
T4-1	354.80	3.35	354.79	351.46	June 21/80 352.88	July 23/80 352.46	June 13/81 352.86
2		14.17	354.79	340.63	352.91	352.45	352.82
3		9.80	354.81	342.02	352.92	352.46	352.80
7		6.96	354.84	347.84	352.90	352.40	352.83
8		4.97	354.83	349.83	352.89	352.40	352.83
9		4.17	354.83	350.63	352.90	352.41	352.83
10		2.67	354.83	352.13	352.90	352.41	352.84
11		6.17	354.83	348.63	352.86	352.38	352.80
12		19.03	354.82	335.77	352.35	352.45	352.80
13		18.48	354.81	333.32	-	352.47	352.85
14		10.18	354.82	344.62	-	352.46	352.84
T5-1	356.06	6.30	356.34	349.76	July 18/80 351.42	Sept.8/80 351.16	June 13/81 351.14
2		5.72	356.06	350.34	351.14	350.90	350.87
3		8.00	356.08	348.06	351.08	350.82	350.80
4		9.00	356.08	347.06	351.05	350.80	350.74
5		10.01	356.06	346.05	350.96	350.74	350.69
6		14.03	356.03	342.03	350.96	350.75	350.62
7		10.93	356.03	345.13	351.03	350.77	350.70
8		13.04	356.02	343.02	351.02	350.77	350.75
T6-1	354.49	5.65	354.49	348.84	July 3/80 350.03	June 13/81 349.78	
2		7.41	354.49	347.08	349.97	349.78	
3		8.06	354.49	346.43	349.97	349.76	
4		9.37	354.49	345.12	349.90	349.70	
5		10.65	354.48	343.83	349.87	349.70	
6		11.65	354.49	342.84	349.93	349.76	
7		13.08	354.49	341.41	349.99	349.73	
8		14.42	354.49	340.07	349.81	349.58	
T7-1	351.89	10.09	351.67	341.60	Aug.6/80 342.82	July 4/80 343.05	June 13/81 343.16
2		9.41	351.68	342.28	342.88	342.99	343.17
3		8.75	351.69	342.94	343.16	343.37	343.41
4		8.05	351.69	343.64	dry	dry	343.68
T8-1	353.50	14.43	353.53	339.07	July 28/80 342.09		June 13/81 342.10
2		12.91	353.52	340.59	342.09		342.11
A		11.29	353.48	342.21	343.51		343.63
B		11.55	353.35	341.95	342.25		342.29
C		11.25	352.46	341.25	342.72		342.79
T9-1	350.34	9.23	350.35	341.11	July 4/80 342.27	July 27/80 342.23	June 13/81 342.22
2		8.23	350.34	342.11	344.89	343.63	344.10
3		8.08	350.34	342.26	344.68	343.44	343.78
4		7.10	350.34	343.24	344.99	343.63	344.12
T10	354.73	15.35	354.73	339.38	June 27/80 344.23	June 13/81 344.47	
Lacroe Tailings*							
LT-1		7.95			Aug. 15/80 0.85	Sept. 7/80 0.85	
2		7.52			0.87	0.85	
3		6.65			0.84	0.83	
4		5.57			0.86	0.86	
5		4.63			0.88	0.84	
6		3.62			1.56	0.82	
7		2.54			0.85	0.84	
9		1.51			0.84	0.85	
Outrea Tailings*							
OT-1		5.0			Sept. 7/80 0.42		
2		4.0			0.41		
3		3.0			0.40		
4		2.0			0.35		
5		1.0			0.29		

*The elevations of these piezometer nests were not determined. Data listed under "Piezometer tip depth below datum" represents approximate depth of piezometer point below ground surface. Data shown under "Hydraulic Head" is the depth to static water level from ground surface.

Notes:

- Datum is arbitrarily chosen to approximate the elevation of the piezometer stand pipes.
- Ground surface is approximately 1 metre below listed datum.
- Elevations of top of piezometer stand pipe from 1980 survey of Noranda Main tailings done by Marshall, Macklin Monaghan Ltd. Consulting Engineers for Rio Algom Ltd.
- Water levels measured to ± 0.5 cm.

Table A 2 Data on piezometer depths and water levels for bundle piezometers in the aquifer underlying the Nordic Main tailings (location designations coincide with tailings piezometer nest designations) (all water levels measured September 8, 1980)

Bundle Piezometer Number	Elevation of Top of Piezometer (m)	Depth to Piezometer Point* (m)	Depth to Static Water Level* (m)	Hydraulic Head (m)
BT3-1	350.82	17.2	7.72	343.10
2		16.2	7.80	343.02
3		15.2	7.80	343.02
4		13.8	7.75	343.07
5		12.9	7.71	343.11
6		12.0	7.70	343.12
7		11.1	7.70	343.12
BT4-1	354.9[1]	20.1	2.67	352.23
2		18.4	2.62	352.28
3		17.3	2.01	352.89
4		16.3	2.79	352.11
5		15.3	2.63	352.27
6		14.3	2.64	352.26
7		13.3	2.73	352.17
8		12.3	2.62	352.28
BT5-1	355.91	21.98	8.97	346.94
2		20.48	8.94	346.97
3		19.48	8.94	346.97
4		18.48	8.94	346.97
5		17.48	8.91	347.00
6		15.98	6.40	349.51
BT7-1	351.33	23.09	8.62	342.71
2		19.13	8.62	342.71
3		18.00	8.78	342.55
4		17.30	8.54	342.79
5		15.17	8.52	342.81
6		13.04	8.52	342.81
7		11.21	8.51	342.82
8		8.92	8.53	342.84
9		7.09	dry	

*Depths are taken relative to the surveyed elevation of the top of the piezometer stand pipe.

[1]The elevation of the top of the bundle piezometer was not surveyed, and the elevation was calculated from the groundsurface elevation and measured pipe stick-up.

Appendix B

ANALYSES OF SATURATED-ZONE PORE-WATER CHEMISTRY

Footnotes for tables B1.1 through B 1.12

[1] Depth measured relative to listed datum, Table A 1

[2] Analyses were done at the following locations: 1) University of Waterloo laboratory, 2) Rio Algom Environmental Control Laboratory, 3) Monenco Analytical Laboratory, 4) EMR CANMET Elliot Lake Laboratory, F) Field analyses.

[3] SO_4 value adjusted to achieve charge balance

All analyses in ppm except pH, pe, specific conductance (µS) and ^{226}Ra (pCi/L).

Table B1.1 Pore water chemistry of piezometer nest T1, Nordic Main tailings area

Piezometer Number		T1-1		T1-2		T1-3	T1-4			T1-5		T1-6
Depth[1] (m)	Lab[2]	13.09		8.52		8.44	7.05			5.52		3.96
Date sampled		July 1980	June 1981	July 1980	June 1981	July 1980	June 1981	July 1980	June 1981	July 1980	June 1981	June 1981
pH	F	6.2	6.01	6.9	6.12	6.69	6.45	6.03	5.96	5.42	5.76	3.82
pe	F	2.0	2.12	1.59	1.17	2.45	1.14	2.26	1.80	4.74	3.66	8.11
Alk (as HCO_3)	F	167	109	79	109	139	15	100	63	46	22	-
Specific conductance	F	2830	3750	5100	7.100	7.000	10,000	9,500	10,200	-	5,400	3,800
Ca	2	417	425	375	390	363	393	382	359	381	369	398
Na	2	32.3	32	23.8	15	17.9	11	5.8	4.9	3.1	6.3	7.3
K	2	49.3	53	64.5	96	80	103	62.5	48	29	26	14
Pb	2	0.20	0.14	0.28	0.29	0.26	0.29	0.56	0.34	0.46	0.14	< 0.03
Zn	2	0.40	0.25	0.05	0.31	0.10	1.6	0.44	0.43	0.57	0.35	0.42
Ni	2	0.13	0.15	0.51	0.88	0.70	0.93	0.50	0.80	3.24	2.6	2.3
Co	2	0.10	0.11	0.04	0.13	0.71	0.46	0.47	1.3	5.65	3.2	1.3
Fe	2	570	390	490	1950	800	4,100	6,260	5,275	5,240	2,575	1,388
Mn	2	26.9	27	9.8	119	114	112	30.9	26	7.60	7.1	3.1
Cu	2	0.08	< 0.01	0.22	0.05	0.03	0.04	0.11	0.06	0.27	0.04	0.13
Mg	2	249	269	1114	878	1157	628	688	308	183	97	78
Al	2	< 0.4	< 0.5	< 0.4	< 0.5	< 0.4	< 0.5	< 0.4	< 0.5	< 0.4	< 0.5	< 0.5
SO_4	1	5290	2500	-	7160	7020	9,480	15,200	10,100	11,000	5,100	3,200
Cl	1	4.75	24.0	-	1.21	2.60	0.58	0.35	< 0.5	0.81	7.28	14.1
SiO_2	1	9.90	19.0	-	21.3	16.9	27.3	28.1	30.4	28.2	28.5	57.5
F	1	< 2.0	-	-	-	< 2.0	-	< 2.0	-	< 2.0	-	-
^{226}Ra	3	8		8		117		119				

Table B1.2 Pore water chemistry of piezometer nest T2, Nordic Main tailings area

Piezometer Number		T2-1		T2-2		T2-3	T2-4			T2-5	
Depth[1] (m)	Lab[2]	12.65		10.96		9.82	8.30			6.86	
Date sampled		July 1980	June 1981	July 1980	June 1981	July 1980	June 1981	July 1980	June 1981	Aug. 1980	June 1981
pH	F	5.95	5.87	7.28	7.3	5.61	5.95	5.65	5.97	5.67	5.36
pe	F	1.47	3.66	2.66	1.91	2.46	2.72	1.58	2.61	6.78	6.85
Alk (as HCO_3^-)	F	125	27	407	389	39	32	65	80	23	7
Specific Conductance	F	2,400	2,920	4,070	4,090	8,500	9,000	10,100	10,100	5,100	3,280
Ca	2	359	365	432	410	350	395	362	386	394	416
Na	2	27.5	23	46.0	36	5.9	4.2	27.5	2.8	2.3	1.8
K	2	65	70	61	155	7.8	191	67	115	63	29
Pb	2	0.16	< 0.03	0.18	< 0.03	0.33	0.37	0.40	0.34	0.32	0.23
Zn	2	0.01	0.080	0.05	0.032	0.12	0.18	2.22	3.2	7.07	2.6
Ni	2	0.05	0.73	0.40	0.68	0.56	0.88	10.2	12	5.91	2.9
Co	2	0.02	0.17	0.06	0.09	4.23	4.6	10.35	11	3.77	1.4
Fe	2	180	241	100	80	4,550	4,725	6,900	6,550	3,070	1,250
Mn	2	6.12	7.7	8.31	8.9	157	109	7.18	6.3	2.15	1.2
Cu	2	0.04	0.09	0.08	< 0.01	0.14	0.05	0.26	0.05	0.41	0.04
Mg	2	191	197	327	408	746	385	186	152	102	32
Al	2	< 0.4	< 0.5	< 0.4	< 0.5	< 0.4	< 0.5	< 0.4	< 0.5	< 0.4	< 0.5
SO_4	1	2,750	1,960	4,350	2,900	12,500	9,720	13,800	10,500	6,680	3,280
Cl	1	34.0	34.1	77.0	64.0	9.53	< 0.5	2.80	< 0.5	3.40	< 0.5
SiO_2	1	10.8	12.7	7.39	6.09	29.5	25.6	29.5	24.7	43.3	39.0
F	1	< 2.0	-	3.4	-	< 2.0	-	< 2.0		3.5	
^{226}Ra	4	11.3	-	132.1	-	142.1					

Table B1.3 Pore water chemistry of piezometer nest T3, Nordic Main tailings area

Piezometer Number		T3-1		T3-2		T3-3	
Depth[1] (m)	Lab[2]	10.54		9.10		8.62	
Date sampled		July 1980	June 1981	July 1980	June 1981	Aug. 1980	June 81
pH	F	5.72	5.88	5.88	5.89	6.03	6.12
pe	F	5.29	3.44	2.94	3.10	2.65	1.73
Alk (as HCO_3)	F	153	105	165	56	133	114
Specific Conductance	F	7,200	7,200	5,900	6,500	5,750	6,900
Ca	2	594	548	396	406	372	398
Na	2	31	24	3.7	2.3	3.7	3.0
K	2	140	136	135	95	148	114
Pb	2	0.11	<0.02	0.51	0.34	0.11	0.40
Zn	2	0.10	0.66	1.0	2.6	0.72	0.77
Ni	2	0.77	1.0	1.3	1.2	1.2	0.92
Co	2	0.33	0.27	1.9	4.3	1.9	2.9
Fe	2	800	745	3,275	2,963	3,870	2,675
Mn	2	95	103	95	32	230	60
Cu	2	0.07	0.10	< 0.01	0.73	0.04	0.12
Mg	2	1,410	1,118	246	166	297	162
Al	2	0.5	< 0.3	1.6	< 0.5	0.3	< 0.5
SO_4	1	8,550	7,200	7,810	6,600	8,680	6,280
Cl	1	7.60	7.63	0.95	< 0.5	< 0.26	< 0.5
SiO_2	1	8.92	6.28	26.7	25.2	26.3	27.1
F	1	< 2.0	-	3.4	-	< 2.0	-
^{226}Ra	4	16.7	-	0.60	-	144.1	-

Table B1.4 Pore water chemistry of piezometer nest T4, Nordic Main tailings area (sampled July 1980)

Piezometer Number		T4-1	T4-2	T4-3	T4-7	T4-8	T4-9	T4-10	T4-11	T4-12	T4-13	T4-14
Depth[1] (m)	Lab[2]	3.35	14.17	0.80	6.96	4.97	4.17	2.67	6.17	19.03	18.48	10.18
pH	F	4.06	8.00	6.05	5.90	5.80	4.40	4.55	6.08	6.50	6.5	7.09
pe	F	7.74	0.90	3.86	2.28	2.12	6.38	6.64	1.48	1.38	2.31	1.77
Alk (as HCO_3)	F	-	218	165	240	157	-	-	201	218	127	141
Specific Conductance	F	4,130	3,320	5,250	6,400	5,800	4,940	2,600	7,500	3,490	3,290	3,500
Ca	2	422	455	398	378	383	395	470	375	448	437	405
Na	2	4.75	113	52.5	39.5	4.95	3.85	3.35	12.05	41.3	55.6	51.3
K	2	57.0	120	241	204	77	38	49	131	72	210	193
Pb	2	2.86	0.19	0.08	0.12	0.12	2.32	0.02	0.18	0.03	0.13	0.14
Zn	2	0.42	0.09	0.32	0.11	2.14	1.78	0.80	2.25	1.21	0.10	0.18
Ni	2	2.06	0.19	0.48	0.52	8.46	3.19	0.80	8.35	0.33	0.32	0.51
Co	2	1.80	0.16	0.34	0.34	4.88	2.08	0.33	4.81	0.27	0.15	0.17
Fe	2	1,930	8	1,930	3,410	3.870	2,620	398	5,120	570	116	113
Mn	2	0.55	0.66	27.7	267	4.73	1.17	0.39	10.23	6.43	28.4	1.84
Cu	2	0.02	0.01	0.02	0.04	0.03	0.02	0.01	0.02	0.02	0.03	0.03
Mg	2	25.0	768	1,030	1,000	305	135	90	1,620	1,610	510	1,045
Al	2	115	5	3	3	3	47	8	3	3	3	3
SO_4	1	5,100	4,320[3]	8,350[3]	11,328[3]	8,600	6,600	2,227[3]	16,224[3]	8,640[3]	3,520	5,376[3]
Cl	1	2.80	39.2	127	78.2	7.50	3.50	2.8	13.4	-	156	88.1
SiO_2	1	116	21.9	24.6	43.2	36.8	81.8	94.9	38.8	-	16.5	10.1
F	1	2.36	< 2.0	< 2.0	< 2.0	2.7	< 2.0	< 2.0	< 2.0	-	< 2.0	3.40
^{226}Ra	4	-	82.7	160.8	154.1	126.4	66.76	-	124.8	121.5	130.4	84.9

Table B1.5 Pore water chemistry of piezometer nest T5, Nordic Main tailings area (sampled July 1980)

Piezometer Number		T5-1	T5-2	T5-4	T5-5	T5-6	T5-7	T5-8
Depth[1] (m)	Lab[2]	6.30	5.72	9.00	10.01	14.03	10.93	13.04
pH	F	2.73	3.85	5.83	5.30	5.98	6.15	6.97
pe	F	9.86	8.16	3.92	2.23	3.50	1.01	0.29
Alk (as HCO_3)	F	-	-	232	116	195	229	345
Specific conductance	F	12,200	9,000	16,200	10,119	6,400	9,500	3,500
Ca	2	380	384	400	396	428	386	480
Na	2	12	10	14	16	46	39	48
K	2	174	72	170	204	144	204	144
Pb	2	4.0	4.0	0.67	0.54	0.36	0.25	0.06
Zn	2	4.9	5.1	7.3	1.5	1.6	0.67	0.27
Ni	2	5.0	6.0	16	5.6	3.0	1.7	0.33
Co	2	6.8	6.3	14	8.3	2.5	3.1	0.12
Fe	2	6,030	5,350	12,520	10,240	2.73	5,790	84
Mn	2	1.2	2.9	15	19	16	30	3.7
Cu	2	49	0.04	0.05	0.09	0.01	0.05	0.01
Mg	2	98	125	460	458	440	510	326
Al	2	933	595	0.79	< 0.3	4.7	< 0.3	< 0.3
SO_4	1	21,700	13,968[3]	28,000	20,640[3]	7,440[3]	13,104[3]	2,654[3]
Cl	1	6.90	9.62	4.90	6.53	48.8	10.1	196
SiO_2	1	238	102	40.4	32.4	34.0	34.0	9.53
F	1	5.0	11.4	< 2.0	2.95	2.2	< 2.0	3.2
^{226}Ra	4	-	-	131.9				

Table B1.6 Pore water chemistry of piezometer nest T6, Nordic Main tailings area

Piezometer Number		T6-1		T6-2		T6-3	T6-4		T6-5		T6-6		T6-7	T6-8		
Depth[1] (m)	Lab[2]	5.65		7.41		8.06	9.37		10.65		11.65		13.08	14.42		
Date sampled		July 1980	June 1981	July 1980	June 1981	July 1980	June 1981	July 1980	June 1981	July 1980	June 1981	July 1980	July 1980	June 1981	July 1980	June 1981
pH	F	3.99	-	3.91	3.98	4.3	4.11	5.66	5.80	5.9	5.95	6.8	6.83	6.51	6.49	6.4	6.68
pe	F	7.69	-	7.76	6.48	7.72	8.25	5.52	3.47	2.64	2.33	2.50	1.59	0.40	1.96	1.64	1.35
Alk (as HCO_3^-)	F	-	-	-	-	-	-	95	14	152	41	196	123	662	126	276	241
Specific Conductance	F	4,300	-	6,100	5,900	7,000	6,000	9,000	8,400	9,800	10,250	3,690	3,650	4,420	5,200	4,520	4,800
Ca	2	432	413	384	406	386	406	388.	409	384	400	470	470	450	465	438	438
Na	2	2.9	4.4	5.9	4.2	8.6	5.2	16	15	18	22	43	47	69	71	3.0	63
K	2	31	105	85	71	130	94	206	172	208	235	174	170	156	155	160	142
Pb	2	2.6	2.0	3.4	2.7	5.6	3.8	0.49	0.29	0.25	< 0.02	0.10	0.14	0.10	0.07	0.09	0.09
Zn	2	0.52	0.77	1.2	1.7	5.3	4.1	8.0	3.6	0.14	.57	0.22	0.18	0.10	0.067	0.48	0.084
Ni	2	1.4	1.8	4.1	3.5	6.2	5.5	9.1	6.6	2.7	2.3	0.44	0.73	0.39	0.73	0.92	0.59
Co	2	1.6	1.8	4.1	2.9	5.1	2.9	7.1	5.2	3.8	2.8	0.06	0.09	0.13	0.14	0.70	0.18
Fe	2	1,710	1,920	3,760	2,713	4,440	2,750	6,030	4,963	5,920	4,850	140	128	290	237	910	155
Mn	2	0.54	0.82	1.0	0.97	1.8	1.4	8.0	13	30	48	1.3	1.3	4.4	4.5	13	8.9
Cu	2	0.02	0.081	0.03	0.016	0.01	0.016	< 0.01	0.14	< 0.01	0.056	0.01	0.040	< 0.01	0.017	0.02	0.033
Mg	2	24	42	50	39	77	47	286	246	658	600	320	317	488	520	488	493
Al	2	116	191	563	180	381	145	41	13	0.3	0.7	< 0.3	< 0.3	0.3	0.7	< 0.3	< .3
SO_4	1	4,800[3]	5,560	12,400	6,160	12,650	6,600	14,100	9,480	15,400	10,500	2,880[3]	2,350	3,950	3,180	5,650	3,200
Cl	1	4.21	3.94	2.6	4.04	5.82	2.83	32.3	26.9	9.8	40.8	157	196	136	134	91.0	99.4
SiO_2	1	125	132	116	98.0	106	90.8	51.5	39.4	46.5	34.2	27.6	18.5	13.8	12.0	5.71	18.5
F	1	2.6	-	8.0	-	84.4	-	32.4	-	3.66	-	< 2.0	-	2.92	-	3.33	-
^{226}Ra	3	95	-	67	-	135	-	412	-	111	-	129	-	117		100	

Table B1.7 Pore water chemistry of piezometer nest T7, Nordic Main tailings area

Piezometer Number		T7-1		T7-2		T7-3	
Depth[1] (m)		10.09		9.41		8.75	
Dated Sampled	Lab[2]	Aug. 1980	June 1981	Aug. 1980	June 1981	Aug. 1980	June 1981
pH	F	5.40	5.51	4.38	5.06	4.1	4.65
pe	F	6.46	4.01	10.11	7.69	9.99	8.60
Alk (as HCO_3)	F	85	55	-	-	-	-
Specific Conductance	F	8,900	9,200	9,100	-	12,000	-
Ca	2	456	473	330	420	358	438
Na	2	12	11	17	301	7.2	16
K	2	180	158	182	137	252	163
Pb	2	0.4	0.20	0.5	0.30	0.9	0.52
Zn	2	0.72	0.74	0.85	5.1	19	46
Ni	2	1.4	0.91	4.4	11	18	30
Co	2	4.7	3.6	5.3	5.9	20	23
Fe	2	5,685	4,200	7,049	5,388	17,965	13,156
Mn	2	78	44	42	14	10	9.8
Cu	2	0.03	0.041	0.05	0.75	0.12	0.77
Mg	2	428	399	340	149	251	323
Al	2	1.3	< 0.4	6.0	36	1.0	11
SO_4	1	-	8,240	-	9,520	-	20,500
Cl	1	13.4	20.7	14.4	23.9	18.8	13.4
SiO_2	1	10.1	10.8	39.8	63.7	60.9	100.4
F	1	-	-	-	-	-	-
^{226}Ra	4	24.4	-	-	-	-	-

Table B 1.8 Pore water chemistry of piezometer nest T8, T9, and T10, Nordic Main tailings

Piezometer Number		T8-1	T8-2	T8-A	T8-B	T8-C	T9-1	T9-2	T9-3	T0-4	T-10
Depth[1] (m)		14.43	12.91	11.29	11.55	11.25		8.23	8.08	7.10	15.35
Date Sampled	Lab[2]	Aug. 1980	Aug. 1980	Aug. 1980	Aug. 1980	Aug. 1980	July 1980	Aug. 1980	July 1980	July 1980	July 1980
pH	F	6.08	6.33	5.80	5.28	5.38	4.9	6.51	6.43	-	6.39
pe	F	5.08	3.61	5.62	8.11	7.81	3.47	5.76	6.86	-	4.38
Alk (as HCO_3)	F	36	258	48	13	46	37	-	50	-	-
Specific Conductance	F	6,300	6,250	6,200	3,490	8,200	4,200	3,400	5,100	-	4,200
Ca	2	410	430	370	390	364	462	418	386	392	472
Na	2	15	23	6.7	6.1	30	38	224	13	8.2	78
K	2	123	132	127	116	100	94	65	66	56	115
Pb	2	0.09	0.22	0.15	0.31	0.94	0.54	0.04	0.11	0.09	0.49
Zn	2	0.53	0.42	1.4	1.8	0.68	1.3	0.41	0.57	0.50	0.15
Ni	2	0.52	1.4	11	5.1	3.5	0.77	0.92	0.15	0.21	0.60
Co	2	1.1	1.5	11	6.2	4.8	0.10	0.58	0.08	0.02	0.17
Fe	2	3,530	2,960	7,740	4,550	10,028	35	600	10	50	910
Mn	2	130	86	9.4	7.8	31	1.5	16	2.8	2.8	12
Cu	2	0.05	0.07	0.07	0.43	0.06	0.11	0.06	0.02	0.01	< 0.01
Mg	2	575	695	168	140	498	440	162	1,326	810	368
Al	2	< 0.3	0.8	0.3	2.4	< 1.0	1.0	< 0.3	< 0.3	0.3	< 1.0
SO_4	1	11,300	20,100	26,700	10,000	-	5,250	4,190	10,100	7,350	-
Cl	1	30.0	23.0	2.0	4.9	-	17.5	15.5	28.3	6.00	-
SiO_2	1	22.5	18.4	39.2	51.6	-	16.2	30.8	10.1	12.8	-
F	1	< 2.0	3.1	< 2.0	< 2.0	-	2.0	< 2.0	2.17	< 2.0	-
^{226}Ra	4	-	98.1	-	51.3	92.3	19.1	-	-	-	-

Table B 1.9 Pore water chemistry of piezometer nest LT, Lacnor tailings area (sampled August, 1980)

Piezometer Number		LT-1	LT-2	LT-3	LT-4	LT-5	LT-6	LT-7	LT-8
Depth[1] (m)		7.95	7.52	6.65	5.57	4.63	3.62	2.54	1.51
	Lab[2]								
pH	F	5.26	6.15	4.11	3.69	3.70	3.40	2.02	1.98
pe	F	3.3	1.38	7.67	7.18	7.17	7.90	8.74	8.94
Alk (as HCO_3)	F	32	109	-	-	-	-	-	-
Specific Conductance	F	3,610	3,590	3,720	3,570	3,510	-	3,890	3,590
Ca	2	349	320	324	327	346	395	405	439
Na	2	11	10	6.7	6.1	4.8	3.7	3.2	7.5
K	2	73	86	87	81	75	60	52	36
Pb	2	2.3	0.3	0.6	0.4	2.9	3.3	2.2	2.5
Zn	2	4.7	110	3.5	110	2.5	0.92	0.59	8.9
Ni	2	1.5	0.2	1.4	2.3	2.1	1.1	0.6	0.5
Co	2	1.3	0.09	1.1	2.3	2.0	0.93	0.92	0.67
Fe	2	2,388	3,638	3,525	2,615	2,183	1,251	1,171	910
Mn	2	1.4	2.3	2.0	0.81	0.84	0.74	0.38	0.25
Cu	2	0.79	0.33	0.02	0.04	0.03	0.03	0.01	0.73
Mg	2	45	66	53	27	28	39	76	80
Al	2	203	5.4	201	404	313	244	76	48
SO_4	1	-	-	-	-	-	-	-	-
Cl	1	20.8	13.4	19.1	24.2	26.7	6.5	24.2	27.7
SiO_2	1	82.6	22.2	50.1	86.7	97.3	199	159	134
F	1	-	-	-	-	-	-	-	-
^{226}Ra	2	85	99	102	115	38	33	23	25

Table B 1.10 Pore water chemistry of piezometer nest QT, Quirke tailings area (sampled September 1980)

Piezometer Number		QT-1	QT-2	QT-3	QT-4	QT-5
Depth[1] (m)		5	4	3	2	1
	Lab[2]					
pH	F	8.72	8.70	8.68	9.15	7.00
pe	F	-	-	-	-	-
Alk (as HCO_3)	F	110	85	85	207	-
Specific Conductance	F	3,200	3,220	3,490	3,660	3,840
Ca	2	624	616	607	704	638
Na	2	27	26	25	25	30
K	2	194	198	140	214	218
Pb	2	0.14	0.12	0.11	0.07	0.14
Zn	2	0.04	0.02	0.02	0.04	0.03
Ni	2	0.02	<0.01	< 0.01	< 0.01	0.14
Co	2	< 0.01	<0.01	< 0.01	< 0.01	0.05
Fe	2	< 3	<3	< 3	< 3	< 3
Mn	2	0.01	<0.01	0.01	0.01	1.4
Cu	< 0.01	< 0.01	<0.01	< 0.01	< 0.01	< 0.01
Mg	2	15	5.5	5.4	1.0	13
Al	2	1.2	1.1	1.1	1.1	1.2
SO_4	1	-	-	-	-	-
Cl	1	23.2	22.1	23.2	28.3	26.2
SiO_2	1	115	108	92.6	78.0	63.9
F	1	-	-	-	-	-
^{226}Ra	2	420	448	492	354	449

Table B 1.11 Pore water chemistry of piezometer nest UW6, Nordic West Arm tailings (sampled June 1981)

Piezometer Number		UW6-1	UW6-2	UW6-3	UW6-4	UW6-5	UW6-6	UW6-7
Depth[4] (m)		6.6	5.5	4.5	3.5	2.5	1.5	8.7
	Lab[2]							
pH	F	7.06	7.29	7.44	6.09	5.56	6.62	6.15
pe	F	1.56	1.14	0.86	2.26	3.87	1.56	2.58
Alk (as HCO_3)	F	779	892	817	187	173	352	29
Specific Conductance	F	3,220	3,040	3,480	7,900	8,100	5,100	3,900
Ca	2	563	585	539	404	418	465	489
Na	2	60	50	56	99	98	198	33
K	2	45	34	38	100	97	106	69
Pb	2	< 0.02	0.18	< 0.02	0.12	0.06	0.07	0.09
Zn	2	0.025	0.021	0.14	0.092	0.17	0.11	0.19
Ni	2	0.30	0.30	0.71	0.57	1.3	0.54	0.14
Co	2	0.15	0.05	< 0.01	0.07	0.43	< 0.01	0.07
Fe	2	65	37	24	3,338	3,325	536	831
Mn	2	1.8	4.1	2.4	8.0	7.9	9.4	8.6
Cu	2	< 0.008	< 0.017	< 0.008	0.042	< 0.008	0.034	< 0.008
Mg	2	225	208	337	450	461	556	227
Al	2	< 0.4	< 0.4	< 0.4	< 0.4	8.2	<0.4	< 0.4
SO_4	1	1,800	1,660	2,060	7,500	8,160	4,000	2,960
Cl	1	125	106	79.4	83.8	81.4	136	63.8
SiO_2	1	10.7	10.7	10.7	35.0	47.0	16.1	19.0

4. Depths are from Blackport and Cherry, 1980

Table B 1.12 Pore water chemistry of piezometer nest UW14, Nordic West Arm tailings (sampled June 1981)

Piezometer Number		UW14-1	UW14-2	UW14-3	UW14-4	UW14-5
Depth[4] (m)		4.3	3.0	2.0	7.8	6.0
	Lab[2]					
pH	F	1.29	1.31	0.97	1.37	1.40
pe	F	10.05	10.56	11.24	9.46	9.81
Alk (as HCO_3)	F	-	-	-	-	-
Specific Conductance	F	29,800	25,500	47,000	20,100	21,500
Ca	2	436	434	481	424	428
Na	2	5.6	3.6	3.9	6.5	4.4
K	2	131	94	90	121	100
Pb	2	2.6	2.1	2.2	2.4	2.2
Zn	2	0.92	0.39	0.74	0.86	1.3
Ni	2	2.7	1.9	4.0	2.6	1.6
Co	2	4.2	3.4	6.6	3.1	2.9
Fe	2	5,125	4,275	10,094	3,625	3,363
Mn	2	0.36	0.26	0.25	0.41	0.26
Cu	2	5.3	3.7	5.6	9.4	4.8
Mg	2	38	29	33	6.8	5.1
Al	2	72	51	37	63	47
SO_4	1	15,400	11,900	26,600	10,700	10,400
Cl	1	3.25	1.91	18.4	16.5	4.3
SiO_2	1	123	113	71.5	118	138

4. Depths are from Blackport and Cherry (1980).

Appendix C

DEVELOPMENT OF A TECHNIQUE FOR THE DETERMINATION OF SOLID CARBONATE MINERAL CONTENT AND RESULTS

Due to the high effectiveness of the dissolution of carbonate minerals for neutralizing low-pH waters, the accurate determination of the solid carbonate mineral content of the tailings was given a high priority. The determination of carbonate mineral content in solid samples from the tailings areas is complicated by the fact that much of the pore waters have high concentrations of Fe^{2+}. Contamination by oxygen during sampling will cause the Fe^{2+} to oxidize to Fe^{3+}, which will precipitate as amorphous ferric hydroxide ($Fe(OH)_3$). This precipitation generates H^+ ions and results in the dissolution of carbonate minerals present in the samples. Approximately 0.1 wt. % $CaCO_3$ could be dissolved by the oxidation and precipitation of 1,400 to 2,000 mg/L of Fe^{2+} (depending on the specific gravity of the sample and the initial water content).

Barker and Chatten (in preparation) published results of preliminary attempts to overcome the problem of high Fe^{2+} pore water by A) washing the sample with distilled water immediately after collection, and B) preventing the creation of acidic pore waters by buffering the sample with dilute NaOH solution immediately after collection. Results are presented in Table C.1. It was found that treatment of samples with known $CaCO_3$ contents and high Fe^{2+} pore water (pH = 5.5) by addition of NaOH before drying caused the samples to gain large amounts of carbonate. Barker and

Chatten (in preparation) attribute this to uptake of CO_2 gas from the atmosphere. Washing the samples with distilled water was found to cause the loss of large amounts of carbonate.

In an attempt to improve on sample preservation, an experiment was designed to test the effectiveness of washing samples with methanol in an inert atmosphere to remove the pore water without allowing iron oxidation. Samples were prepared by the addition of ground calcite in two grain size ranges (60 - 80 mesh and 230 - 325 mesh) to a carbonate free sand to produce mixtures with approximately 0.01, 0.1 and 1.0 wt. % $CaCO_3$. Prior to mixing, the ground calcite was washed with mildly acidic water and resieved to remove very fine $CaCO_3$ powder which has abnormally high disslution rates. In each trial 5 ml of a 1 molar aqueous solution of ferrous sulphate (approximately 5,500 mg/L Fe^{2+}) was added to 20 grams of solid sample in a nitrogen-filled glove box. After standing times of 1 or 5 minutes, the samples were washed by vacuum filtering four successive 50 ml aliquots of methanol through the sample.

Results show a correlation between loss of $CaCO_3$ and initial pH of the ferrous solution added (Table C.2). Contrary to expectations based on an increase in dissolution rate with decreasing grain size, larger proportions of total $CaCO_3$ were lost from the samples containing the coarser grained calcite. Overall, in runs with initial pH's greater than 5.0, the loss of carbonate was comparable to or less than that produced by washing with distilled water. Although no major difference between the two methods was found, the methanol wash method was selected as it is least likely to produce changes in the solid phase composition of the tailings samples.

During the preliminary analyses of tailings cores further work was done to test the effects of various sample preparation methods. Core recovered from T5 at a depth of approximately 13 m was analyzed with 5 different preparation methods: 1) samples were transferred directly into the 50 ml syringe without drying ('wet') 2) samples were dried in an oven at a temperature of approximately 105^0C; 3) samples were air dried; 4) samples were methanol washed in the air and 5) samples were methanol washed in a N_2 gas-filled glove box.

Results of the analyses on core from T5 are presented in TableC3. The analyses were found to be fairly precise with reasonably small variations in the results for triplicate runs for each method. In general, the results for the 5 methods differ only slightly with an average of 0.015 wt. % $CaCO_3$ overall. The samples analyzed wet contained, on the average, a higher weight % $CaCO_3$ (0.019 wt. %) than the methanol washed samples. This difference can be attributed to a contribution of carbonate by the pore water; a problem recognized by Barker and Chatten (in preparation). The maximum measured alkalinity in the groundwater at T5 was 5.7 millimoles/L HCO_3^-. At the measured field pH of 6.97 an addition 1.4 millimoles/L of aqueous carbonate species would be 7.1×10^{-3} millimoles per ml of solution, which would contribute 0.025 wt. % $CaCO_3$ to the analysis (using specific gravity = 2.8 and solid:liquid volume ratio of 1:1). However, during removal of samples from the T5 core the solid tailings were observed to have small open pockets, or "bubbles", near the sample tube end. These "bubbles" were probably produced by degassing of the sample (due to agitation and increase in temperature) during transportation and storage. Analyses of a wet sample from T6 also produced a higher wt. % $CaCO_3$ (28% increase above average)

than analyses on dry samples. In this case, however, the observed difference (0.064 wt. % $CaCO_3$) is greater than the possible contribution by carbonate dissolved in the pore water (0.034 wt. %). Because it is believed that much of the dissolved carbonate was lost via CO_2 degassing during storage, the observed variation is probably due to variation in carbonate mineral content of the tailings over small distances.

Additional comparisons of the data show the oven-dried samples from T5 to have an average of 0.004 wt. % less $CaCO_3$ than the methanol washed (in air) samples. Pore waters extracted from the base of the T5 core (13.5 m) were found to have 36 mg/L of Fe^{2+}, the oxidation and precipitation of which could account for the removal of 0.002 to 0.003 wt. % $CaCO_3$. It is possible that the lower carbonate mineral content of the oven-dried example is due to removal of $CaCO_3$ by $Fe(OH)_3$ precipitation. However, samples from the same level that were air dried had the same wt. % $CaCO_3$ as the methanol washed samples in spite of the fact that they should have been subject to the same process of ferric hydroxide precipitation as the oven-dried samples. Fine scale compositional variations within the sample are again suggested as an explanation of this variation. In addition, the observed variations are near a level that may be attributed to other aspects of sample preparation for carbonate anaysis*.

Results show that variations in $CaCO_3$ content that could be attributed to the precipitation of $Fe(OH)_3$ were on the same order of magnitude as other unidentified sources of variation. This is probably due to the low concentrations of iron in the pore waters of this core. Although the results

---

Barker and Chatten (in preparation) reports that six replicate analyses on samples prepared to contain 0.075 wt. % $CaCO_3$ produced a mean of 0.079 wt. % $CaCO_3$ with a standard deviation of 4.7% of the mean, or 0.0037 wt. % $CaCO_3$.

are inconclusive, all samples were methanol washed as rapidly as possible upon exposure to the atmosphere in the belief that this procedure can help limit carbonate mineral removal by ferric iron precipitation.

Table C1

Results of tests on carbonate solid sample preservation by washing with distilled water or titration with NaOH (apparent loss or gain of carbonate reported relative to the original carbonate content of the samples). (from Barker and Chatten, in preparation).

Synthetic Control	after H_2O wash		after NaOH wash	
Wt% $CaCO_3$	Wt% $CaCO_3$	% apparent loss	Wt% $CaCO_3$	% apparent gain
0.014	0.007	50	0.10	610
0.014	0.012	14	0.14	900
0.018	0.006	67	0.091	410
0.023	0.006	74	0.13	470
0.061	0.018	70	0.16	160
0.11	0.041	63	0.20	82

Table C 2

Results of tests on carbonate solid sample preservation by washing with methanol

$CaCO_3$ grain size range	Control (average of 4 samples) wt% $CaCO_3$	After Methanol wash (average of 3 trials) wt% $CaCO_3$	% apparent loss 1 minute standing time	% apparent loss 5 minute standing time	pH at start
60-80 mesh	1.055	0.375	65	90	4.55-4.81
	0.099	0.03	70	90	5.09-5.34
	0.022	0.004	82	82	4.08-4.12
230-325 mesh	0.84	0.67	20	30	5.47-5.55
	0.147	0.07	52	66	5.20-5.30
	0.033	0.015	55	55	5.25-5.36

Table C 3

Results of analysis of tailings samples for carbonate mineral content

Sample Location and Depth (m)	Sample Treatment		wt % $CaCO_3$
T5	wet	-1	0.022
13.54 m		-2	0.019
		-3	0.017
			0.019 average
T5	oven dried	-1	0.012
13.54 m		-2	0.013
		-3	0.011
			0.012 average
T5	air dried	-1	0.014
13.54 m		-2	0.019
		-3	0.015
			0.016 average
T5	methanol wash		
13.54 m	in air	-1	0.018
		-2	0.015
		-3	0.016
			0.016 average
T5	methanol wash		
13.54 m	in N_2 atmosphere	-1	0.008
		-2	0.008

Table C 4

Summary of analyses of carbonate mineral content of tailings samples from sites T1, T5, and T6, in the Nordic Main tailings area, September 11, 1981. (results expressed as weight percent $CaCO_3$).

T1[1] Depth (m)	T1[1] wt % $CaCO_3$	T5 Depth (m)	T5 wt % $CaCO_3$	No. of Analyses	T6 Depth (m)	T6 wt % $CaCO_3$	No. of Analyses
3.45	BD[2]	4.3	0.004	ave. of 2	4.4	BD	1
3.85	0.005	4.7	0.001	"	4.8	0.005	"
4.25	0.002	5.1	BD	"	5.2	BD	"
4.65	0.003	5.5	BD	"	5.6	0.002	"
5.05	0.001	5.9	0.002	"	6.0	BD	"
5.45	0.009	6.3	0.001	"	6.4	BD	"
5.85	0.002	6.7	0.006	"	6.8	BD	"
6.25	0.002	6.9	0.001	"	7.0	0.002	ave. of 2
6.65	0.004	7.2	0.004	"	7.2	0.003	"
7.05	BD	7.4	0.005	"	7.4	0.003	"
7.45	0.001	7.6	0.004	"	7.6	0.005	"
7.85	0.009	7.8	0.002	"	7.8	0.004	"
8.25	0.013	8.0	0.003	"	8.0	0.001	ave. of 3
8.65	0.006	8.2	0.003	"	8.2	0.010	"
9.05	0.022	8.4	0.003	"	8.4	0.017	"
9.40	0.056	8.6	0.002	"	8.6	0.007	"
		8.8	0.005	"	8.8	0.003	"
		9.0	0.025	"	9.0	0.004	"
		9.2	0.038	"	9.2	0.003	"
		9.4	0.007	ave. of 3	9.4	0.015	"
		9.6	0.004	"	9.6	0.009	"
		9.8	0.005	"	9.8	0.016	ave. of 2
		10.0	0.017	"	10.1	0.024	ave. of 4
		10.2	0.025	"			
		10.3	0.007	ave. of 5	10.2	0.023[3]	ave. of 3
		10.4	0.039	"	10.4	0.238[3]	"
		10.5	0.016	"	10.8	0.227[3]	"

1. all data represent single analyses
2. BD: below detection

3. These samples of tailings were interbedded with thin layers of peat and are not believed to be representative of the tailings mass.

Appendix D

TEMPERATURE DATA FOR THE FOUR INCUBATORS DURING THE OXIDATION PERIOD

Appendix

Table D.1: Summary of incubator temperatures during the oxidation experiment

YEAR	MONTH	DAY	TIME (hrs)	TEMPERATURE OF DESSICABS (°C)			
				D1	D2	D3	B4
82	03	10	1600	6.6	6.9	26.8	27.0
82	03	11	0930	3.9	3.9	26.8	27.2
82	03	11	1600	3.8	3.8	26.6	27.0
82	03	12	0900	3.9	3.9	27.1	26.8
82	03	12	1600	5.8	5.8	27.2	27.8
82	03	15	0900	4.0	3.9	27.2	27.8
82	03	15	1600	4.2	4.2	27.5	27.9
82	03	16	0900	4.1	4.0	27.3	27.7
82	03	16	1630	4.2	4.2	27.4	-
82	03	17	0900	4.1	4.1	27.3	-
82	03	17	1600	4.1	4.2	27.9	-
82	03	18	0900	4.1	4.2	27.6	-
82	03	18	1630	4.1	4.1	26.8	-
82	03	19	0900	4.1	4.2	26.9	-
82	03	22	0900	4.6	4.5	26.8	-
82	03	22	1630	4.5	4.4	27.1	27.6
82	03	23	0900	4.3	4.3	27.0	27.3
83	03	23	1600	4.5	4.5	27.8	28.0
82	03	24	0900	4.8	4.7	27.9	28.1
82	03	24	1600	4.1	4.4	27.9	28.1
82	03	25	0900	4.2	4.2	27.8	28.0
82	03	25	1600	1.5	1.7	27.5	27.8
82	03	26	0900	1.5	1.6	27.2	27.7
82	03	26	1600	1.7	1.8	27.7	27.9
82	03	29	0900	1.8	1.9	26.4	26.8
82	03	29	1630	4.9	4.9	26.9	27.1
82	03	30	0900	4.7	4.5	27.1	27.5
82	03	30	1615	4.8	4.6	27.8	27.9
82	03	31	0900	4.7	4.6	24.8	24.8
82	03	31	1600	5.3	5.1	28.2	28.3
82	04	01	0900	5.0	4.8	22.9	23.1
82	04	01	1630	5.6	5.3	28.1	28.1
82	04	02	0900	5.8	5.5	27.5	27.8
82	04	02	1600	5.3	5.1	27.7	27.8
82	04	03	0900	5.3	5.1	27.9	28.0
82	04	03	1600	5.1	5.1	28.9	28.9
82	04	05	0900	5.5	5.2	26.0	26.0
82	04	06	0900	5.4	5.0	26.8	27.0
82	04	06	1600	5.4	5.0	26.8	26.9
82	04	07	0900	5.6	5.3	26.3	26.7
82	04	07	1630	5.6	5.3	26.6	26.9
82	04	08	0900	5.6	5.2	26.6	26.8
82	04	08	1600	5.6	5.2	27.1	27.2
82	04	12	0900	6.2	5.9	27.0	27.2
82	04	12	1600	6.5	6.4	27.5	27.8
82	04	13	0900	6.2	5.8	27.2	27.7

Table D.1 : Summary of incubator temperatures during the oxidation experiment

YEAR	MONTH	DAY	TIME (hrs)	TEMPERATURE OF DESSICABS (°C)			
				D1	D2	D3	D4
82	04	13	1600	6.4	6.0	27.8	28.1
82	04	14	0900	6.3	5.9	27.2	27.8
82	04	14	1600	6.4	5.9	27.8	28.0
82	04	15	0900	6.3	5.9	27.5	27.8
82	04	15	1600	6.3	6.2	27.9	28.2
82	04	16	0930	6.4	6.1	28.0	28.2
82	04	16	1400	5.5	5.2	28.2	28.5
82	04	16	1600	5.4	5.2	29.0	29.2
82	04	19	0900	5.3	5.1	26.8	27.1
82	04	19	1600	5.4	5.1	27.0	27.1
82	04	20	1630	5.4	5.2	28.2	28.3
82	04	21	0900	5.2	5.0	27.7	28.0
82	04	21	1630	5.2	5.0	27.8	27.9
82	04	22	0900	5.2	5.0	27.4	27.8
82	04	22	1630	5.3	5.0	27.2	27.2
82	04	23	0900	5.1	4.7	27.0	27.2
82	04	23	1600	5.1	5.0	27.2	27.2
82	04	26	0900	5.0	4.6	27.9	28.2
82	04	26	1600	6.0	5.7	29.0	29.1
82	04	27	0900	5.1	4.8	28.2	28.8
82	04	27	1630	4.8	4.5	28.5	28.8
82	04	28	0900	4.5	4.3	28.1	28.6
82	04	28	1630	4.7	4.6	28.5	28.9
82	04	29	0900	5.1	4.8	27.9	28.2
82	04	29	1630	4.9	4.5	28.5	28.8
82	04	30	0900	4.4	4.0	28.0	28.3
82	04	30	1630	4.4	4.4	28.7	29.0
82	05	03	0930	4.5	4.3	28.6	28.8

Appendix E

OXYGEN AND CARBON DIOXIDE CONTENTS OF THE INCUBATOR ATMOSPHERES

Table E.1: Summary of incubator gas compositions during the oxidation experiment

YEAR	MONTH	DAY	DESSICABS D1		D2		D3		D4	
			% O_2	% CO_2	% O_2	% CO_2	% O_2	% CO_2	% O_2	% CO_2
82	03	30	19.967	1.022	0.500	0.987	19.825	1.035	0.516	0.996
82	04	07	20.000	1.015	0.494	0.990	19.955	1.038	0.517	1.240
82	04	12	20.166	1.029	0.580	0.983	20.230	1.026	0.580	0.992
82	04	15	20.122	1.029	0.524	0.994	20.046	1.024	0.506	1.028
82	04	22	20.616	1.031	0.523	0.989	20.641	1.339	0.506	1.000